THERMAL QUENCHING OF LUMINESCENCE IN QUARTZ

BY

RASHMI NANJUNDASWAMY

Master of Science

Saurashtra University

Rajkot, India

Submitted to the Faculty of the
Graduate College of the
Oklahoma State University
in partial fulfillment of
the requirements for
the Degree of
MASTER OF SCIENCE
August, 2002

THERMAL QUENCHING OF LUMINESCENCE

IN QUARTZ

Thesis Approved:

Thesis Advisor

Dean of Graduate College

To,

Amma, Appa,

Pammi, Ranju, Pali, Chinni

&

Mukul

Acknowledgement

I would like to thank Dr. S.W.S. McKeever for giving me the opportunity to work under him. I would also like to thank him for his guidance, inspiration and understanding during the tough time that I was going through. I would also like to thank my committee members Dr. Wicksted, Dr. Rosenberger and Dr. Westhaus for their helpful comments and suggestions. I also want to thank the Department of Physics at Oklahoma State University for supporting me these 3 years. I would like to thank Mike Lucas of the instrument shop for building the radioluminescence set up and also for patiently making the many changes that I wanted in it.

I would also like to thank Dr. Kenneth Lepper, Dr. Jerimy Polf, Dr. Eduardo Yukihara, Dr. Von Whitely, Dr. Debrata Banerjee and Michael Blair for all the help they have given me. I would like to thank my parents and my family for their continued encouragement and support.

Finally I would like to say a special thanks to my dearest husband Mukul. Without him continuously encouraging me and helping me, I would not have been able to finish this thesis.

Table of Contents

List of Figures

Chapter 2

Chapter 3

Chapter 4

Chapter 5

List of Tables

Chapter 1

Introduction

In recent years luminescence dating of geological sediments has gained widespread popularity. The dating of sediments is important for several different reasons. Not only does it provide correlation between spatially separated deposits but also the time at which extinctions and the environmental reconstructions occurred. Perhaps more importantly the sediment dating may provide information about contemporary climatic changes by providing a timescale for paleoclimatic changes.

In the following sections the method of "optical dating" (or "optically stimulated luminescence dating") based on natural quartz will be discussed. This is one of the main luminescence techniques used for dating of sediments. Also discussed are the effects of thermal treatments on the luminescence and their relevance to laboratory dating procedures.

1.1 Optically Stimulated Luminescence:

In optically stimulated luminescence (OSL), luminescence is observed in specific wavelength regions by stimulating the sample with energetic light from other wavelength regions. A complete discussion can be found in [1]. The initial trials of optical dating [2] were conducted in order to find a better method for dating of sediments than thermoluminescence (TL). Later it was also found to be useful in radiation dosimetry and

detecting the irradiation of consumables (food etc.,). The principal minerals used are quartz and feldspars. This thesis, however is concerned only with the properties of quartz. The usual procedure is to use either a high power arc lamp source, along with a monochromator and/or a filter system to select the excitation wavelength, or a laser of constant intensity light operating at or near the desired wavelength. The stimulated luminescence from an irradiated sample is monitored continuously as long as the excitation source is on (i.e. continuous wave OSL, CW-OSL). In order to separate the emitted light from the excited light, and to prevent scattered excitation light from entering the detector, narrow band and/or cut-off filters are used. Luminescence is monitored from the instant the excitation light is switched on. In general the emitted OSL is found to follow a decaying curve where the total area under the curve represents the total absorbed dose since it was last exposed to light. The luminescence ceases when all traps are emptied.

Through comparison of the natural signal against those following known doses of radiation, the unknown natural absorbed dose can be obtained. By comparing this to the environmental dose rate the age of the sample can be obtained, through the relation:

$$\text{Age} = \text{Dose}/\text{Dose rate},$$

assuming the dose rate to be constant over the age of the sample.

1.2 New Techniques in OSL Dating:

The basic process used in OSL is to stimulate an irradiated sample with light from a specific wavelength region and to read the emitted signal at a different wavelength

region. A variety of stimulation modes is available, known as continuous wave-OSL (CW-OSL), linearly modulated OSL (LM-OSL) and pulsed OSL (POSL).

The mode that is most widely used in sediment dating is CW-OSL, however, brief descriptions of all the three are provided as follows. For a more complete description refer to [3].

CW-OSL: This has been discussed above and is the most widely used method in dating of sediments.

LM-OSL: In this method, rather than illuminating the irradiated sample with a constant intensity light source, the intensity of the stimulation light is made to linearly increase with time. This then gives rise to what is termed as a linearly modulated OSL signal, which is found to increase initially with time and the increase in power of the stimulation light, and then to fall rapidly to zero as the traps get depleted.

POSL: In this method the stimulation light instead of being on continuously is pulsed at a specific frequency wherein the time between the pulses is shorter than the lifetime of the luminescence emitted. Thus time rather than wavelength is used to discriminate between the emitted light and the excitation light.

There are basically two different procedures that have gained popularity. In one of these, a single aliquot (portion) is used, and the same sample is used for all the irradiation and measurements. In the other multiple aliquots (portions) of the sample are used, and a different aliquot is used for each irradiation and measurement. There is also the choice between adding a calibration dose to the natural dose (additive dose technique) or measuring the natural signal first and then trying to regenerate the measured signal by then giving a laboratory dose to the sample (regeneration technique).

The most recent developments have been in the single aliquot regeneration technique or more commonly called the SAR procedure. A full description of SAR procedures can be found in Wintle [4]. A brief description is provided here.

A small aliquot of sample is stimulated with light from the appropriate wavelength region. For quartz, either blue or green light is usually used. The CW-OSL is then recorded. The procedure after this is a set of steps in which different doses from a calibrated laboratory source are given to the sample and the CW-OSL is recorded for each dose. A plot of OSL versus dose is made and by comparison of the OSL signal from the natural dose to this plot an estimate of the natural dose is obtained. However, the repeated use of the same sample results in sensitivity changes, thus the SAR procedures have to take into account the possible sensitivity (defined, as the OSL output in response to a small test irradiation) changes. If sensitivity changes are occurring, the irradiation of a sample by the same test dose will result in different OSL outputs. The SAR procedures account for this by interspersing the irradiations and the OSL measurements with test irradiations and measurements of the OSL due to these test doses [6]. Thus corrections can be made for the sensitivity changes.

Since the ultimate goal is to use the OSL signal as a measure of the length of time the sample has been irradiated in nature, it is also necessary that the OSL signal used to determine the age of the sample be stable over the natural lifetime of the sample. To do this various preheat procedures are adopted to remove any unstable signals, wherein the sample is heated to a specific temperature after irradiation but before the OSL is recorded. Furthermore, the OSL readings themselves may be performed at elevated temperatures.

1.3 Thermal Quenching:

Thermal quenching of luminescence is a phenomenon in which the luminescence efficiency decreases as the temperature of the sample is raised above room temperature. Wintle [5] first described this phenomenon for quartz in a seminal paper in which she monitored Radioluminescence (RL – the instantaneous emission of light or the 'prompt' emission of light during exposure to radiation) as a function of temperature for quartz. The measurements were made at several different wavelengths using narrow band filters. The dependence of luminescence efficiency on temperature was described by an equation of the type

$$\eta = \frac{1}{1 + C\exp(-W/kT)} \qquad (1.1)$$

where η is the luminescence efficiency, W is the thermal activation energy (eV), C is a constant, k is Botlzmann's constant (eV. K^{-1}), and T is the temperature in degrees Kelvin. Recent techniques of OSL measurements used in dating of natural samples require that the signal be stable over the age of the sample. In order to remove the low temperature unstable signal, the OSL measurements are often performed at elevated temperatures. This technique, however, introduces thermal quenching into the picture. Measurements of OSL signal versus temperature indicated a decrease in efficiency in accordance with equation 1 [3,5,6].

Wintle [5] found that for luminescence measured with a filter centered at 465nm the values of C and W were 2.8×10^7 and 0.64 eV, respectively. A note by her also indicated that these values remain almost the same for emission at other wavelengths, using filters centered at 310nm, 370nm, and 410nm. However, she reported that emission in the 495nm region shows very little quenching. Recent experiments conducted by Wintle and

Murray [6] indicated that OSL data could be fitted to similar parameters. They found the values of C and W to be C = 3.4 x 10^7 and 2.0 x 10^7, and W = 0.636 and 0.61 eV respectively. Data by McKeever *et al.* [3] quote C = 7.9 x 10^6 and W = 0.60 eV (using Hoya U-340 nm filter). In both cases the results were obtained for OSL emitted in the UV emission region of the spectrum.

1.4 This Thesis:

The purpose of this investigation is to provide further insight into thermal quenching of OSL in quartz measuring of the thermal quenching characteristics from natural quartz using the various luminescence techniques of TL, RL, and OSL. The intent was to examine the quenching response at two different luminescence wavelength regions, namely the UV (340nm) emission region and the blue (450nm) emission region, and also to discuss the potential of the Mott-Seitz model as the appropriate model to describe luminescence quenching in this material.

Chapter 2

Theory & Background

2.1 General Luminescence Processes:

When a material absorbs external energy, luminescence may be emitted. Depending on the type of radiation used to excite the emission, luminescence phenomena are given different names [7], for example if the radiation used for excitation is optical or ultraviolet then the resulting emission is termed as *photoluminescence.* Similarly, if radiation used for excitation is nuclear i.e. γ-rays or β-rays etc., then the resulting emission is termed as *radioluminescence*. Similarly *cathodoluminescence* is emitted when stimulation is by an electron beam and *sonoluminescence* is stimulated by sound energy.

Luminescence can be sub-classified into *fluorescence* and *phosphorescence* [8]. The most practical and useful way of distinguishing between the two is to study their temperature dependence. *Fluorescence* is essentially independent of temperature, whereas *phosphorescence* decay exhibits strong temperature dependence.

In general, let us consider a ground state *g* and an excited state *e* as shown in Fig 2.1 (a, b). Luminescence occurs when energy is transferred from the radiation to the electrons in the solid and the transition occurs from ground state *g* to excited state *e* (transition (i) in Fig 2.1 (a)) and the electron in the excited state returns to the ground state with the emission of a photon (transition (ii) in Fig 2.1 (a)). However the transition can be delayed by a transition into and out of a metastable state *m* as in Fig 2.1 (b).

Fig 2.1: Absorption and emission process in (a) fluorescence, and (b) phosphorescence.

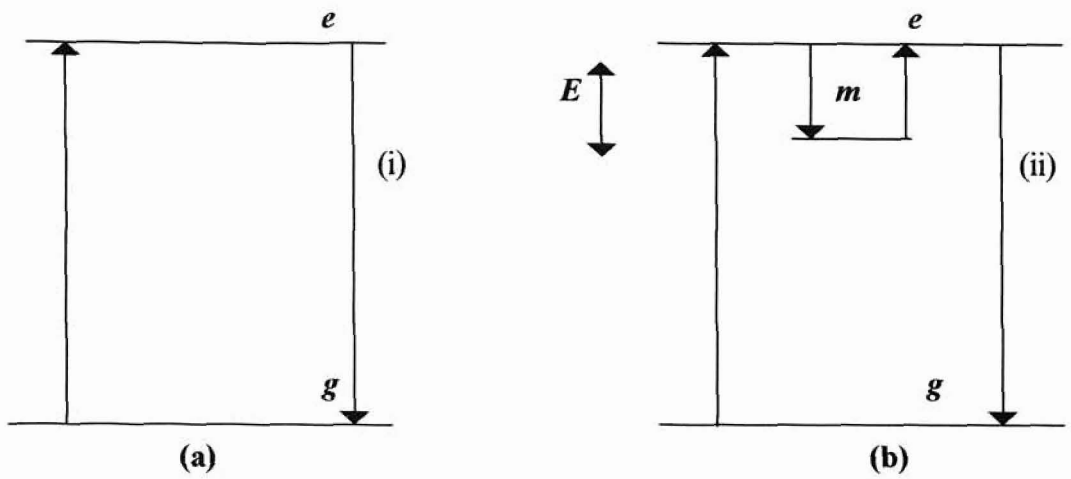

The electron trapped in the metastable state *m* (Fig 2.1 (b)) needs to gain an amount of energy *E* before it can decay to the ground state *g* with the emission of a photon. Thus, the delay observed in phosphorescence corresponds to the time the electron spends in the metastable state *m*.

Using thermodynamic arguments it can be shown that the mean time spent in a trap at temperature *T* is given by:

$$\tau = s^{-1} * \exp(E/kT) \qquad (2.1)$$

where *s* a is constant usually called the 'attempt to escape frequency', *E* is the trap depth and *k* is the Boltzmann's constant.

2.1 (a) Photoluminescence:

Optically stimulated luminescence is to be distinguished from Photoluminescence, which results because of an internal transition between the energy levels of a defect. There is no ionization and hence no electron-hole pair production involved in this process [8]. These transitions do not involve the transfer of charges from one defect to another and thus do not affect the TL signal. On the other hand OSL involves the optical ionization of trapped charge from a defect and subsequent recombination with charge of the opposite sign. If the recombination is radiation, OSL is emitted. This is described in more detail in the next section, and these measurements can be useful in yielding information about luminescent sites.

2.1(b) Emission Process in Optically Stimulated Luminescence:

The amount of energy that the electron needs in order to come out of the metastable m state and decay to the ground state g can be acquired by different means viz., by absorption of thermal or optical energy. The luminescence resulting from stimulation of the trapped charges by light is referred to as Optically Stimulated Luminescence (OSL). The emission of OSL can be understood using the band gap diagram similar to the one represented in Fig 2.1(a, b) [1]. Fig 2.2 (a, b) shows the energy level representation of the OSL process. Fig 2.2 (a) depicts the ionization in the sample due the exposure to radiation. The electrons and the holes get trapped at the defects T and L respectively.

Fig 2.2(b) represents the eviction process due to absorption of light by the trapped electrons and the subsequent emission of OSL due to recombination of the still-trapped holes and the freed electrons. The ionization is due to exposure of the crystal to

Fig 2.2(a) Ionization process in Optically Stimulated Luminescence "Trap Filling":

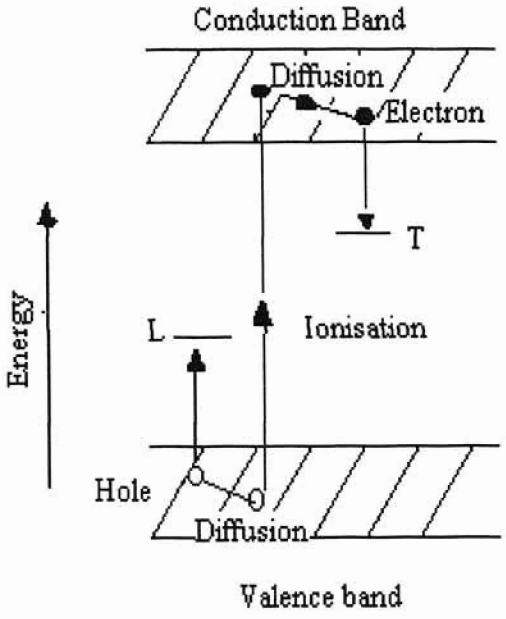

Fig 2.2(b) Eviction process in Optically Stimulated Luminescence "Trap Emptying":

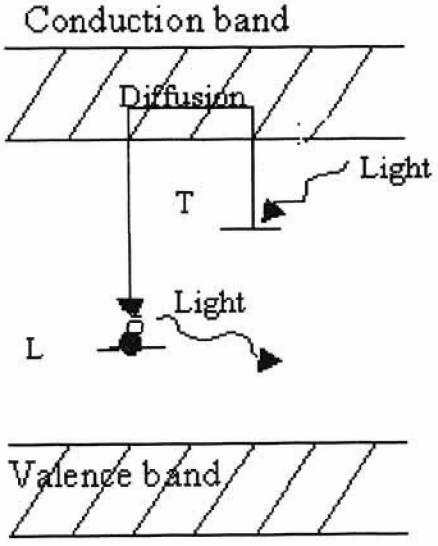

radiation. This results in the trapping of electrons and holes at defects T and L respectively.

By shining light of appropriate wavelength onto the sample, electrons are evicted from traps and light is emitted when recombination takes place at the luminescence centers. The process by which OSL can be produced (as shown in Fig 2.2) is by transport via the conduction band. The simplest model to describe this is the one electron-trap and one hole-trap (recombination center) model.

In order to develop this OSL model the following assumptions and definitions need to be made [8]:

Trap: These are states at which the probability of transition to the conduction band of the trapped charge is greater than the probability of recombination of a free charge of the opposite sign at the state.

Recombination center: These are sites in which the probability of recombination of charge is higher than the probability of release of the charge.

All transitions to and from the localized levels take place through the delocalised bands (i.e. conduction band for electrons and valence band for holes).

Transitions of electrons from the delocalised bands into the localized traps are non-radiative producing only phonons, and transitions of electrons into recombination sites are radiative producing photons.

Lastly, for simplification, we assume that only one type of charge, i.e. electrons, is released during the whole process (note that it can very well be holes that are released).

An analysis of the rate equations associated with the flow of charges between the various energy levels can be useful in understanding the OSL process. These are in the form of simultaneous coupled differential equations.

In general the intensity of the luminescence produced is proportional to the rate at which the recombination takes place and from the above assumption that no trapped holes are released during the process, we can write,

$$I_{OSL} \propto \left| \frac{dn_h}{dt} \right| \tag{2.2}$$

where n_h is the concentration of holes in the recombination center. Since the intensity is actually proportional to the rate at which the number of these holes decrease, equation (2.2) can be further written as

$$I_{OSL} = -\eta \frac{dn_h}{dt} \tag{2.3}$$

where η is a constant indicating the efficiency of the process and is usually taken to be unity and the negative sign indicates that the concentration of holes is decreasing. Figure 2.3 indicates the allowed transitions in the simplest model of OSL.

Fig 2.3 Simplest model for OSL, involving one electron trap and one hole trap (acting as a radiative recombination center).

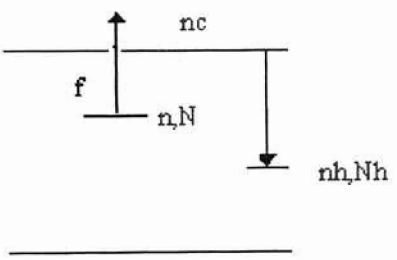

The following equations can thus be written during optical stimulation of the trapped electrons,

$$\frac{dn}{dt} = -nf + n_c A(N - n) \tag{2.4}$$

$$\frac{dn_c}{dt} = nf - n_c(N - n)A - n_c n_h A_r \tag{2.5}$$

$$n + n_c = n_h \tag{2.6}$$

$$\frac{dn_c}{dt} = -\frac{dn}{dt} + \frac{dn_h}{dt} \tag{2.7}$$

Here, f is the optical excitation rate at which the electrons are excited into the conduction band, n_c is the concentration of electrons in the conduction band, n is the concentration of electrons in the trap, n_h is the concentration of holes in the recombination center, N is the concentration of traps, and A is the transition coefficient for free electrons and A_r is the recombination transition coefficient.

Equation (2.6) represents the charge neutrality condition.

The recombination at hole centers of electrons and holes result in an OSL intensity of I_{OSL}. In order to solve these equations analytically certain assumptions need to be made.

The most important is the Quasi-Equilibrium (QE) condition, according to which, the optically stimulated charge carriers are relaxed almost instantly either into the recombination centers or into vacant traps, or more simply, the number of electrons in the conduction band change much slower than the number of trapped charges, i.e.:

$$dn_c/dt << dn/dt,\ dn_h/dt \tag{2.8}$$

$$\&\quad n_c << n,\ n_h \tag{2.9}$$

As an additional constraint we assume that once released, the probability of the electrons getting retrapped is negligible. Then the OSL intensity can be given by:

$$I_{OSL} = -\frac{dn_h}{dt} = -\frac{dn}{dt} = nf \tag{2.10}$$

with $\eta = 1$. The solution of 2.10 is

$$I_{OSL} = n_o f \exp(-tf) = I_o \exp(-t/\tau) \tag{2.11}$$

where n_o and I_o are the trapped electron concentration and the initial OSL intensity, respectively, at time $t = 0$, and $\tau = 1/f$ is the OSL decay constant. Detailed discussion about more complicated models can be found in [3]. An experimental example of an OSL decay curve is given in Fig 2.4. The OSL decay curve was measured for the powdered Arkansas quartz sample (grain size 90-106μm) in the UV emission region. The stimulation light was in the blue region. Two UV-340 nm filters were used for measuring the signal.

Fig 2.4 OSL decay curve of Arkansas quartz sample:

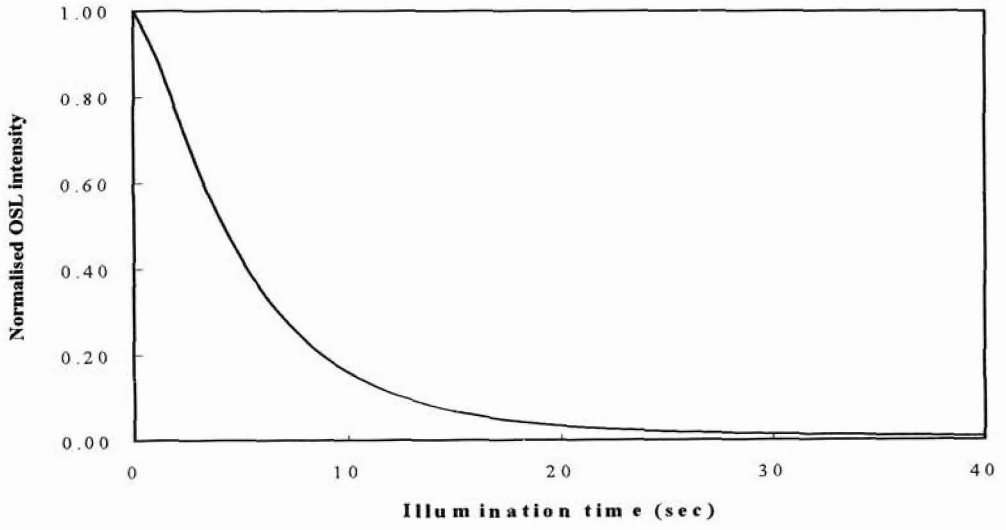

2.1 (c) Thermally Stimulated Luminescence:

The electrons trapped in a metastable state can also be released by raising the temperature of the sample. Given a Maxwellian distribution of trap energies, the probability p per unit time of thermal excitation is exponentially dependent on the temperature as

$$p = s * \exp(-E/kT) \qquad (2.12)$$

Where s, E, k, and T have definitions as before. If the temperature of the sample is increased at an arbitrary constant rate $\beta = dT/dt$ then the probability that an electron will be released from a trap will increase according to equation (2.12) producing an increase in the luminescence emission. As the temperature of the sample is increased further the trap gets depleted, after which the intensity falls down to zero. The resulting shape of the curve is in the form of a peak. An example is given in figure (2.5).

As this emission is controlled by temperature it is referred to as Thermally Stimulated Luminescence, or simply, Thermoluminescence (TL). In order to describe the TL process the same definitions and assumptions made in analyzing the simple OSL model need to be made (cf. pg. 11).

The heating of the sample is done at a linear rate according to the equation

$$T(t) = T_o + \beta t$$

Where T_o is the initial temperature and β is the heating rate given by dT/dt.

The intensity of TL $I_{TL}(t)$ during the heating of the sample is proportional to the rate of recombination of holes and electrons as in OSL.

The intensity $I_{TL}(t)$, can be thus written by an equation similar to equation (2.3):

$$I_{TL}(t) = -dn_h/dt, \text{ with } \eta = 1 \qquad (2.14)$$

Here the efficiency η has been taken to be unity and the negative sign indicates the reduction in the concentration of trapped holes. The position of the glow peak maximum in a TL experiment is related to both, the trap depth E and the 'attempt to escape frequency' s, and the heating rate β. The size of the TL peak is related to the concentration of the trapped electrons. An analysis of the TL peaks thus provides important information about the distribution of traps in the sample. It is also advantageous to further analyze the TL model and the rate equations associated with the flow of charges between the various energy levels. Expressions for the change in the number of trapped electrons, trapped holes and free electrons in the conduction band during heating of the sample can be written in the form of simultaneous coupled differential equations, thus:

$$dn/dt = - ns \exp(-E/kT) + n_c (N - n) A \quad (2.15)$$

$$dn_h/dt = -n_c n_h A_r \quad (2.16)$$

$$n + n_c = n_h \quad (2.17)$$

$$dn_c/dt = dn_h/dt - dn/dt \quad (2.18)$$

All the terms are as defined before.

Equations (2.15)-(2.16) are the rate equations depicting the movement of the charge carriers whereas equation (2.17) expresses the charge neutrality condition, and (2.18) is derived from (2.17). As these rate equations are analytically insolvable, certain assumptions again need to be made in order to find an analytical expression for $I_{TL}(T)$, i.e. the intensity of TL as a function of temperature.

In solving the rate equations for OSL the Quasi-Equilibrium (QE) condition was again made to solve the rate equations analytically. This condition assumes that the thermally

stimulated charge carriers are relaxed almost instantly either into the recombination centers or into vacant traps or more simply, that the number of electrons in the conduction band change much more slowly than the number of trapped charges:

$$dn_c/dt << dn/dt \tag{2.19}$$

$$\& \quad n_c << n \tag{2.20}$$

Applying (2.19) to equation (2.18),

$$dn_h/dt = - dn/dt \tag{2.21}$$

Substituting (2.15) & (2.16) into (2.21) and solving for n_c,

$$n_c = \frac{ns\, exp(-E/kT)}{n_h A_r + (N - n) A} \tag{2.22}$$

Substituting this result into equation (2.16) and using equation (2.14),

$$I_{TL}(t) = \frac{- dn_h}{dt} = n\, s\, exp(-E/kT) * \frac{n_h A_r}{[n_h A_r + (N - n) A\,]} \tag{2.23}$$

This equation can be used for finding TL intensities provided an expression for n, i.e. the concentration of trapped electrons is known. In order to find n, we substitute (2.21) into (2.23):

$$I_{TL}(t) = \frac{dn}{dt} = n\, s\, exp(-E/kT) * \frac{n_h A_r}{[n_h A_r + (N - n) A\,]} \tag{2.24}$$

Which can be rewritten as:

$$I_{TL}(t) = n\, s\, exp(-E/kT) * [1 - \frac{(N - n) A}{n_h A_r + (N - n) A}\,] \tag{2.25}$$

According to the criteria of Randall & Wilkins [7,8] the model will yield a first-order kinetics if the probability of retrapping is negligible as compared to the probability of recombination, expressed as:

$$n_h A_r >> (N - n) A \tag{2.26}$$

Applying (2.26) to (2.24) yields:

$$I_{TL}(t) = dn/dt = n\, s\, exp\,(-E/kT) \tag{2.27}$$

Integrating from $T=T_o$, assuming a linear heating rate as per equation (2.13) gives,

$$I_{TL}(T) = n\, s\, exp\,(-E/kT)\, exp\left[(s/\beta) \int_{To}^{T} exp(-E/kT)\, dT \right] \tag{2.28}$$

Equation (2.28) is called the Randall-Wilkins equation for first-order kinetics since it depends on the first power of the carrier concentration. The first-order TL intensity equation (2.28) produces asymmetric peaks with the peak position depending on the activation energy, frequency factor, and heating rate.

Fig 2.5 is an example of a TL glow curve obtained from the Arkansas quartz sample. A dose of 1Gy was given to the sample.

Fig 2.5 A TL glow curve for Arkansas quartz sample at a heating rate of 0.1K/s

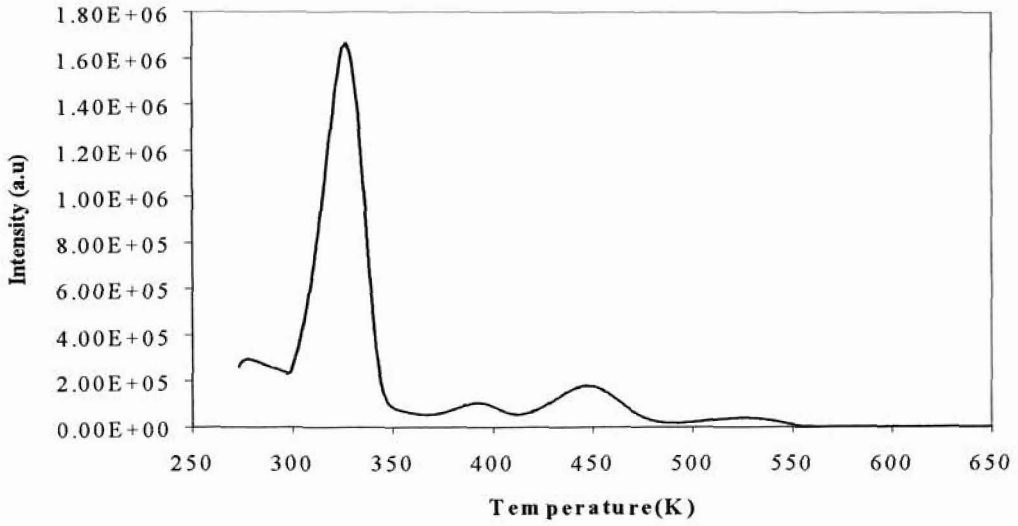

The heating rate used was 0.1 K/s and the emission was measured in the UV region with 2 UV 340nm filters. Several TL peaks are seen, suggesting individual processes of the type hereby described. A more complete discussion can be found in chapter 4 in analysis of results.

2.1 (d) Radioluminescence:

Instantaneous emission of light or the 'prompt' emission of light during exposure to irradiation is termed Radioluminescence (RL). This results from the immediate recombination of the electrons and holes at the luminescence centers. The kinetics described in TL can be applied to RL with some modifications. The most important being, that in case of TL the band-to-band transitions are considered negligible and hence the term does not appear in the rate equations. In case of RL, however the band-to-band transitions cannot be neglected.

Rate equations for the emission process for RL can be developed as in TL and OSL. In order to do so we make the same assumptions that we made in writing down the rate equations for the TL and OSL process (cf pg 11).

The charge neutrality condition can be written as:

$$n + n_c = n_h \tag{2.29}$$

and from the above equation,

$$dn_c/dt = dn_h/dt - dn/dt \tag{2.30}$$

The following set of simultaneous differential equations can thus be written:

$$\frac{dn_c}{dt} = \Gamma\frac{dD}{dt} - n_c(N-n)A - n_c n_h A_r \tag{2.31}$$

$$\frac{dn}{dt} = n_c(N - n)A \tag{2.32}$$

$$\frac{dn_h}{dt} = -n_c n_h A_r + n_v(N_h - n_h)A_h \tag{2.33}$$

where dD/dt is the dose rate of the radiation used to stimulate the luminescence and Γ is a constant.

It can be seen that the equations for RL are similar to the rate equations of OSL. However in RL the rate of excitation of electrons into the conduction band are governed by the dose rate of the radiation used for stimulating the luminescence.

In order to solve these simultaneous coupled differential equations we again make the Quasi-Equilibrium (QE) conditions as in OSL and TL, i.e. $dn_c/dt << dn/dt$ & $n_c << n$.

Using the QE condition and from equation (2.31) solving for n_c, i.e. the concentration of electrons in the conduction band, yields

$$n_c = \frac{\Gamma \dot{D}}{A(N - n) + A_r n_h} \tag{2.34}$$

where $\dot{D} = dD/dt$. The intensity of Radioluminescence, I_{RL} is given by the rate of recombination of the trapped holes, thus

$$I_{RL} = -n_c n_h A_r \tag{2.35}$$

Substituting n_c back into equation (2.33), and using QE condition the intensity of RL can be expressed as:

$$I_{RL} = \Gamma \dot{D} \left[1 - \frac{A(N - n)}{A(N - n) + A_r n_h} \right] \tag{2.36}$$

When the concentration of the traps equals the concentration of the electrons, i.e.

$A\ (N - n) \rightarrow 0$, the intensity of RL will be proportional to the dose rate of the stimulating radiation, thus

$$I_{RL} = \Gamma \dot{D} \tag{2.37}$$

Detailed discussion about more complicated models can be found in [10]. RL emission in the infrared region (IR-RL) has found applications in dating of feldspars [11]. An example of RL intensity as a function of stimulation time for Arkansas quartz sample is shown in Figure 2.6. A dose of 4.53 Gy was give during the total time of the measurement. The total measurement time was 200 s.

Fig 2.6: RL intensity of Arkansas quartz sample as a function of illumination time in the UV emission region:

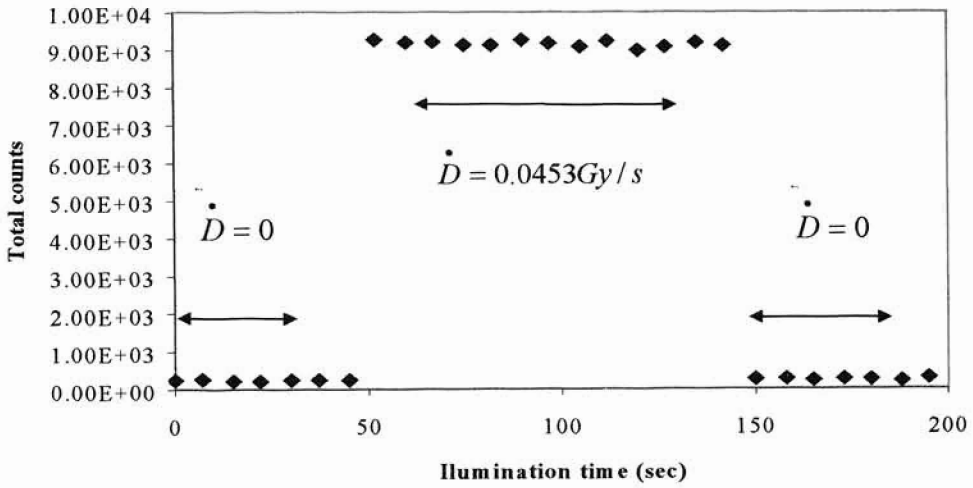

2.2 Thermal Quenching of Luminescence:

As the term itself implies thermal quenching is a decrease in efficiency of luminescence at high temperature. Specifically, thermal quenching is concerned with the decreased likelihood that an excited luminescence center will de-excite by emission of a photon rather than dissipate its excess energy as heat in the form of enhanced lattice vibrations. Thermal quenching of the luminescence from natural quartz was first described in a paper by Wintle [5] in which she monitored the radioluminescence from natural quartz as a function of temperature. The measurements were made at several emission wavelengths using a variety of narrow-band filters. As mentioned in chapter 1, the dependence of the luminescence efficiency η on the temperature T was described by a function of the type:

$$\eta = \frac{1}{1 + C\exp(-W/kT)} \qquad (1.1)$$

where W is the thermal activation energy (eV) for luminescence quenching, and C is a constant; k is the usual Boltzmann's constant ($eV.K^{-1}$) and T is in Kelvin. In general, a plot of normalized intensities of the luminescence obtained as a function of temperature yields the "quenching curve". An example of a quenching curve is shown in Fig (2.7). Two models have been put forth in order to explain thermal quenching. They are the Mott-Seitz model and the Schön-Klassens model.

2.2(a) Mott-Seitz model:

The Mott-Seitz model dates back to the early work by Seitz and Mott & Gurney [8-9] who considered the electron transitions between a ground state and an excited state within the same atom in terms of a coordinate configuration diagram (Fig 2.8).

Fig 2.7: Plot of the quenching curve obtained for equation (1.1) using Wintle's published values for C and W (3.4*10^7, 0.636 eV):

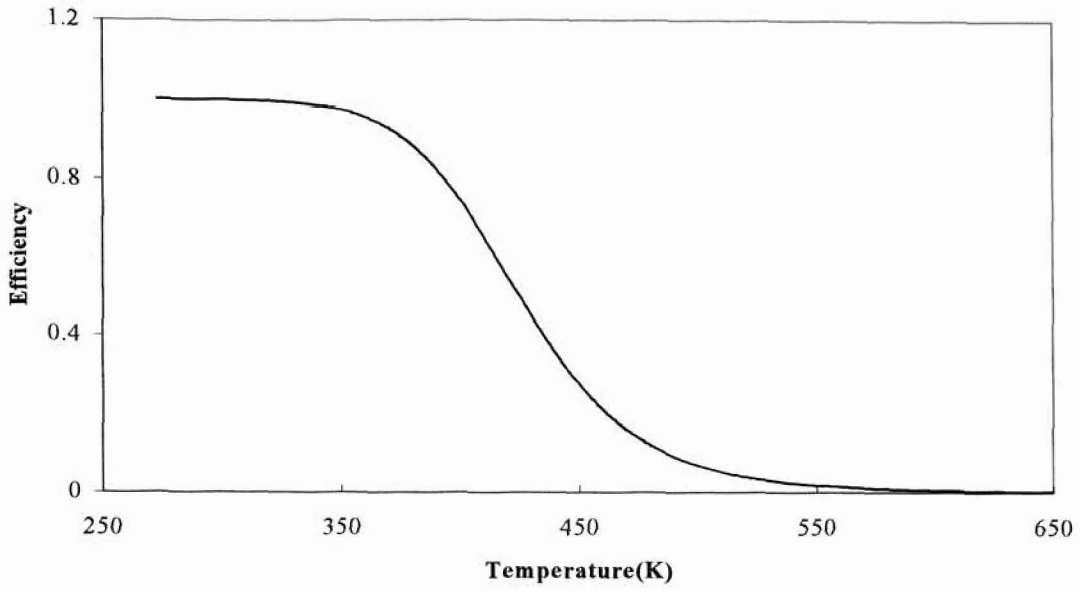

The configurational coordinate is the displacement of atoms in the neighborhood of the defect. At equilibrium in the ground state the electron takes on minimum energy (point **A**). Absorption of energy from radiation results in a transition to an excited state **B** without an adjustment in the configurational coordinate (Frank-Condon principle). However the minimum energy in the excited state is not the same as in the ground state and thus the electron has to lose an amount of energy $\mathbf{E_1}$, dissipated as heat in order to reach a new energy minimum **C.** Transition C-D now results in luminescence and the electron again loses energy in the form of heat to come back to the energy minimum **A.** Thus from the figure it can be seen that the absorbed energy is less than the luminescence energy by an amount $\mathbf{E_1 + E_2}$, and that the emission bands lie on the long wavelength side of the corresponding absorption bands (Stoke's shift).

An additional route by which the excited electron can return to its ground state is suggested in the configuration coordinate diagram. If the electron absorbs an amount of thermal energy **ΔE** while in its excited state, then a transition from **C** to **E** can take place. The electron now transfers easily to the ground state without the emission of radiation, but with just the dissipation of heat causing the return of the electron to the minimum energy at **A**.

Whether or not a material will exhibit luminescence following the absorption of energy depends on the relative probabilities of radiative and non-radiative transitions. In general, the luminescence efficiency of a phosphor, η, is related to the probability of a luminescence transition, P_r, and the probability of non-radiative transition P_{nr} by

$$\eta = P_r /(P_r + P_{nr}) \tag{2.38}$$

Thus in the Mott-Seitz model it can be seen that the probability of non-radiative transition P_{nr} is related to the temperature by a Boltzmann's factor $exp\ (-\Delta E/kT)$. The radiative probability P_r is unaffected by the temperature and thus the efficiency can be written in the form of equation (1.1)

$$\eta = \frac{1}{1 + C_1 exp(-\Delta E / kT)} \tag{2.39}$$

Comparing Equation (2.39) to (1.1), it can be seen that ΔE has the same meaning as W and C_1 has the same meaning as C.

Fig 2.8 Possible variations of electron energy with configuration coordinate for excited and ground states of an atom:

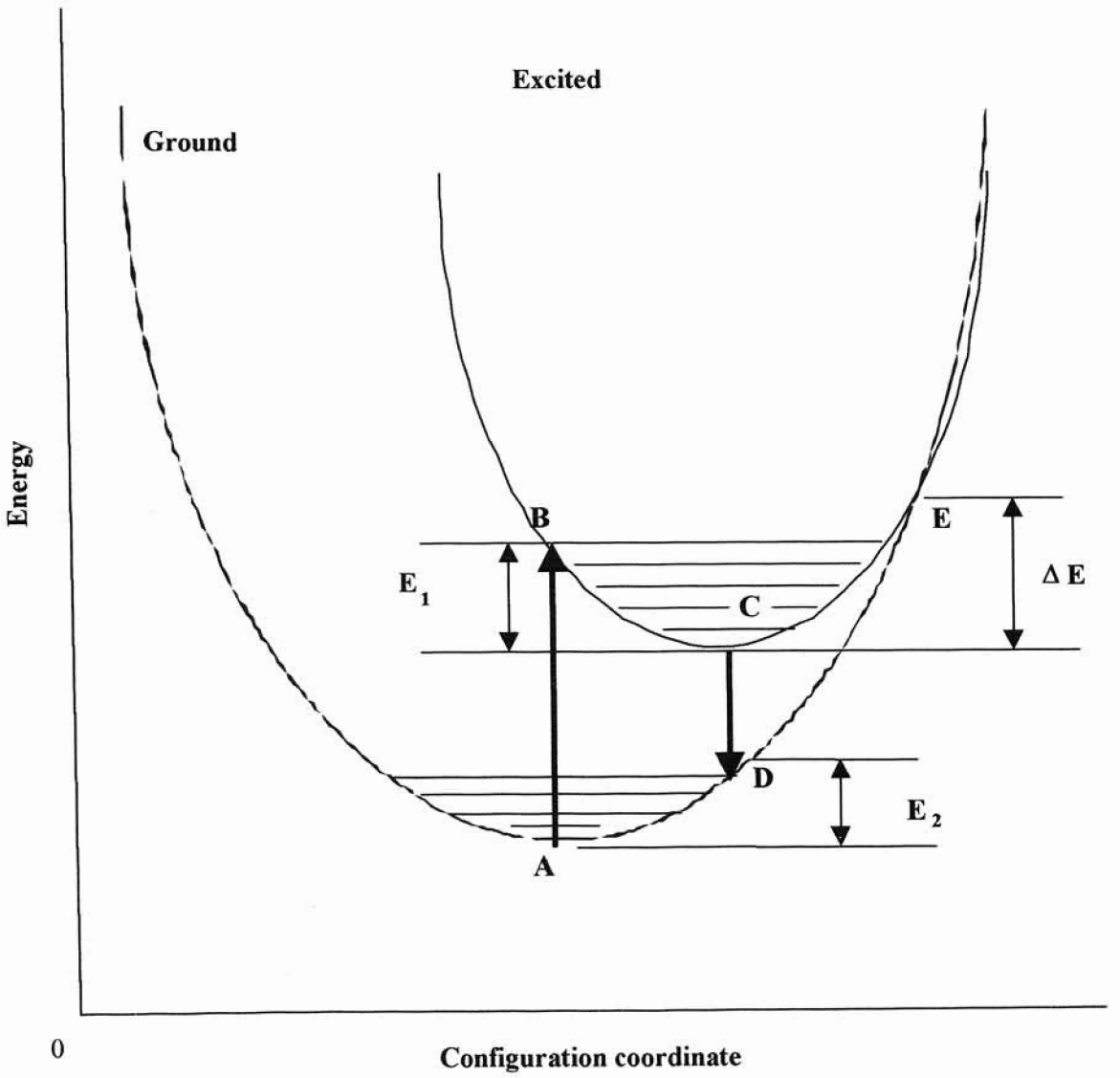

2.2 (b) Schön-Klassens model:

The Schön-Klassens model was the alternative model suggested in order to explain the thermal quenching in quartz. This is based directly on the energy band model and was independently advanced by Schön and by Klassens [8-9] for those materials in which the recombination involves displacement of charge carriers through the crystal lattice. Luminescence is a result of recombination of electrons with trapped holes in order to give luminescence. At high temperatures, however, it is possible that holes may be thermally released and the free holes may migrate and become trapped at other centers termed as killer centers (Fig 2.9). Here the free electrons may recombine without the emission of luminescence due to phonon interaction. An increase in these 'killer center' concentrations and/or an increase in temperature can thus be seen to increase the probability of a non-radiative recombination. Thus, the efficiency in this case with which a free electron will recombine at the luminescence center is given as:

$$\eta = \frac{1}{1 + C_2 exp(-\Delta E_h / kT)} \tag{2.40}$$

Comparing equation (2.40) with (1.1), it can be seen that constant C_2 is the same as C and ΔE_h has the same meaning as W, the activation energy. The luminescence center acts as a recombination center at low temperatures, and as a hole-trap at high temperatures. For the 'killer' center to act as a recombination center at high temperatures, its trap depth has to be more than $W = \Delta E_h$.

Fig 2.9 Schön-Klassens model: 1- Radiative recombination, 2-Thermal release of a hole, 3- Hole migration, 4-Hole trapping at a killer center, 5- Non-radiative recombination; solid circles-electrons; open circles-holes.

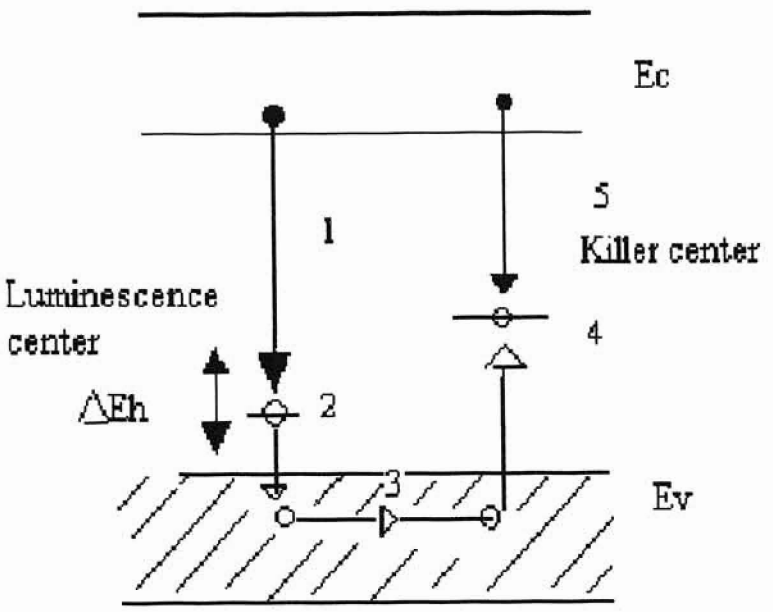

2.3 Thermal Quenching in TL of Quartz:

In thermoluminescence (TL) the temperature of a TL peak shifts to higher values as the heating rate increases. Thus, at low heating rates the TL peak may appear in a range where thermal quenching is minimal, whereas at higher heating rates the peak temperature may be such that thermal quenching is strong. A plot of the area under the TL peak as a function of peak position for a variety of heating rates will yield the thermal quenching curve similar to the one shown in figure (2.7).

The intensity of TL is related to the rate of reduction of the recombination centers, and can be given by

$$I_{TL} = \eta \left| \frac{dn_h}{dt} \right| \tag{2.41}$$

where we have now included η, the luminescence efficiency. The integral under the glow peak with respect to time is:

$$\int_0^\infty I_{TL}(t)\, dt = \frac{1}{\beta} \int_0^\infty I_{TL}(T)\, dT = \eta\, n_{ho} \tag{2.42}$$

Where n_{ho} is the initial concentration of holes and β is the heating rate and is given by dT/dt. If the efficiency i.e. the proportionality constant η is a constant then the areas under the different glow peaks should not change with heating rate i.e. the integral $\int_0^\infty I_{TL}(t)dt$ should be a constant. Otherwise if the efficiency η itself will be a function of temperature, then the integral $\int_0^\infty I_{TL}(t)dt$ will decrease as β increases.

The above analysis relies upon a fixed temperature range over which thermal quenching is observed. With the Schön-Klassens model, the thermal emission of holes from the recombination site will also shift to higher temperatures with heating rate since this process is governed by the same thermally activated kinetics that control the thermal emission of electrons from the trapping site. Effectively, this means that the plot of area under the TL peak versus peak position (temperature) curve will not follow the simple relationship defined in Equation (2.26). In contrast, the Mott-Seitz model predicts a shape and form for η which is independent of heating rate. Thus, analysis of thermal quenching in this described manner should reveal which model is most descriptive of the thermal quenching process. Fig 2.10 shows an example of a glow peaks unaffected by thermal

Fig 2.10 Simulated glow curves unaffected by thermal quenching:

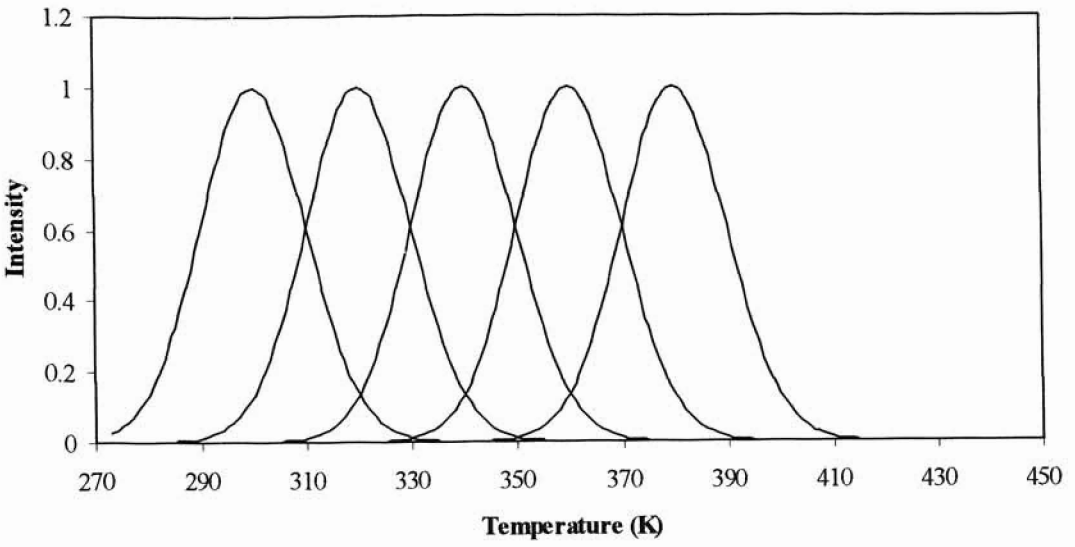

Fig 2.11 Simulated glow curves affected by thermal quenching:

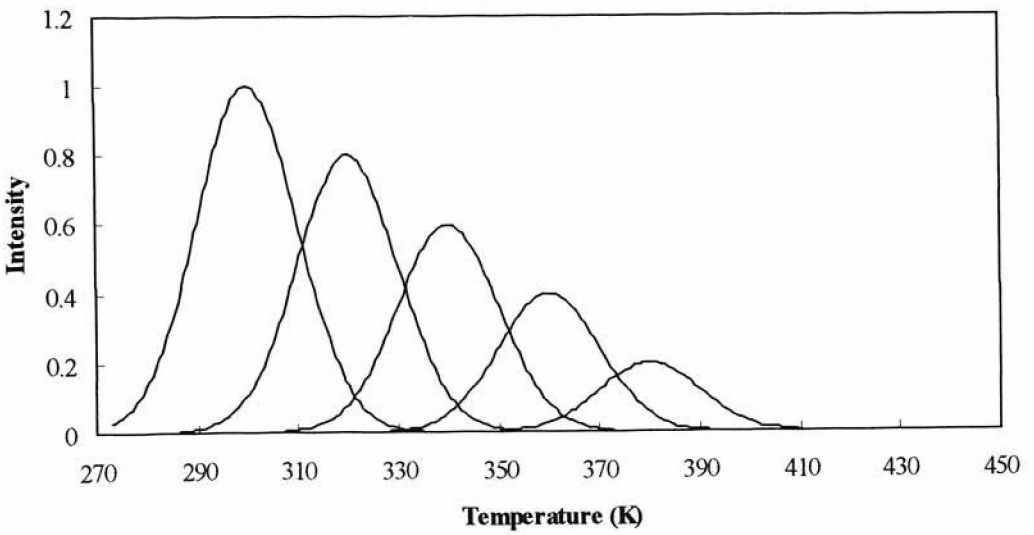

quenching. In order to simulate these curves a Gaussian shaped curve was assumed and the FWHM were taken from experimental data. Fig 2.11 shows an example of simulated glow curves affected by thermal quenching. However, experimentally obtained quenched peaks are not as symmetrical and will be distorted because the higher temperature end of a peak will be affected by quenching to a larger extent than the lower end. Fig 2.12 shows the plot of TL peak areas as a function of peak positions from experimental data for the Arkansas quartz sample for different heating rates in the UV emission region. A dose of 1 Gy was given to the sample and heating rates from 0.01K/s to 9 K/s were used. The peak areas as functions of peak positions were obtained after the glow curves were deconvoluted into its constituent peaks. The data sets numbered 1, 2, 3, 4, and 5 are the different peaks in each glow curve. As the heating rate is increased the peaks shift to higher temperatures and also decrease in intensity due to thermal quenching. This is discussed in more detail in Ch 4.

Fig 2.12: Quenching curve (peak area versus peak position) obtained for the Arkansas quartz sample in the UV emission region:

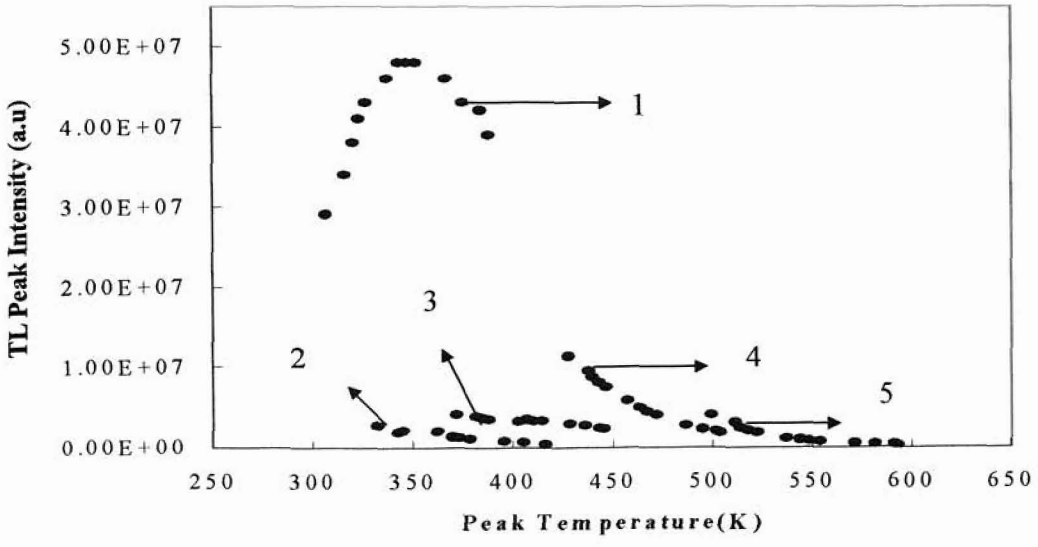

2.4 Thermal Quenching in OSL:

Measurements of optically stimulated luminescence (OSL) from natural quartz are often performed at elevated temperatures in order to remove the adverse effects of shallow traps, which may be thermally unstable over the period of irradiation of the sample. This, however, introduces thermal quenching into the picture, which causes the efficiency of luminescence centers (i.e. photon emission per electron arriving) to decrease as the temperature is increased. Here non-radiative pathways become available as the temperature is increased. The Schön-Klassens model can explain the cause of such effects: at high temperatures the holes are thermally excited into the valence band before the recombination with free electrons can take place. Alternatively the Mott-Seitz model can also be used to explain the phenomenon.

In order to obtain the quenching curve in OSL, the OSL experiments are performed at different temperatures. The total area under each decay curve can then be obtained. A plot of the area under the decay curve as a function of the temperature at which the experiment was performed yields the quenching curve.

An example of a OSL quenching curve obtained for the Arkansas quartz sample in the UV emission region is shown in Fig 2.13. The stimulation light used was from blue LED's. Each data point represents an individual sequence in the experiment. A dose of 1 Gy was given to the sample in each sequence. Each sequence was performed at different sample temperatures. Each sequence yielded a decay curve and each data point in the quenching curve shown represents the total integrated signal under each curve.

Fig 2.13: Quenching curve (plot of area under the OSL decay curve as a function of sample temperature) for the Arkansas quartz sample in the UV emission region:

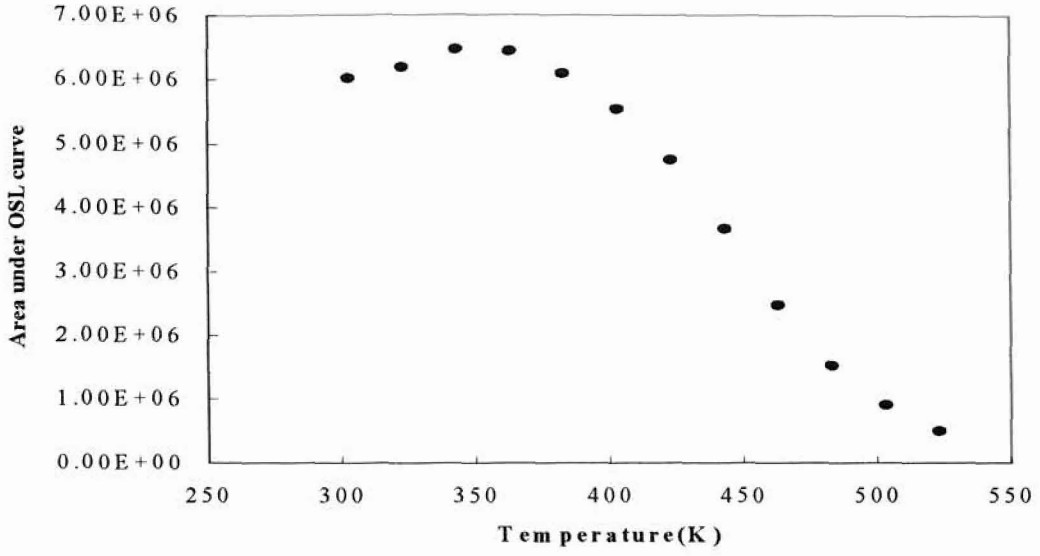

2.5 Thermal Quenching in RL:

As mentioned before, Wintle first discussed thermal quenching of RL in quartz in 1975 [5]. She monitored RL as a function of temperature at different emission wavelengths.

RL is the 'prompt' emission of luminescence during irradiation of the sample. A plot of obtained RL intensity as a function of illumination time is shown in Fig 2.6. If the temperature of the sample is increased, then, it is observed that the intensity of the resulting luminescence decreases. Thus RL experiments can be performed at different sample temperatures. A sum total of the signal can then be obtained as a function of the temperature. A plot of the total RL signal versus the temperature yields the quenching curve.

An example of the quenching curve obtained for the Arkansas quartz sample in the UV emission region is shown in Fig 2.14. The data points shown in this quenching curve

were obtained for the cooling cycle with sample temperatures varying from 570 K to room temperature. A single UV 340nm filter was used to measure the signal. Analysis of this data can be found in Chapter 4.

Fig 2.14: Quenching curve (plot of total RL signal as a function of temperature) for the Arkansas quartz sample in the UV emission region:

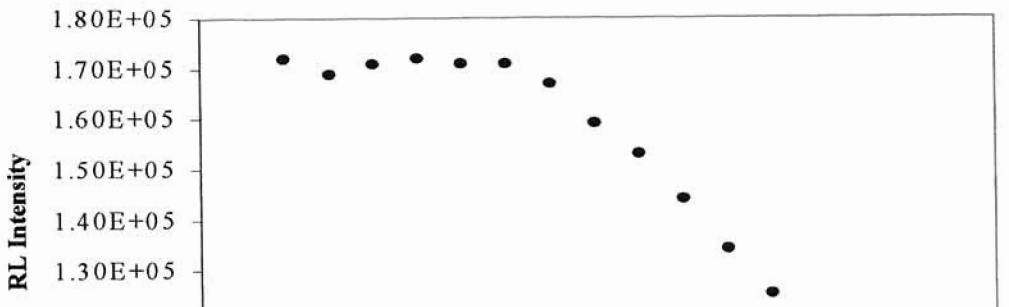

Chapter 3

Experimental Setup and Procedures

3.1 Samples:

Several quartz samples were used in these experiments. These included samples of rock crystal from Arkansas, Oklahoma and Alaska, Premium-Q and Electronic Grade synthetic quartz from Sawyer Inc., and quartz from two sedimentary deposits in Denmark. Dr. Andrew Murray of Risø National Laboratory (Denmark) kindly provided the latter. Among these the Arkansas quartz sample and the Danish quartz sample (QQ-974703) were primarily used in the experiments because of the stability of the signal they produced.

3.1 (a) Sample Preparation:

The Danish sedimentary quartz (or Danish QQ-974703) is a fine grain sedimentary quartz sample. It was obtained as a finely ground sample. The Arkansas, Oklahoma, Alaska and the synthetic quartz samples were all obtained as single crystals. The crystals were first ground into a fine powder and then grain sizes between 90 to 106μm were separated using sieves. The ground quartz samples were affixed onto aluminum disks using a silicone spray (Silko Spray). This was done in order to minimize the thermal gradient across the sample and to ensure that there was a good thermal contact between the sample and the disks.

3.1 (b) Sample Selection:

It was necessary to select only those samples in which the TL signal was found to be stable. In this context the signal was stable if there was no change in either the intensity of the signal or the shape of the glow curve when repeated measurements were made at the same heating rate. In order to ensure that the TL signal produced by these quartz samples was stable the following experiment was performed on each quartz sample:

(i) Each of the quartz samples was given a beta dose of 1 to 50 Gy (depending on the intensity of the signal they produced) using the inbuilt source in the Risø system (dose rate = 0.0936 Gy/sec).

(ii) The samples were then held at room temperature for 300 sec in order to ensure that the phosphorescence was not measured.

(iii) A TL measurement was then performed at a heating rate of 3 $K.s^{-1}$ from room temperature to 723 K (450 °C).

These three steps were performed repeatedly on the samples until the signal obtained became stable. Only those samples that had very stable signals and more than one strong peak in their signal were chosen. The Arkansas rock crystal quartz sample and the Danish QQ-974703 quartz sample were found to have both these characteristics. An example of the glow curves recorded for such an experiment on the Arkansas quartz sample is shown in Fig 3.1. Curve 1 in the Fig is the first measurement that was performed on the sample. The intensity of signal in this curve is larger than the second curve. Curve 2 was measured next, and it can be seen that the glow curve retains its shape but decreases in intensity. This decrease in intensity from curve 1 to curve 2 indicates a change in sensitivity. Repeated measurements on this sample yielded curve 2 without any change in

either the intensity or the shape. Thus this sample was found to be very stable. Some of the samples that were measured in this way did not yield stable signals and thus were not used in the experiments.

Notation:

It is necessary here to explain notation that will be used in referring to the different TL peaks and the traps that give rise to these peaks in the measured glow curves. Quartz, in the UV emission region has 3 main traps, the '110°C' trap, the '220°C' trap and the '325°C' trap. These traps give raise to the three main TL peaks in a TL measurement performed at a heating rate of 10K/s. Though in a TL experiment the peak centers of these peaks change with heating rate, these TL peaks and the traps that give rise to them are referred to by the peak center position. This notation is widely used in the scientific community, and thus it is being used in this thesis for easy reference.

3.2 Filters:

The thermoluminescence, radioluminescence experiments were performed in two different emission wavelength regions, UV and Blue. The optically stimulated luminescence experiment was performed only in the UV emission region. The filters used for measuring the signal in these regions were: (i) 2.54 mm thick U-340 filter with a peak maximum at 340 nm and a bandwidth (full-width-half-maximum) of 30 nm. (ii) Corion P10-450 filter centered at 450 nm with a bandwidth of 40 nm. The transmission spectra of the filters are shown in Fig 3.2 (a) and (b).

Fig 3.1 Glow curves of Arkansas quartz sample from stability tests:

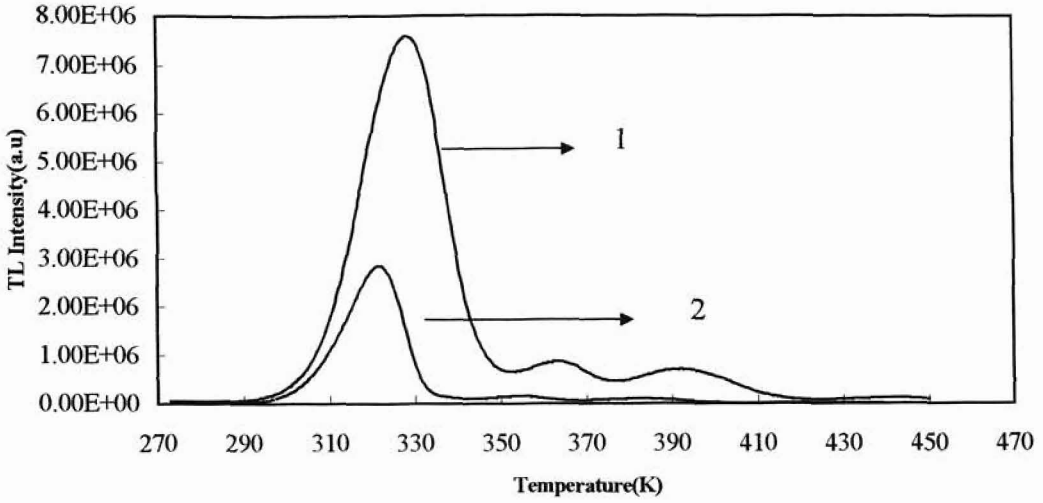

Fig 3.2 (a) Transmission spectra of the U-340nm filter:

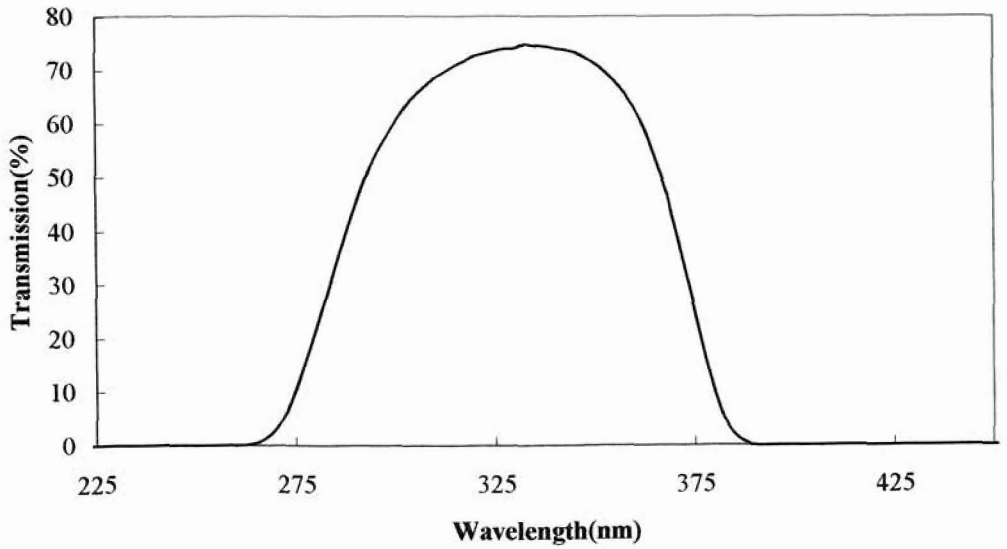

Fig 3.2 (b) Transmission spectra of Blue Corion-P10-450nm filter:

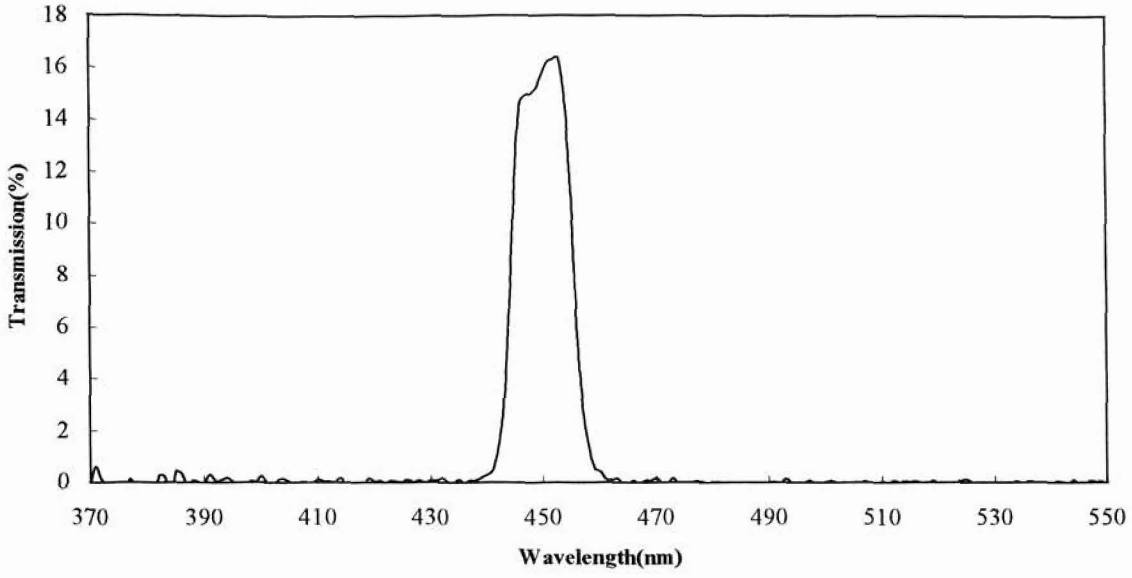

3.3 Apparatus and Procedures:

The Risø System:

The Risø TL/OSL DA-15 system was used for making TL as well as the OSL measurements. A brief description of the system is provided as follows [12]:

The automated Risø TL reader was first introduced almost 15 years ago. A mini computer "Mini-Sys" controls the latest version of the reader. All direct hardware control has been incorporated into this mini computer. Control software for creating, editing and executing TL/OSL sequences for both DOS and Windows are provided. The system also has a Sr-90/Y-90 beta irradiator attachment. They come equipped with IR laser diodes, and an array of LEDs.

The dosimetry laboratory here at Oklahoma State University is equipped with two Risø readers. One of them is equipped with an array of blue LEDs, which can provide stimulation light of 470nm with a bandwidth of 20nm, and an IR laser diode, which can provide a stimulation light of 830nm with a bandwidth of 30nm. The other system is equipped with a halogen lamp, IR laser diodes and an array of green LEDs as stimulation sources. The lamp with appropriate filters can provide a stimulation band from 420-550nm. The IR laser diodes can provide stimulation light of 870nm with a bandwidth of 25nm and the green LED can provide stimulation light of 520nm with a bandwidth of 30nm. The dose rate of the beta sources in each reader is 0.12Gy/sec and 0.0936 Gy/sec, respectively.

The Risø system is an extremely user-friendly device and is used world wide in TL and OSL dating, retrospective dosimetry, environmental dosimetry and material characterization.

3.3(a) Thermoluminescence:

The TL experiments were performed on both the Arkansas quartz sample and the Danish QQ-974703 quartz sample. TL experiments were performed in both the UV emission region and the Blue emission region on the samples. Each sequence in a TL experiment consisted of the following three steps:

(i) Beta dose of 1Gy.

(ii) Pause of 300 s at room temperature.

(iii) TL measurement performed at different heating rates from room temperature to 450°C (723 K). The exception being the measurement of the Danish quartz sample in the

blue emission region. The Danish quartz sample in the blue emission region has a high temperature peak centered around 450°C, thus the TL measurement was performed from room temperature to 650°C (923K).

The sequence was repeated for heating rates from 0.01 $K.s^{-1}$ to 9 $K.s^{-1}$. Glow curves were thus recorded for both the samples in the two emission wavelength regions.

3.3(b) Optically Stimulated Luminescence:

The OSL experiments were performed on the samples only in the UV emission region. In order to perform the OSL experiments it was necessary that the wavelength region of the emission from the sample did not overlap with the wavelength region of the stimulation light. This was not possible to achieve in the blue emission region.

Fig 3.3 Emission spectra of the Blue LED's in the Risø system:

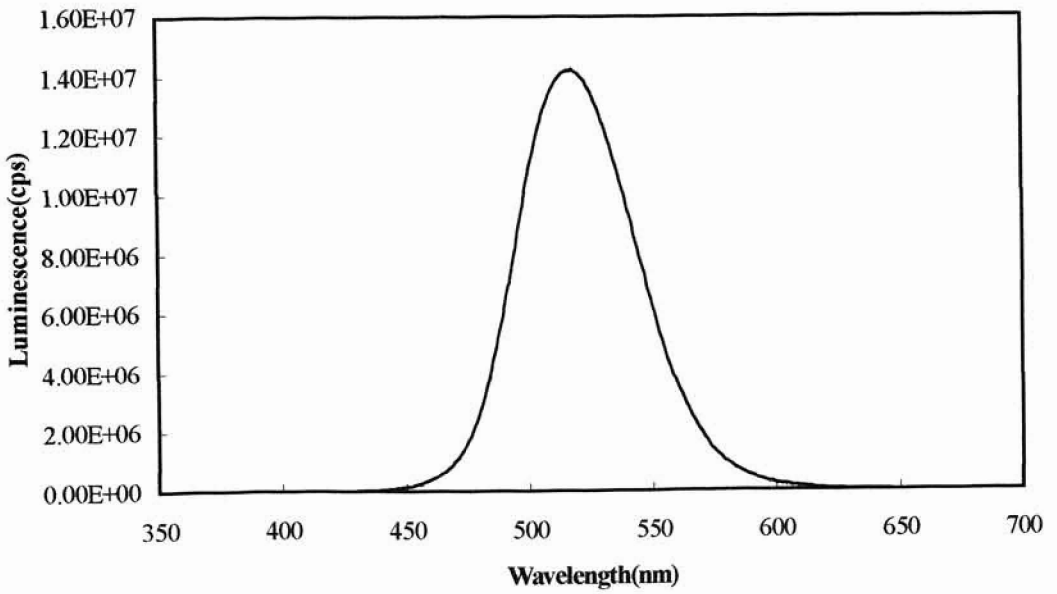

As shown in Fig 3.3 the emission spectra of the green LEDs in the Risø system is in the 450nm to 600nm region and the blue filter (Fig 3.2(b)) is centered at 450nm.

Thus, as the excitation and emission regions overlap luminescence in the blue emission region could not be measured. The possibility of using the halogen lamp with appropriate filters was explored but resulted in the same problems as with the green LEDs. The IR laser diode could not be used for this purpose because quartz material does not respond to excitation by IR light [13]. Thus the OSL experiments were performed only in the UV emission region for the quartz sample.

OSL experiments were performed for different sample temperatures for both the heating and cooling cycles. Each sequence in an OSL experiment had the following 6 steps:

(i) Beta dose of 1 Gy.

(ii) Pause of 300 s at room temperature.

(iii) Apply pre-heat of 260°C at 5K/s and hold for 10s.

(v) Heat (or cool) to specific sample temperatures at 5K/s.

(iv) OSL measurement performed by stimulating with Blue LED's for an illumination time of 40s.

OSL measurements were performed for different sample temperatures at 20-degree intervals starting from 30°C (303 K) to 250 °C (523 K) for the heating cycle and from 523 K to 303 K for the cooling cycle.

Many researchers have verified that the OSL signal from natural quartz samples is primarily due to the 325°C trap [23, 33-34]. Thus, the OSL experiments are performed only by stimulating the '325 °C' trap. This is done by applying suitable preheats to empty out the charge from the other traps. It is necessary to empty the other two traps because

the signal from the 220°C trap is known to be optically inactive i.e. it does not respond to stimulation and that from the 110°C trap is only partially optically active [1,23]. Moreover the lifetime of the charge trapped at the 110°C trap is very short. In order to identify appropriate preheat necessary to isolate the signal from the 325°C trap, TL experiments can be performed and by applying different preheats after irradiating the sample and measuring the TL glow curve, appropriate preheat can be determined.

Fig 3.4 shows the test TL experiments performed on the Arkansas quartz sample to find the appropriate preheat. In these experiments TL sequences were performed on the sample in which different preheats were used. In Fig 3.4 the curves shown are numbered 1, 2, 3, 4, and 5 for preheat of 180°C, 200°C, 220°C, 240°C, and 260°C respectively. For curve 1 i.e. for preheat of 180°C, three peaks can be seen clearly. As preheat is increased the first two peaks are removed. In case of preheat of 220°C, peak 1 is removed partially but is still much stronger than the 325°C peak.

Fig 3.4 Effect of different preheats on the Arkansas quartz sample:

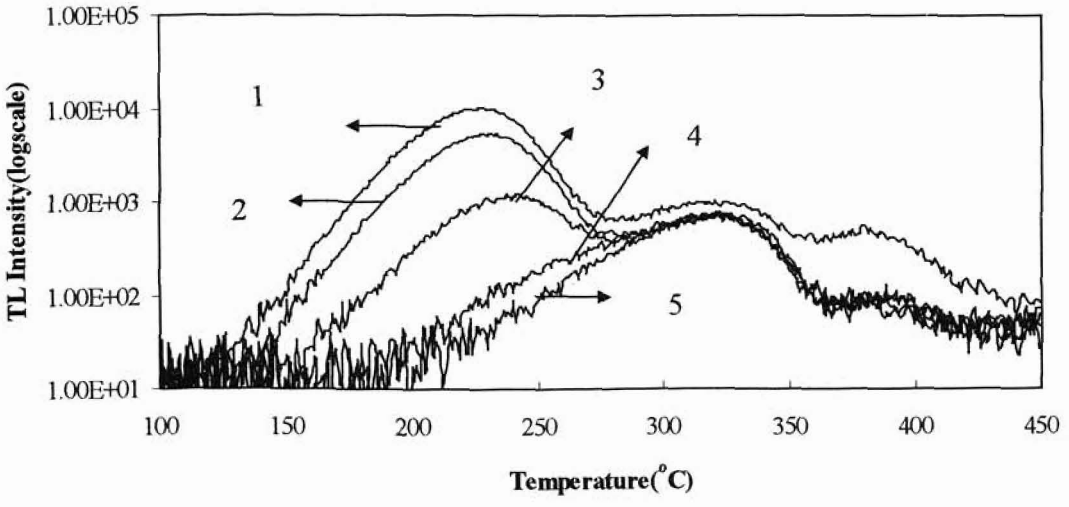

At preheat of 200°C, the intensity of the 220°C peak has gone down further, and at 220°C preheat the two peaks, i.e. the 220°C peak and the 325°C peak have nearly the same intensity. Curves 4 and 5 i.e. for preheats of 240°C and 260°C, the 220°C peak has been removed. But curve 4 shows a small hump, which is due to some signal from the 220°C peak. Thus preheat of 260°C was chosen. Similar experiment was performed for the Danish quartz sample and a preheat of 260°C was chosen. OSL experiments were then performed on the two samples and decay curves were recorded in the UV emission region.

3.3 (c) Radioluminescence:

Fig 3.5 shows the cross sectional view of the experimental arrangement used for making the RL measurements. The sample is placed on a nickel sample holder embedded in ceramic. The ceramic is attached to the lead shielding with glass spacers. The fiber optic cable is made of silica and has a diameter of 400μm and a length of 1m. The cable is connected to the PMT (photo-multiplier tube). The beta source provides a dose rate of 0.0453 Gy/sec. The pencil heater and the thermocouple are inserted into the nickel holder and connected to the temperature controller on the other end. The temperature controller sets the temperature of the sample for the RL measurement. The temperature of the sample is varied from room temperature to 300°C.

The RL experiments were performed in both the UV and the Blue emission regions. They were also performed in both the heating and cooling cycles. Each sequence in the experiments consisted of the following steps:

(i) Set sample temperature.

(ii) Record background counts for 50 s.

(iii) Open the shutter of the beta-source and record signal for 100 s.

(iv) Close the shutter of the source and record background for 50s.

The sample temperature was varied from room temperature to 300 °C for the heating cycle and from 300°C to room temperature for the cooling cycle.

Fig 3.5 Cross-sectional view of the radioluminescence experimental setup:

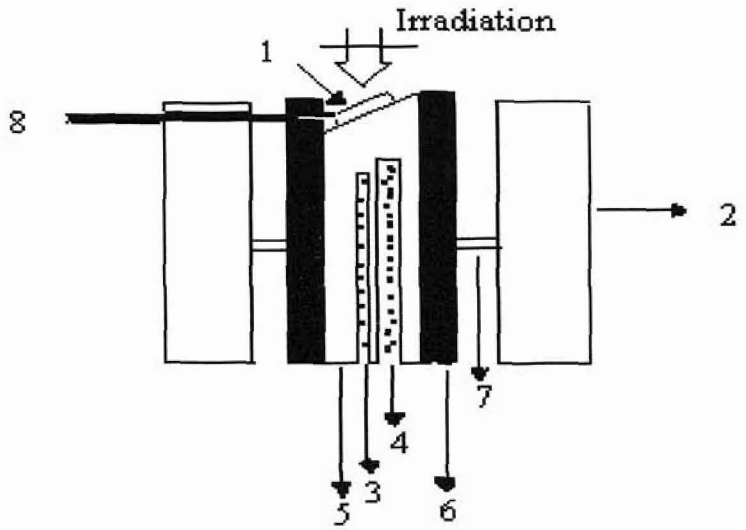

1.Sample, 2.Lead holder, 3.Thermocouple, 4.Heater cartridge, 5.Nickel holder, 6.Ceramic insulator, 7.Glass spacers, 8.Fiber optic cable.

3.4 TL Spectral Emission Measurements:

TL spectral measurements were performed on both the Arkansas quartz and the Danish quartz samples. The spectroflurometer was used for this purpose. A brief description of the system is provided as follows.

Spectrofluorometer: The Jobin-Yvon Flurolog-3 spectroflurometer mainly consists of optical components, a personal computer and software for Windows, which drives the hardware. This system is widely used for florometry, phosphorimetry and other luminescence measurements. It has the following attributes.

A source of light, which filtered by an excitation monochromator, allows a single wavelength of light to reach the sample. The resulting radiation is filtered by an emission monochromator that feeds the signal to a photomultiplier detector. By stepping either or both monochromators through a wavelength region and recording the variation in intensity as a function of wavelength, a spectrum can be produced. For measuring the TL spectra, however, only the source was kept off and the TL emission was analyzed through the emission monochromator.

Measurements: In order to take the TL spectral measurements, the sample was kept on a sample holder to which two pencil heaters and a thermocouple was connected. A temperature controller was used for changing the sample temperature. The samples were given a high beta dose of 225 Gy with a beta source having a dose rate of 0.188 Gy/sec. Then the TL emission spectrum was recorded during the heating of the sample using the spectroflurometer, for the emission wavelength region between 220nm to 800nm at 5nm intervals. The temperature of the sample was raised at a heating rate of 1 $K.s^{-1}$.

Chapter 4

Results, Analysis and Discussion

4.1 Results Obtained in TL Experiments:

The glow curves obtained for the Arkansas quartz sample and the Danish quartz sample in the two emission regions of UV and Blue are shown in Fig 4.1 and Fig 4.2. The heating rates vary from 0.01K/sec to 9K/sec. A representative set of curves is shown for each sample in the two emission regions, although a complete data set was obtained for the full range of heating rates.

Fig 4.1(a) Glow curves of Arkansas quartz sample in the UV emission region:

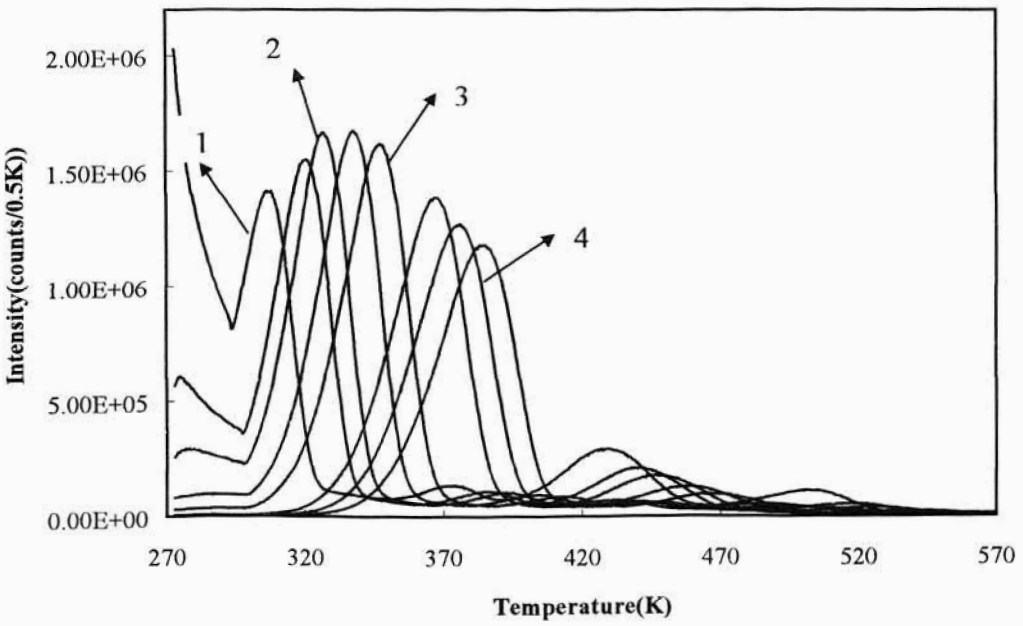

Fig 4.1(b) Glow curves of the Arkansas quartz sample in the Blue emission region:

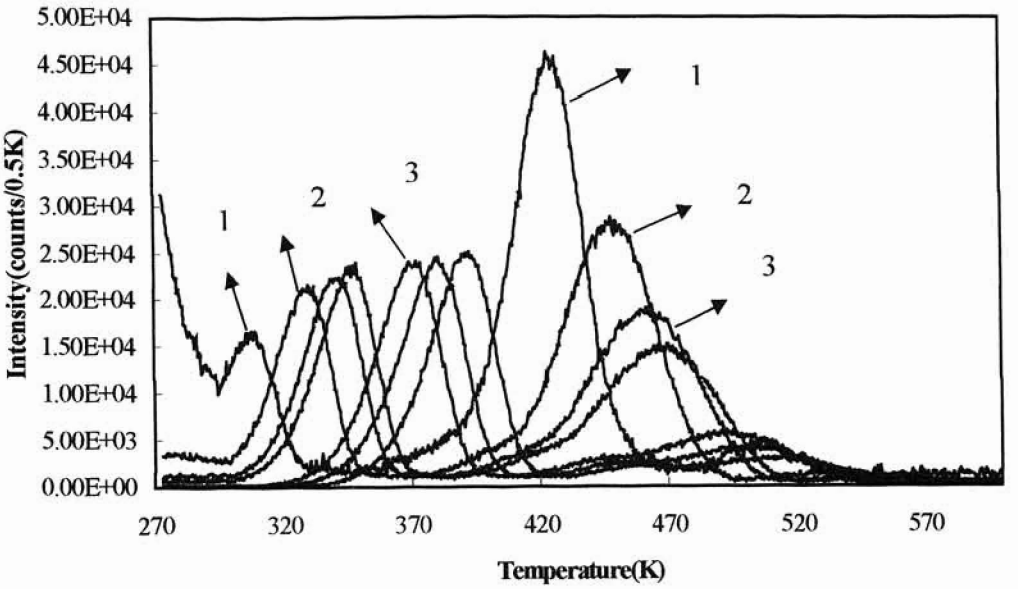

Fig 4.2(a) Glow curves of the Danish QQ-974703 quartz sample in the UV emission region:

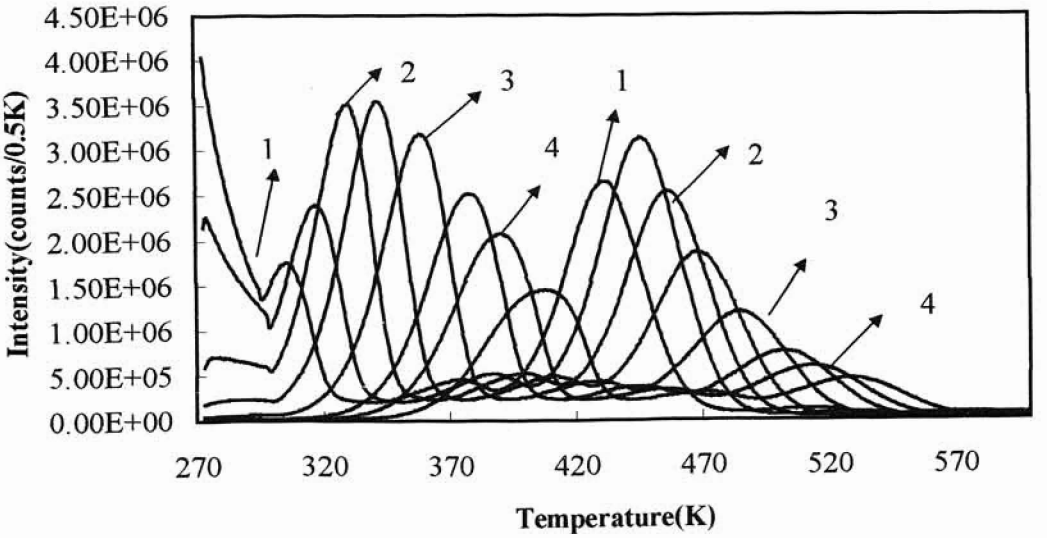

Fig 4.2(b) Glow curves of the Danish QQ-974703 quartz sample in the Blue emission region:

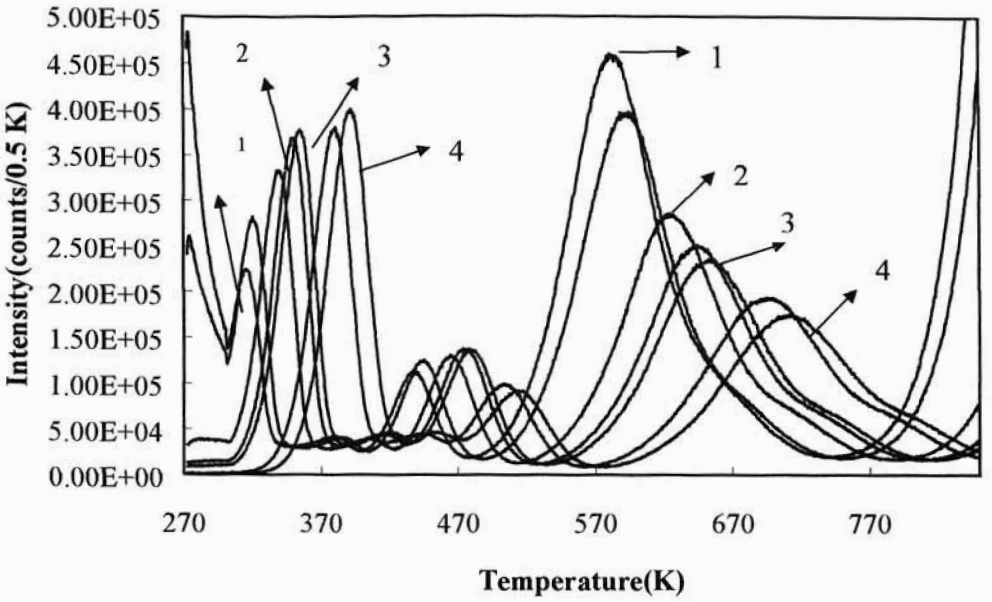

4.2 Discussion:

Arkansas Quartz sample: UV emission

Fig 4.1(a) depicts the glow curves obtained for the Arkansas quartz sample in the UV emission region. TL measurements ranging from 0.01 K/s to 9 K/s were obtained. In the figure curve 1 is heating rate 0.01K/s, curve 2 is 0.1 K/s, curve 3 is 1 K/s and curve 4 is 9 K/s. In this emission region the sample has three main peaks. For a heating rate of 1 K/s the peak positions are 420 K (the '110 °C' peak), 500 K (the '220 °C' peak) and 600 K (the '325 °C' peak). It can be seen from the graphs that as the heating rate increases the glow curves shift to higher peak temperatures. It can be seen that peak 1 occurs around 350 K for the lowest heating rate and for the highest heating rate of 9 K/s it occurs around

480 K. Thus the shift to higher temperatures with heating rates is in accordance with theory.

It can be observed from the graph that for peak 1 the peak intensity increases for the first few heating rates. This increase in the peak intensity at low heating rates is not related to thermal quenching. This effect is because of the 'dead time' effect of the delay time effect in the Risø system. In the system, though the electronic ramp stars at 0°C, the actual temperature of the sample is not increased until the electronic temperature T_e equals the actual temperature T_a. Length of the dead time is governed by the heating rate. Slower the heating rate, longer is the dead time, and higher the heating rate, shorter the dead time. Thus, at lower heating rates, fading of the signal occurs. Thus the increase in intensity at low heating rates can be seen.

At higher heating rates, however, a decrease in the intensity of the signal can be observed. This is especially true for the higher temperature peaks and is due to thermal quenching. At higher heating rates, the peaks do not appear until high temperatures, at which the probability of non-radiative transitions increases during recombination as compared to the probability of radiative transition. This results in a decrease of the luminescence efficiency, and therefore a decrease in the TL intensity.

Arkansas Quartz sample: Blue emission

Arkansas quartz emission in the Blue region is shown in Fig 4.1 (b). Glow curves for heating rates 0.01 K/s, 0.03 K/s, and 5 K/s are numbered 1, 2, and 3 respectively. Again the shift of the peak centers to higher temperatures as the heating rate increases can be observed. An increase in the luminescence intensity at low heating rates for peak 1 can be

seen in the Fig., and this is again due to the thermal fading of the signal as discussed for the UV emission region of the Arkansas quartz sample. It can also be seen that even at the highest heating rate shown, i.e. 9 K/s thermal quenching cannot be observed in peak 1. In case of peak 2, however the opposite can be observed. Thermal fading is not observed even at the lowest heating rate of 0.01 K/s, but thermal quenching of peak 2 can be clearly seen in all the heating rates shown starting from 0.01 K/s to 9 K/s. Since the Risø system is optimized for heating rates between 0.01 k/s and 9 K/s, measurements outside this range could be not taken.

Danish QQ-974703 quartz sample: UV emission region

The TL glow curves for the Danish quartz sample in the UV emission region are shown in Fig 4.2(a). Glow curves of heating rates of 0.01 K/s, 0.1 K/s, 0.7 K/s, and 5 K/s are numbered 1, 2, 3, and 4 respectively. As with the Arkansas quartz sample, here too the observation that the position of the peak center is dependent upon the heating rate can be made. It can be seen that in this emission region, the two main peaks 1 and 2 both exhibit thermal fading at low heating rates as well as thermal quenching at high heating rates. From heating rate 0.01 K/s to 0.1 K/s thermal fading can be observed in peak 1. In the case of peak 2 however, thermal fading can be observed in only the lowest heating rate of 0.01 K/s. From 0.5 K/s thermal quenching can be observed in peak 1. Thus for this sample it was possible to go down to low enough heating rates to observe thermal fading in both the peaks and it was also possible to go to high enough heating rates to observe thermal quenching in both the peaks.

Danish QQ-974703 quartz sample: Blue emission

The TL glow curves obtained for the Danish quartz sample in the blue emission region are depicted in Fig 4.2 (b). In this emission region the Danish sample has a peak centered around 670 K (400 °C) for the lowest heating rate. As the heating rate is increased to 7 K/s, the peak temperature shifts to 770 K (500 °C). Thus it was necessary to make the TL measurement from room temperature to 923 K (650°C). The glow curves with heating rates of 0.03 K/s, 0.3 K/s, 1K/s, and 9 K/s are numbered, 1, 2, 3, and 4 respectively. It can be seen from the figure that beyond 770 K, an increasing signal can be seen partially. This signal is not a TL peak but is incandescence, or black body radiation emitted from the sample or the holder, or both at very high temperatures. It does not take the form of a peak but follows approximately the Stephan- Boltzmann law ($\propto T^4$). Incandescence is not heating rate dependent but is a constant irrespective of the heating rate. The intensity in the TL glow curves shown above is measured as 'counts/0.5 K'. If this intensity is plotted as 'counts/sec' against Temperature then the portion of the glow curve beyond 800 K can be seen to be independent of the heating rate. This is shown in Fig 4.3. The curves numbered 1, 2, 3, and 4 are the highest heating rates of 9 K/s, 7 K/s, 5 K/s, and 3 K/s. These four curves appear to be shifted from the others. This shifting is not in intensity but is due to the shift of the TL peaks to high temperatures at high heating rates. At very high heating rates the high temperature peak centered at 800 K moves into the temperature region wherein the incandescence is being emitted. Thus the high heating rates appear shifted from the lower heating rates.

It can be seen from Fig 4.2(b) that there are 4 main peaks in this emission region. As before the peaks shift to higher temperatures as the heating rate is increased. The lowest

temperature peak, peak 1 exhibits the increase in luminescence intensity due to thermal instability. However at high heating rates it does not exhibit thermal quenching. Peak 2 exhibits the increase in intensity at low heating rates as well as thermal quenching at high heating rates. Peak 3 and peak 4 are not distinctly separate but overlap each other at all the heating rates. They both exhibit thermal quenching.

Fig 4.3 Luminescence intensity (counts/sec) of Danish quartz sample in Blue emission region:

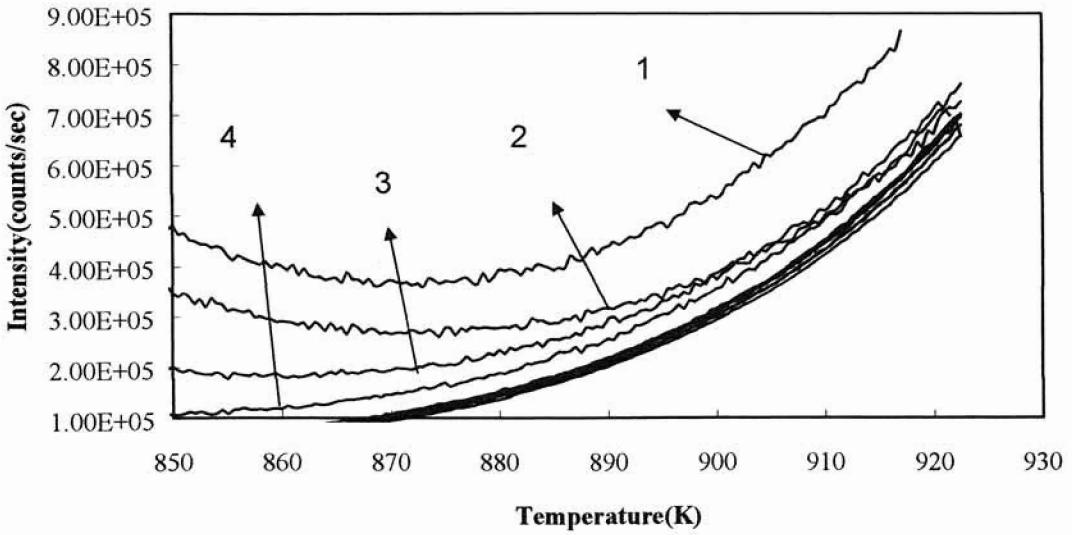

4.3 Analysis of TL Experimental Data:

The analysis of the TL data performed in order to find the luminescence efficiency curve for each of the samples in the two emission regions of UV and Blue is discussed in the following sections.

4.3(a) Summary of Theory:

A brief summary of the theory and equations necessary for the analysis of the TL data (for a detailed explanation, see Ch 2) is given below.

Thermal quenching in quartz was first described by Ann Wintle [5], wherein she monitored RL as a function of temperature. She measured the RL signal in different wavelength emission regions. The dependence of luminescence efficiency η as a function of temperature T was given by a function of the type:

$$\eta = \frac{1}{1 + C\exp(-E/kT)} \tag{4.1}$$

where E is the thermal activation energy (eV) for luminescence quenching, and C is a constant; k is the Boltzmann's constant ($eV.K^{-1}$) and T, the temperature is in Kelvin.

In order to perform the analysis, the known principle that the temperature of a TL peak shifts to higher values as the heating rate increases, is used. Thus, at low heating rates the TL peak may appear in a temperature range were thermal quenching is minimal, whereas at higher heating rates the peak temperature may be such that thermal quenching is strong. Data to this effect has been shown in Fig 4.1 and Fig 4.2. By monitoring the peak areas as a function of the peak position for different heating rates, the thermal quenching curve (cf.Ch2.Section 2.2) can be obtained. This may be understood from an examination of the equations describing the variation of the TL intensity I_{TL} with time t during trap emptying. I_{TL} is proportional to the rate of decrease of recombination centers n_h, and thus we may write:

$$I_{TL}(t) = \eta \frac{dn_h}{dt} \tag{4.2}$$

The integral under the glow peak with respect to time is:

$$\int_0^\infty I_{TL}(t)dt = \frac{1}{\beta}\int_0^\infty I_{TL}(T)dT = \eta * n_{h0} \tag{4.3}$$

where n_{ho} is the initial concentration of trapped holes, and $\beta = dT/dt$ is the heating rate. If the proportionality constant η (*i.e.* the efficiency) is constant and independent of temperature, then the obtained integral $\int_0^\infty I_{TL}(t)dt$ should be independent of β. Conversely, if η is itself a function of temperature (*e.g.* Eq. (4.1)), then the obtained integral will also be the same function of temperature (as defined by the peak position).

One should note that the above analysis relies upon a fixed temperature range over which thermal quenching is observed. With the Schön-Klassens model, however, the thermal emission of holes from the recombination site will also shift to higher temperatures with heating rate since this process is governed by the same thermally activated kinetics that control the thermal emission of electrons from the trapping site. Effectively, this means that the obtained TL versus peak temperature curve will not follow the simple relationship defined in Eq. (4.1). In contrast, the Mott-Seitz model predicts a shape and form for η which is independent of heating rate. Thus, analysis of thermal quenching in this described manner should reveal which model is most descriptive of the thermal quenching process.

Furthermore, by monitoring the TL at fixed wavelengths, or in narrow wavelength bands, one can follow the thermal quenching characteristics as a function of the wavelength of the luminescence.

4.3(b) Analysis and Fitting of Glow Curves:

Having obtained TL data, it is now necessary to deconvolute the glow curves to extract the individual peak intensity and follow their behavior as a function of the heating rate. The most popular procedure is to either assume a kinetic order or to allow the kinetic order to vary as a free parameter. In this analysis first-order kinetics was assumed and the Randall-Wilkins first order equation with Keating's approximation was used with E (activation energy), s (frequency factor) and n_o (initial concentration) as fitting parameters (cf. Ch. 2. Eq2.28). As discussed in Ch.2 the Randall-Wilkins equation assumes no interaction between the trapping centers. It generates asymmetrical peaks with peak position depending upon frequency factor, activation energy and heating rate [7,8].

The method that was used in the analysis of the glow curves is referred to as the whole curve analysis. The analysis takes into account the whole of the glow curve rather than a single peak in it. It is based on separating a glow curve into its constituent peaks, and analyzing the individual peaks to obtain their areas as a function of their peak positions. Previous methods to isolate individual TL peak [14] have only been able to analyze one TL peak from the glow curve (the "325°C" peak) in order to extract data on thermal quenching. In the present case, however, several TL peaks were used. In order to analyze the glow curves, 'Peak Fit' software was used. It uses a method called the Marquardt-Levenberg's non-linear method of least square fitting. Since the glow curves in the obtained data contained overlapping peaks, the analysis proceeded with a simple superposition of these peaks. Each of the 3 variable parameters for each peak within a glow curve was independently varied until a 'best fit' was obtained. The 'best fit' is usually recognized as the minimization of an error function between the experimental

data and the linear superposition of the assumed functions. Convergence to a minimum of this function is taken as an indication of the 'best fit'. An example of the 'best fit' for one of the glow curves in the Arkansas quartz sample in the UV emission region is shown in Fig 4.4. The Fig shows the actual glow curve (1), the fit of the individual peak (2) and the 'best fit' of the whole curve.

Deconvolution of the glow curve was performed to separate a glow curve into its constituent peaks and the area of each peak was determined as a function of its peak position. In order do so, the individual peaks in these glow curves were fitted with peaks whose areas could be calculated by the software. For peaks in the temperature range where quenching is weak, the curve for fitting was generated by the Randall-Wilkins first-order equation with the Keating approximation. The Randall-Wilkins first order equation with the Keating's approximation is given as:

$$I_{RWK} = n_o * s * \exp\left(\frac{-E}{kT}\right) * \exp\left[\left(\frac{-s}{\beta}\right) * \left(\frac{kT^2}{E}\right) * \left(1 - \frac{3kT}{E}\right) * \exp\left(\frac{-E}{kT}\right)\right] \qquad (4.4)$$

where E is the activation energy, n_o is the initial concentration, and s is the frequency factor. T and k have the usual definitions of the temperature and the Boltzmann's constant.

For temperatures over which quenching is significant, however, the Randall-Wilkins peak shape is inappropriate since the quenching process distorts the first-order peak shape. Thus, since the purpose of curve fitting was only to find the area under each thermally quenched peak, Gaussian peak shapes were used for the higher temperature peaks. The error induced by this approximation is thought not to adversely affect the analysis, but the use of Gaussian line shapes greatly speeds up the glow curve deconvolution.

Peak 1 has been fitted with a peak generated from the Randall-Wilkins equation with the Keating's approximation and all the other peaks have been fitted with Gaussian peaks. The software also provides a table of peak areas and their peak center positions for the 'best fit' of each glow curve. A plot of the peak areas against their peak position yields the quenching curve for the sample in the specific emission region.

Fig 4.4 A Peak Fit example for the Arkansas quartz sample: Squares: Experimental glow curve, Dots: Individual peak fits, Solid Line: 'Best fit' (curve fit).

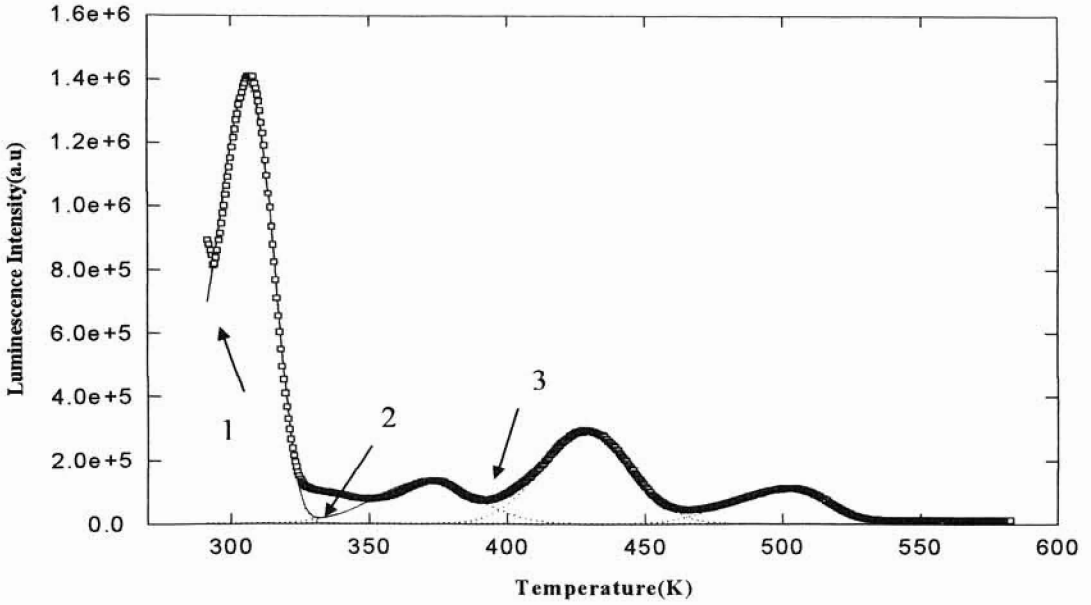

It is important to note here that luminescence emission from quartz in the UV emission region has been reported in literature to shift to longer wavelengths with increasing temperature [16,17]. Since, measurements of luminescence emission (RL, OSL or TL) are made with optical filters of fixed wavelength and bandwidth, a shift of the emission wavelength with temperature may need to be accounted for, if correct analysis of the

thermal quenching parameters is to be achieved. This subject is discussed in further detail in later sections.

4.3 (c) Thermal Quenching Curves:

Thus, once the peak intensities were determined as a function of their peak centers for each of the samples in the two emission regions, the quenching curve was obtained by plotting the peak intensities, as a function of the peak temperature. Quenching curves obtained for each of the samples in the two emission regions are shown in Fig 4.5(a), 4.5(b), 4.6(a) and 4.6(b).

In each graph, the different peaks are shown by a different symbol. The data points having the same symbol are a specific peak at different heating rates. For example, in Fig 4.5(a) the circles are all the same peak, but each circle is from a different heating rate. The lowest temperature data point being the lowest heating rate and the highest temperature data point being the highest heating rate. The plots of peak intensities as functions of peak temperature do not yield smooth quenching curves. The reason as discussed before, is that, it is not possible to go down to low enough heating rates for the high temperature peaks to show the unquenched intensities. At the same time it is not possible to go to high enough heating rates for the low temperature peaks to show the quenched intensities.

Fig 4.5(a) Quenching curve: Arkansas quartz UV emission

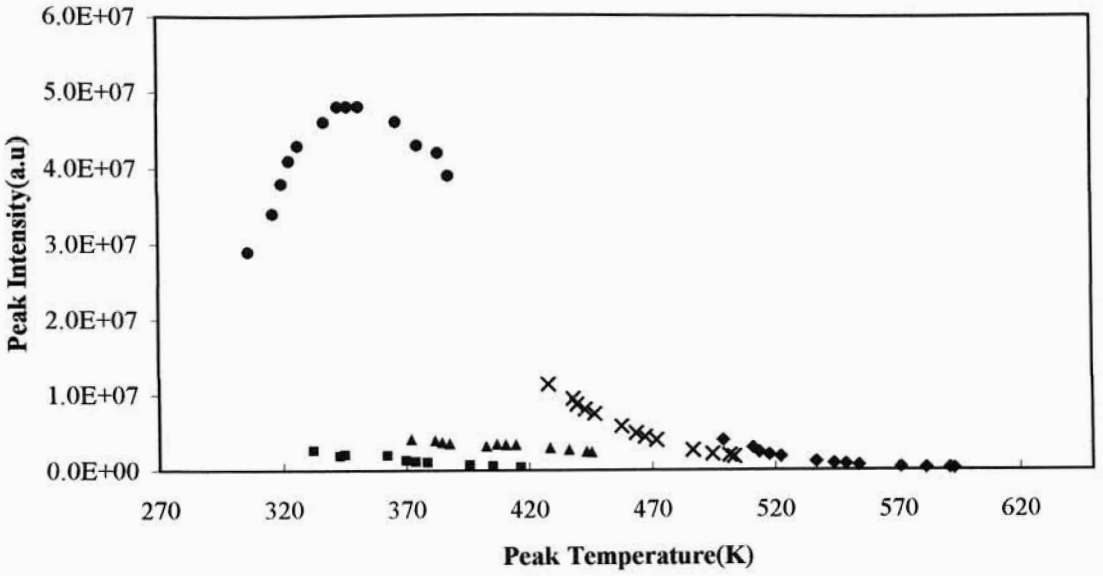

Fig 4.5(b) Quenching curve: Arkansas quartz Blue emission

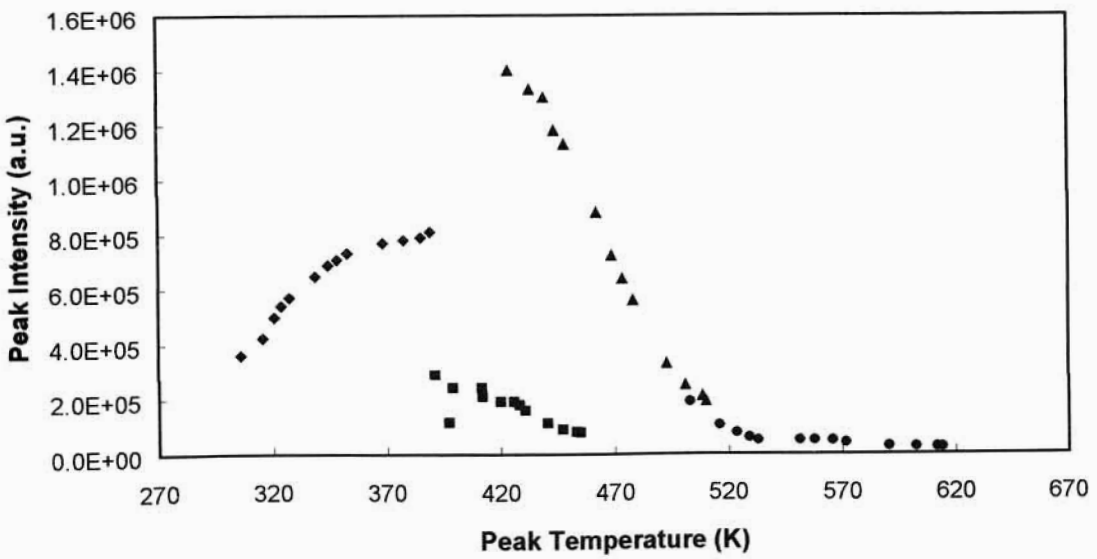

Fig 4.6(a) Quenching curve: Danish quartz UV emission

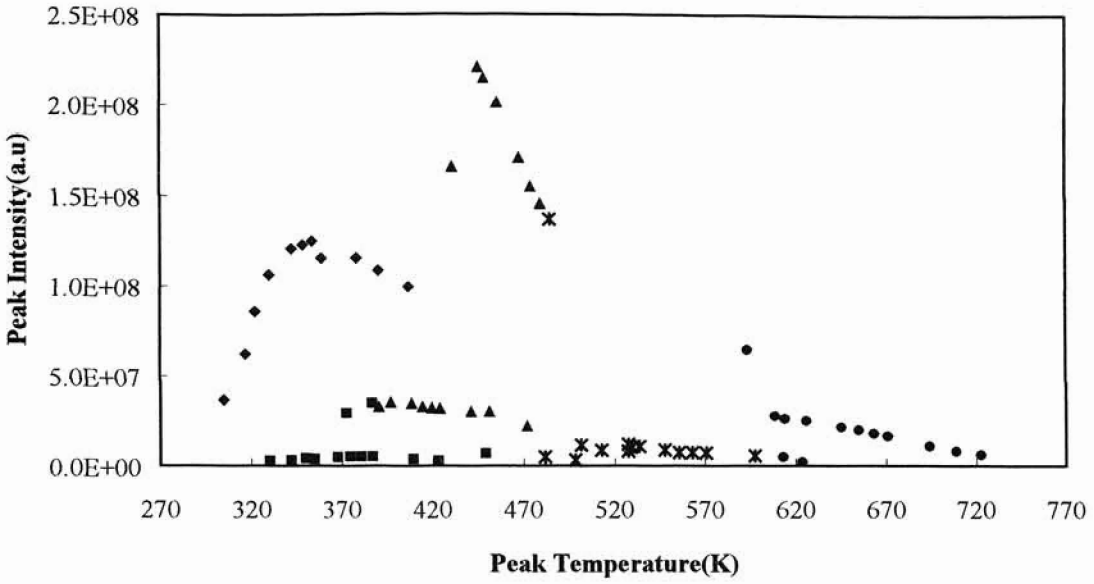

Fig 4.6(b) Quenching curve: Danish quartz Blue emission

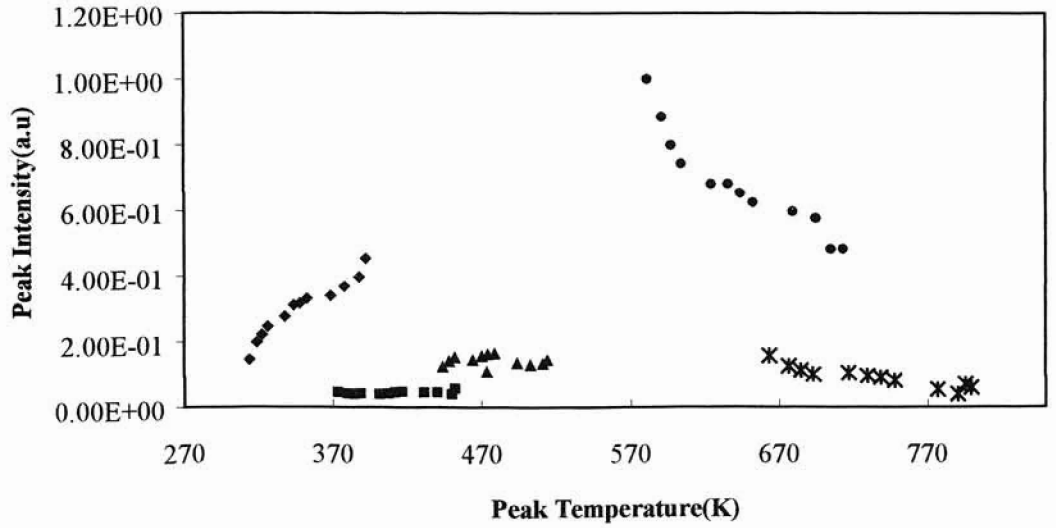

In order to solve this problem and to obtain smooth quenching curves, a scaling procedure was utilized. However, this procedure is somewhat arbitrary and relies to some extent on judgement, for accuracy. Thus the resulting curves may not be very dependable. An illustration of how this was performed is given below for the Arkansas quartz sample in the UV emission region (Fig 4.7(a)). For the Blue emission region of the Arkansas quartz sample and for the Danish quartz sample (both the emission regions) the scaled data has been displayed in Fig 4.7(b), Fig 4.8(a) and Fig 4.8(b).

The 'raw data' i.e. the unscaled data are displayed as filled symbols and the open circles are the scaled data points. The arrows indicate the scaling that was performed on each set of peaks to get the smooth quenching curve. Similarly scaling procedures were used on the other sample in both the emission regions to obtain smooth quenching curves.

Fig 4.7(a) Scaling Procedure for Arkansas Quartz Sample in the UV Emission Region:

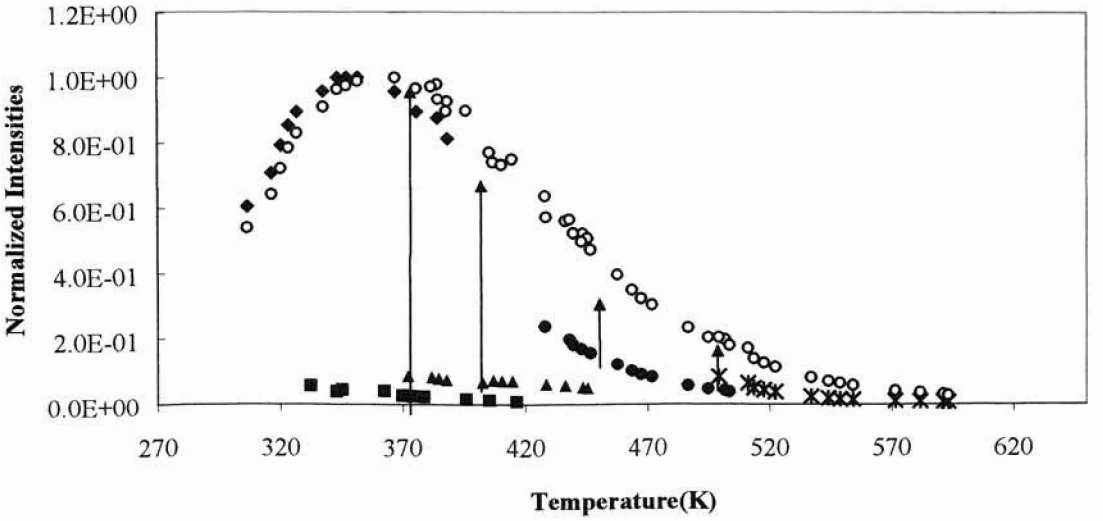

Fig 4.7(b) Scaled data for Arkansas quartz sample in the Blue emission region:

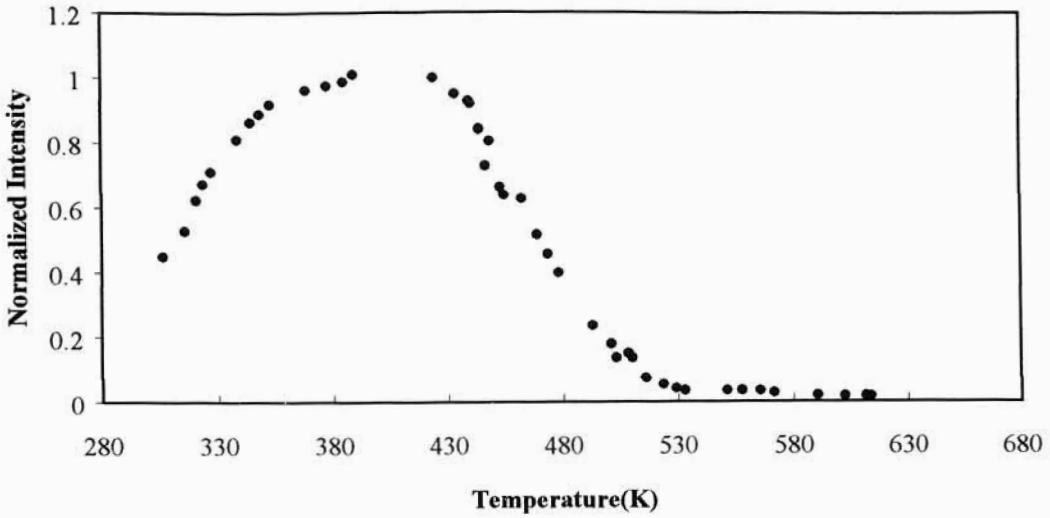

Fig 4.8(a) Scaled data for Danish quartz sample in the UV emission region:

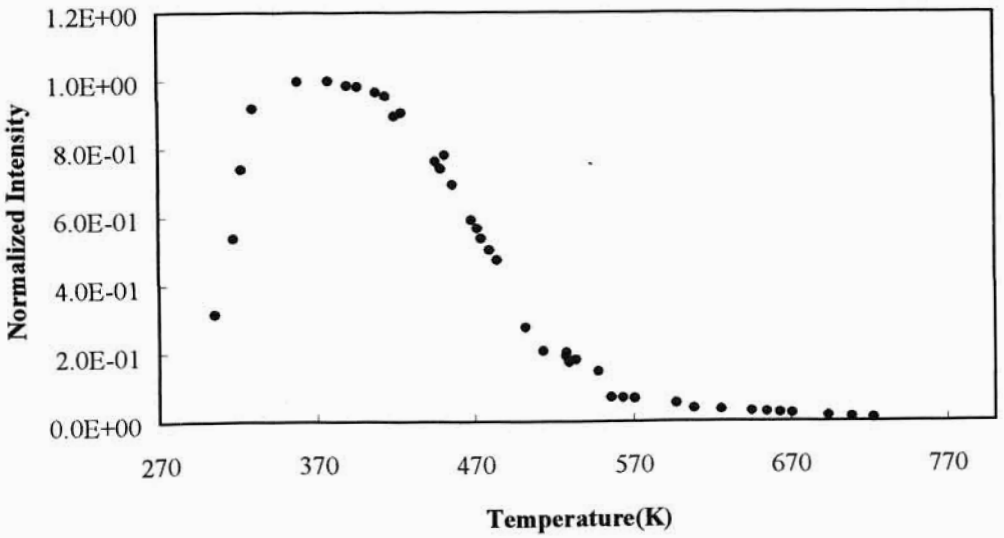

Fig 4.8(b) Scaled data for Danish quartz sample in the Blue emission region:

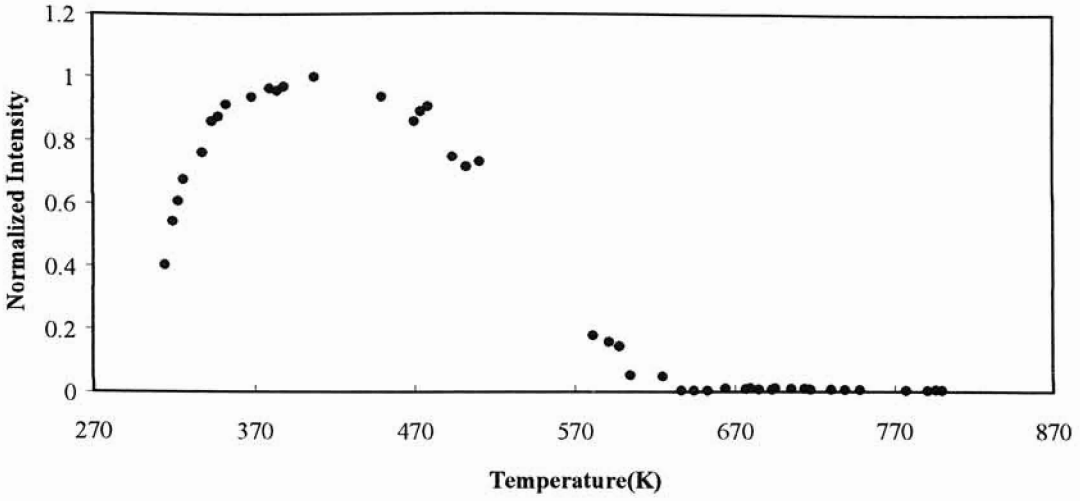

4.3(d) Emission Shift of Luminescence:

The TL measurements made in the UV emission region were with a UV-340 nm filter with a peak maximum at 340nm and a band width of 40nm.This filter falls in the wavelength region which is claimed to shift to higher emission wavelengths with increasing temperature [16,17]. The shift of the TL peak across wavelength with the increase in temperature is 22°C/360nm, 100°C/375nm, 175°C/392nm, 225°C/410nm, and at 325°C/430nm. If true, this is a significant shift in emission region, and with a fixed emission window this causes a decrease in the intensity of the signal unrelated to thermal quenching. The following procedure can be used to correct for this effect.

A convolution of the transmission spectra of the filter (cf.Ch.3.Fig 3.1(a)) and the spectral response of the photo multiplier tube (model –133 Bialkali with quartz window) in the Risø system was performed to get the 'system detection response' curve. Fig 4.9 shows the photo multiplier tube response (1), the filter response (2) and the convolution

of the two (3). The convolution thus gives the 'system detection response' or the 'detection window'.

In order to predict the emission shift, a Gaussian shaped peak was assumed with a FWHM from Huntley's data [18]. This was expressed as function of emission energy. Using the data provided by Krbetschek [16], the variation in the peak maximum with temperature of these Gaussian peaks was then plotted along with the system detection response curve. This is shown in Fig 4.10. The six curves shown are: 1. 'System detection response' curve, 2. Gaussian curve at 22°C/360nm, 3. Gaussian curve at 100°C/375nm, 4. Gaussian curve at 175°C/392nm, 5.Gaussian curve at 225°C/410nm, and 6.Gaussian curve at 325°C/430nm.

Fig 4.9 'System Detection Response' curve:

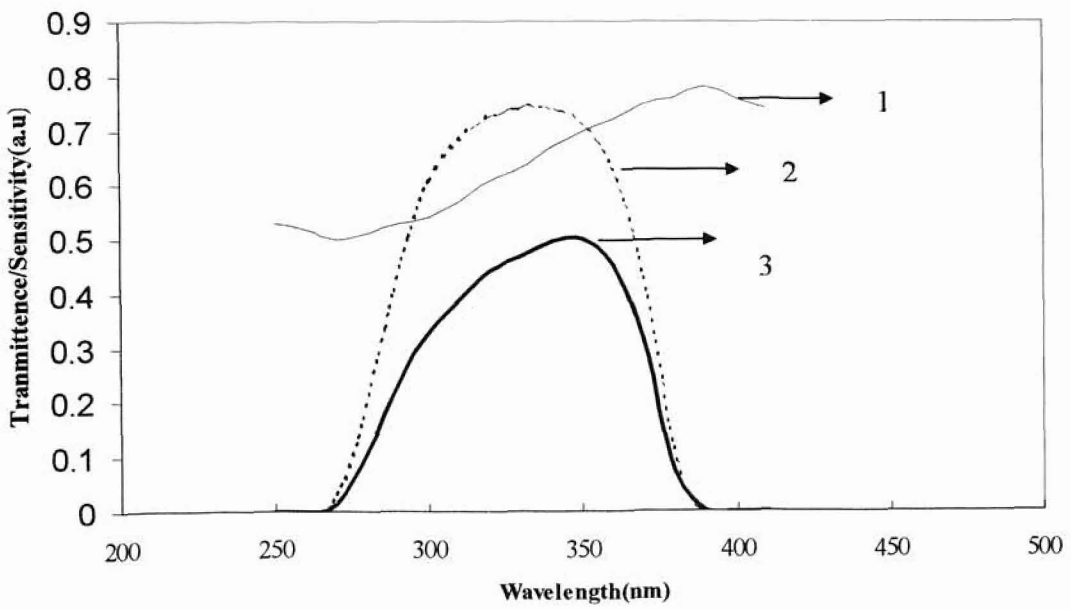

Fig 4.10 Variation of Peak Position with Temperature:

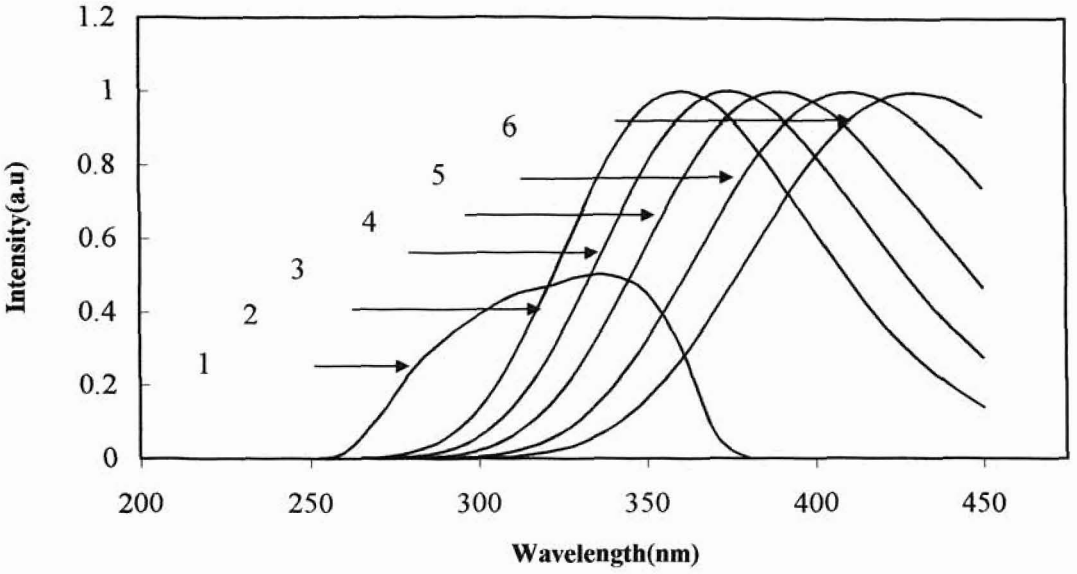

A convolution of each of the Gaussian curves with the system detection response curve was then plotted in order to find the degree of overlap between the two. This is shown in Fig 4.11. The shared area between the system detection response and each of the Gaussian peaks was then estimated as a function of peak temperature. This data was then fitted to a polynomial to predict the shift in the peak maximum for any temperature, and for a TL peak appearing at a temperature T, the predicted wavelength of the peak emission was estimated using this polynomial. These data and the polynomial fit to it, are shown in Fig 4.12. The dashed line is the trend-line of the polynomial fit and the markers are the data points.

Fig 4.11 Convolution of the Gaussian curves with the System Detection Response curve:

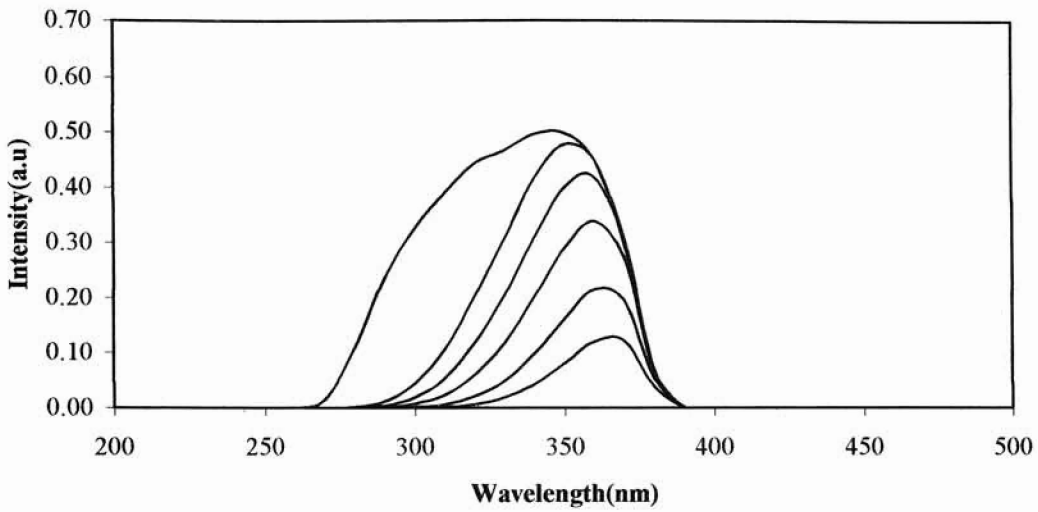

Fig 4.12 Shared area of the Gaussian peaks and its polynomial fit:

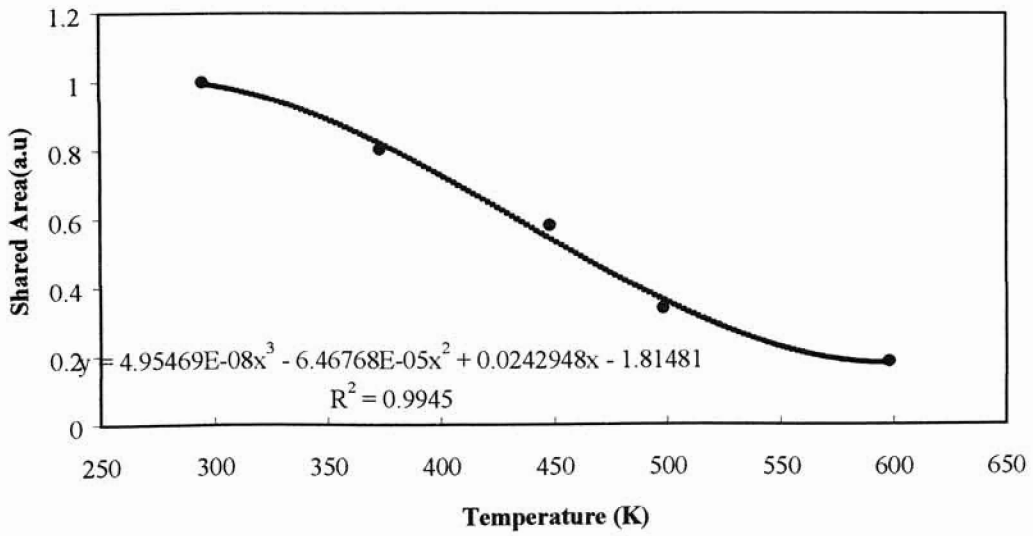

4.3 (e) Theoretical Discussion of Emission Shift:

The possibility of luminescence emission shifting across wavelength with increase in temperature has not been widely discussed. One of the few references that does mention it, is the book by 'Townsend and Kelly' on imperfections in insulators and semiconductors [25].

Based on the configuarational co-ordinate diagram (cf. Ch.2, Pg. 26) the process of optical absorption and luminescence can be described. However, in order to understand the nature of the recombination center it is necessary to begin with the lattice model and compute the wavefunctions that result. In order to calculate the absorption or emission curves it is necessary to compute the shape of the ground and excited states and the distribution of vibrational levels, which are thermally populated. The simplest assumptions of binding forces of an electron to a defect are Hooke's law type forces. The result is a simple harmonic oscillator of frequency ν and parabolic energy bands.

Furthermore, Townsend and Kelly also give an expression for the absorption/emission probability:

$$P(E) = \left(\frac{C}{\pi kT}\right)^{1/2} * Exp\left(\frac{-CX^2}{kT}\right) * \left(\frac{dX}{dE}\right) \tag{4.5}$$

where E is an energy difference between the ground and excited state, C is a constant and X is the displacement from the equilibrium position. In order to match the classical expression to the quantum mechanical expression an effective temperature is used, which is given as in Eq 4.6, wherein ν is the vibrational oscillator frequency. From this, the shift in the peak energy of absorption/emission with temperature can be predicted.

$$T1 = \frac{h\nu}{2k} Coth\left(\frac{h\nu}{2kT}\right) \tag{4.6}$$

Franklin *et al.* [17] suggests that, the configuration coordinate model does provide for temperature dependence of emission wavelength in terms of the increased population of higher vibrational states with temperature. However, it can also be explained as due to change in lattice spacing because of thermal expansion. Another possibility that is also mentioned in this paper is that this shift may be due to the distortion of the lattice.

4.3 (f) Effect of Correction for Emission Shift: 'To Correct or Not To Correct'

The data obtained for the UV emission region was corrected for the emission shift after the scaling procedure was performed. If this correction is performed before the scaling procedure then the effect of the emission shift will not be apparent. This procedure was not done for the data in the Blue emission region because the peaks in the Blue emission region are not known to shift across wavelength as a function of temperature [16].

The quenching curves obtained after scaling and the effect of the emission shift correction (and renormalized) on them is shown for the two samples in Fig 4.13(a) and Fig 4.13(b). In the two curves shown the closed symbols are the uncorrected quenching curves and the open symbols are the emission shift corrected (renormalized) quenching curves. In the both Fig 4.13 (a) and Fig 4.13(b) it can be seen that the correction of the emission shift makes a considerable change to the quenching curve, which is expected, if the reported shift in the literature is true.

Fig 4.13(a) Arkansas quartz in UV emission region: Effect of emission shift

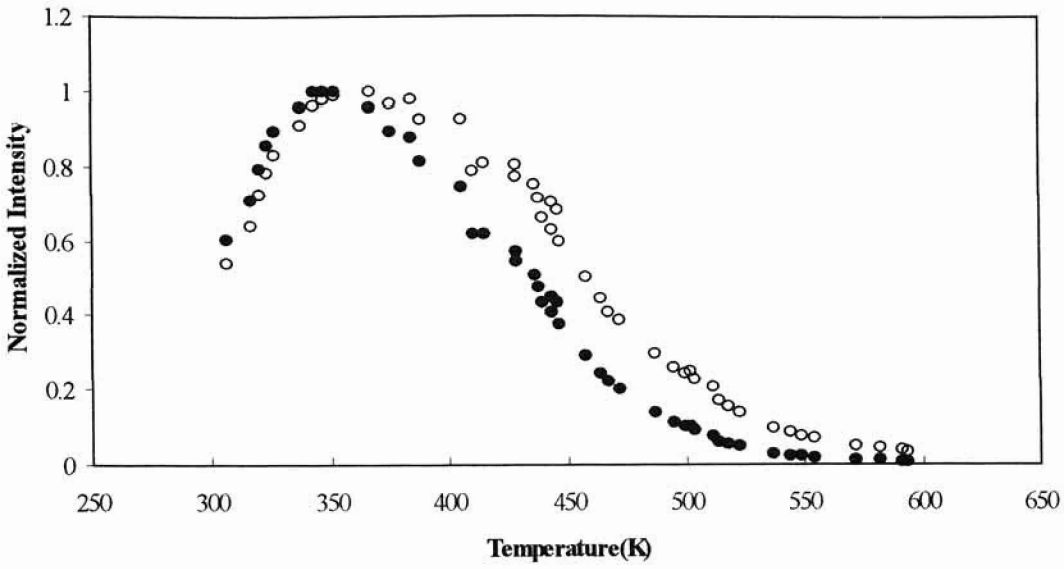

Fig 4.13(b) Danish quartz in UV emission region: Effect of emission shift

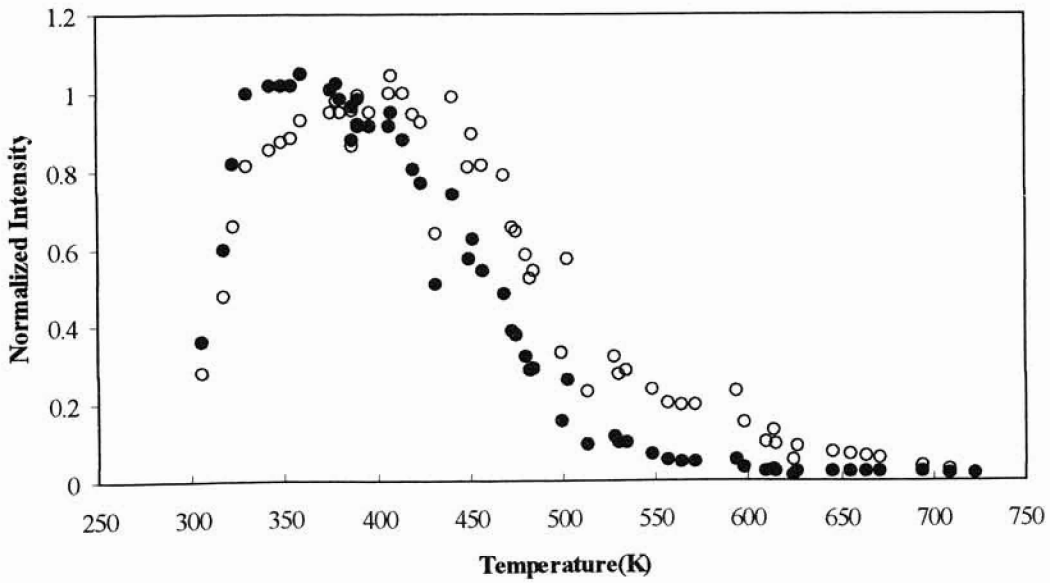

However, here it can also be seen that, not only is the peak in the quenching curve at the low temperatures magnified, but also its shape is broadened and center shifted. The presence of this peak is due to the instability of the low temperature '110°C' glow peak in the TL curve. Thus, the increase in the signal of this unstable peak is understandable but the instability shifting to higher heating rates, as a result of the correction is not. Essentially, this correction, is shifting the peak center of the '110°C' peak to higher temperatures where the peak is not known to occur. Moreover, the correction is also changing the shape of the quenching curve. Due to the correction, the shape no longer follows the shape of the curve resulting from Eq 4.1. However, the resulting curve can be indeed be fit to the quenching equation given in Eq 4.1, but the resulting parameters are no where near the expected values. The thermal activation energy for the quenching in the UV emission region has been confirmed by variety of experiments to be around 0.6eV. When the emission shift correction was applied to the data obtained here in these experiments, the value of activation energy was found to be around 1.5eV. This is almost twice the expected value of 0.6eV. However, without the emission shift correction the quenching curves for the two samples yielded activation energies of 0.59eV and 0.58eV (Fig 4.14(a) and Fig 4.14(b)). These values agree very well with published values [3,6]. This will be further confirmed when the OSL and RL data is presented. It is clear from the theoretical background that a shift in the emission wavelength in the UV emission region does occur at high temperatures. But the effect on the data as shown in Fig 4.13(a) and (b) indicates that the shift cannot be to the large extent suggested in the published data [17]. Thus, for the purpose of this thesis, emission shift correction on quenching curves in the UV emission region will not be performed.

4.3(g) Analysis of the Quenching Curves:

In order to obtain E and C parameters 'Origin 5.0' software was used. This software, like 'peak fit' uses the Levenberg-Marquardt non-linear least square fitting method to find the 'best-fit'. The 'best fit' for the quenching curves obtained in the UV emission region for the two samples are shown in Fig 4.14(a) and Fig 4.14(b).

However, it was not as easy to fit the quenching curves for the blue emission region. The instability in the 110°C peak at low heating rates contributes most to 'undependable' part of each scaled data set. The data sets were normalized to unity by dividing all data points by the data point having the maximum value. Since this value to which all the other data points were being normalized depended to a large extent on the scaling procedure, it was possible that this data point was not really the maximum of the curve. Thus, more weight was given to the quenching part of the curve and the tail end of the curve than the maximum. The other problem that resulted from this was, that, depending on the extent of weighting the quenching parameters tends to differ from fit to fit. Fig 4.15(a) and Fig 4.15(b) show two different fits to the same set of data. In these graphs data from the Arkansas quartz sample in the Blue emission region have been shown.

For the two samples in the UV emission region the parameters obtained are as follows. Arkansas quartz has E and C as 0.59eV and 7.9*10^6. Danish quartz sample has E and C of 0.63eV and 8.8*10^6

Fig 4.14 (a) Arkansas quartz sample in the UV emission region:

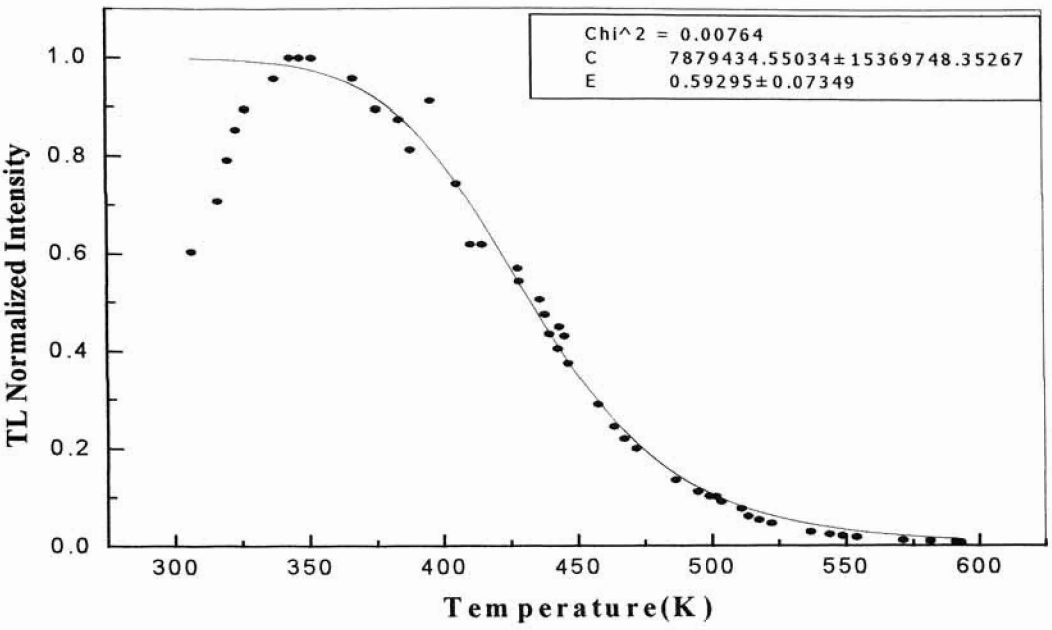

Fig 4.14 (b) Danish quartz sample in the UV emission region:

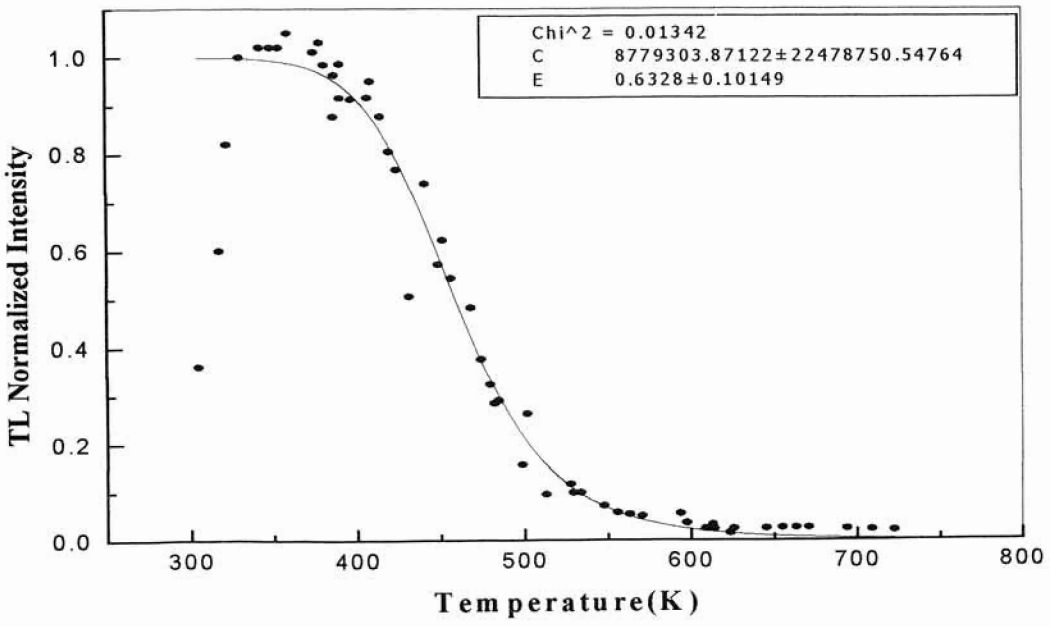

Fig 4.15 (a) Arkansas quartz sample Blue emission- Fit 1:

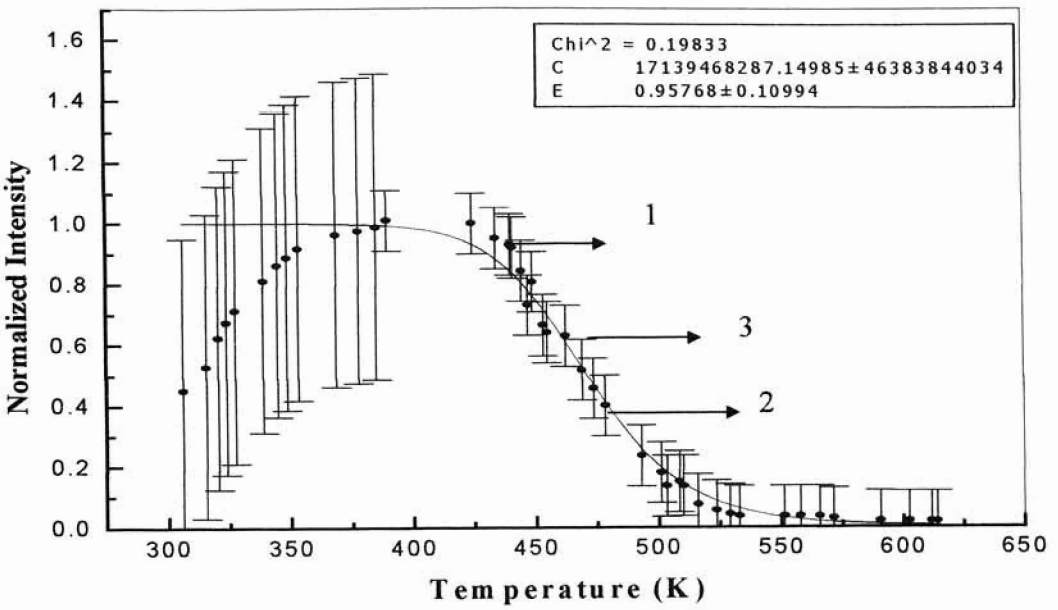

Fig 4.15 (b) Arkansas quartz sample Blue emission- Fit 2:

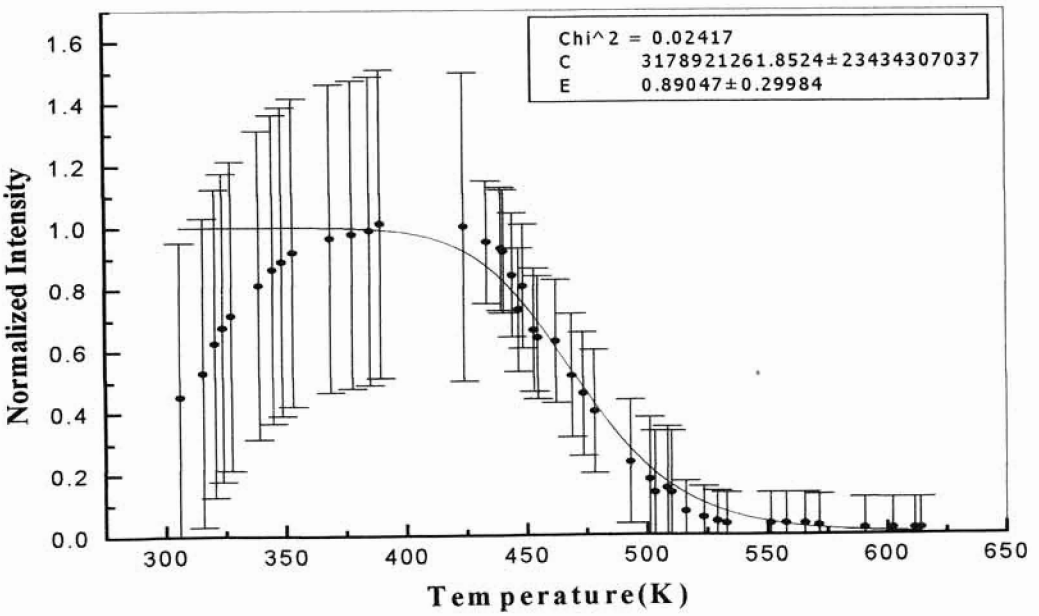

In Fig 4.15(a), filled circles indicate the data points (1), and the solid line indicates the fit (2). Also shown are the resulting fitting parameters for E and C as 0.96eV and 1.7*10^10 respectively. More weight was given to the quenching part of the curve. This can be seen as error bars (3). The length of the error bars indicated the extent of weighting. Long error bars indicate weighting to a lesser extent and smaller bars indicate weighting to a larger extent. However all the data points in the quenching region do not have the same weighting. The tail end of the curve has been give less weight.

Now by changing the extent of weight being given to the tail end of the curve, the values of E and C can be changed. This can be seen in Fig 4.15 (b). As in Fig 4.15(a), the data points are shown by solid circle, the fitting curve by a solid line and the weighting by error bars. All the data points in the quenching region have been given the weight. It can be seen that this fit gives the values of the parameters to be 0.89eV and 3.2*10^9. Thus, the fitting is not completely exact and depends on judgement to yield the best fit. But it can also be seen that in either fit the value of the thermal activation energy is much higher than the values obtained for the UV emission region.

For the Danish quartz sample in the Blue emission region a similar fitting procedure was used and the resulting fit is shown in Fig 4.15(c). The obtained parameters of E and C are 0.83eV and 8.2*10^7.

Fig 4.15 (c) Fitting of Danish quartz sample in Blue emission:

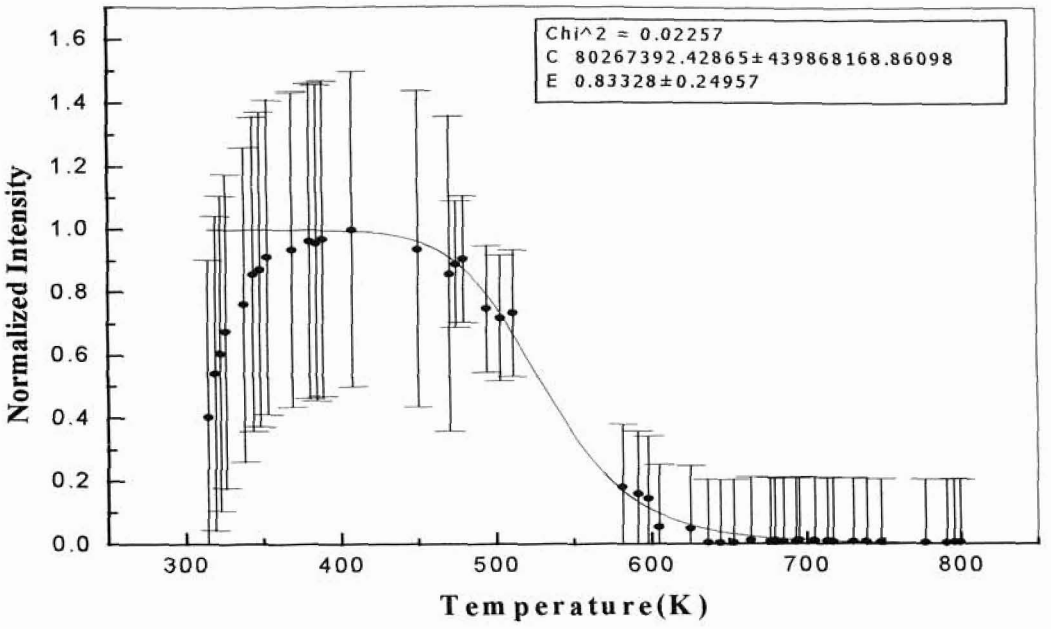

4.4 Optically Stimulated Luminescence Experiments: Results and Discussion

The OSL experiments were performed with the Risø system on the quartz samples in the UV emission region. Results for the UV emission region, and the problems due to which these experiments were not performed in the Blue emission, region are discussed in the following sections.

4.4 (a) OSL Results in the UV Emission Region:

OSL decay curves were obtained for both the samples for temperatures from 30°C through to 250°C at 20°C intervals for both heating and cooling cycles. A representative set of curves is shown for each sample in the following figures, although a full data set

was obtained in each case. The decay curves obtained for each of the samples are shown in Fig 4.16(a) and (b), Fig 4.17(a) and (b).

Fig 4.16(a) OSL decay curves obtained for the Arkansas quartz sample in the UV emission region: Heating Cycle

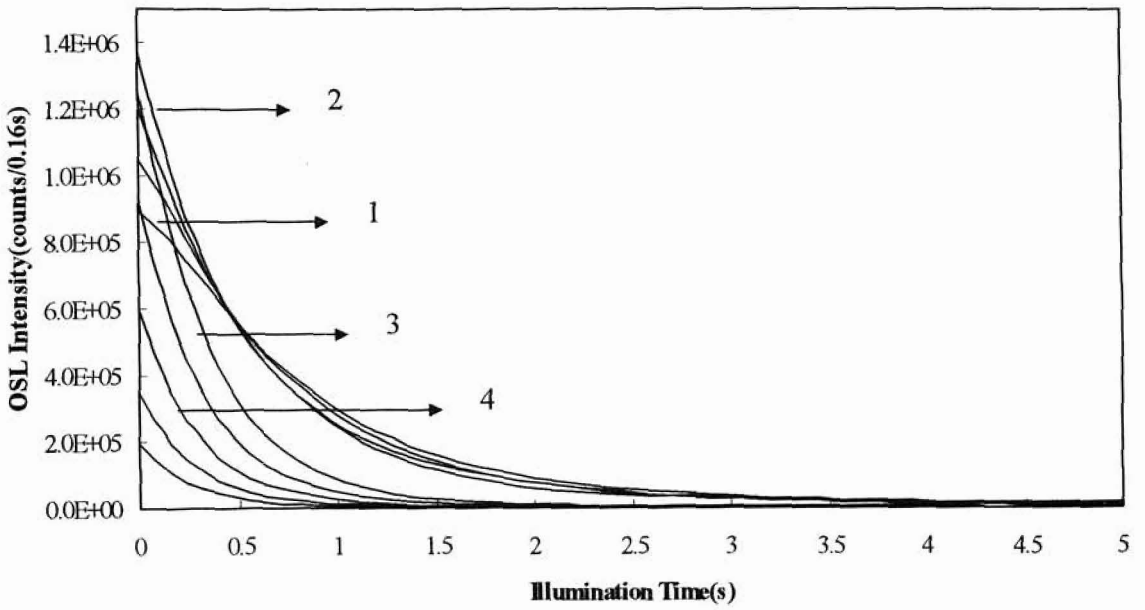

Arkansas Quartz Sample in the UV Emission Region:

Fig 4.16 (a) depicts the OSL decay curves obtained for the Arkansas quartz sample in the UV emission region during the heating cycle. As mentioned in Ch.3 a preheat of 260°C (533 K) was applied to this sample prior to the OSL measurement. These decay curves exhibit long tails and are not exactly exponential decays. The curves numbered 1, 2, 3,

and 4 are decay curves measured at sample temperatures of 303 K, 383 K, 443 K, and 483 K.

It can be seen that the maximum intensity, i.e. the intensity during the first few seconds of illumination of the sample, increases for sample temperatures from 303K to 383K, after which there is a steady decrease in the intensity for higher sample temperatures. This feature is explained in detail below when discussing the quenching curves.

Fig 4.16(b) OSL decay curves obtained for the Arkansas quartz sample in the UV emission region: Cooling Cycle

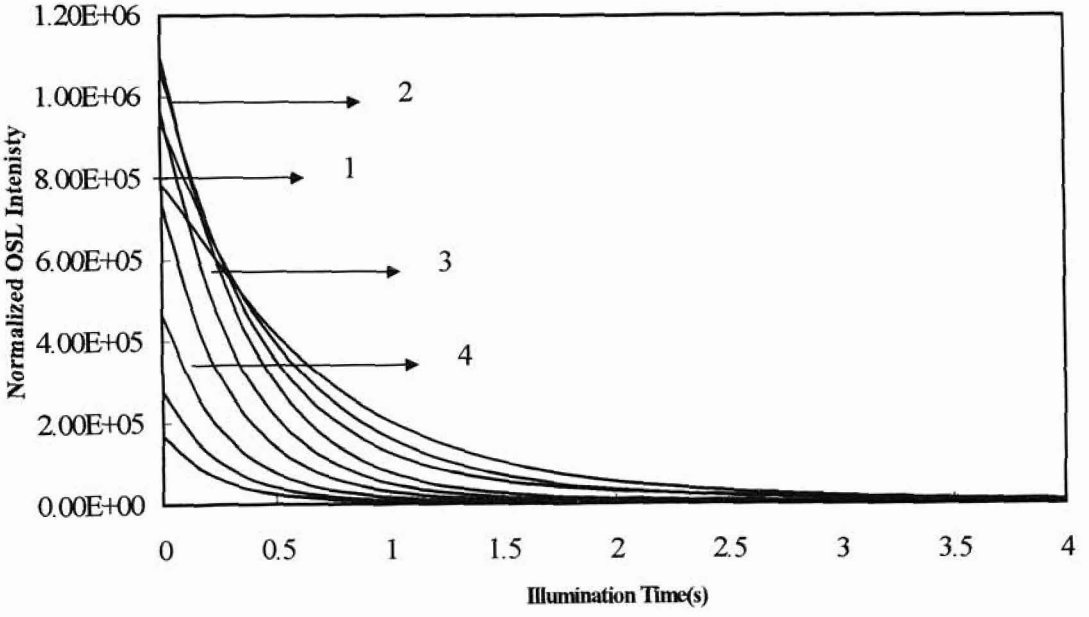

Fig 4.16(b) shows the OSL decay curves during cooling cycle for the Arkansas quartz sample. The increase in intensity at low temperatures can be observed here too; however, it is not as prominent as when observed during the heating cycle. The maximum intensity

in both cases at 303K, is around 8.0*10^5. However, the intensity during the heating cycle, goes up to 1.4*10^6 at 383 K and in the case of the cooling cycle the intensity increases only to 1.0*10^5.

The area under the curve is directly proportional to the absorbed dose. Thus, the amount of luminescence resulting from the irradiation is seen to decrease at higher temperatures. This can be explained as being due to the increase in the probability of non-radiative decay of the trapped charge, and a decrease in the probability of the radiative transition. Thus, a plot of the integration of the area from 0 to 40s under each curve against the sample temperature gives the thermal quenching curve described in section 4.4(b).

Fig 4.17(a) Danish quartz sample in the UV emission region: Heating Cycle

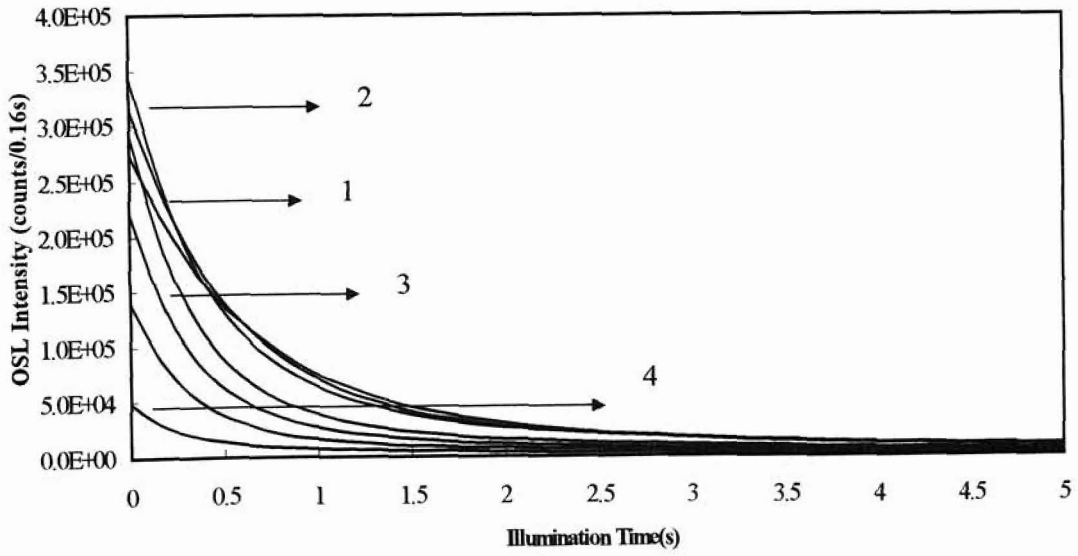

Fig 4.17(b) Danish quartz sample in the UV emission region: Cooling Cycle

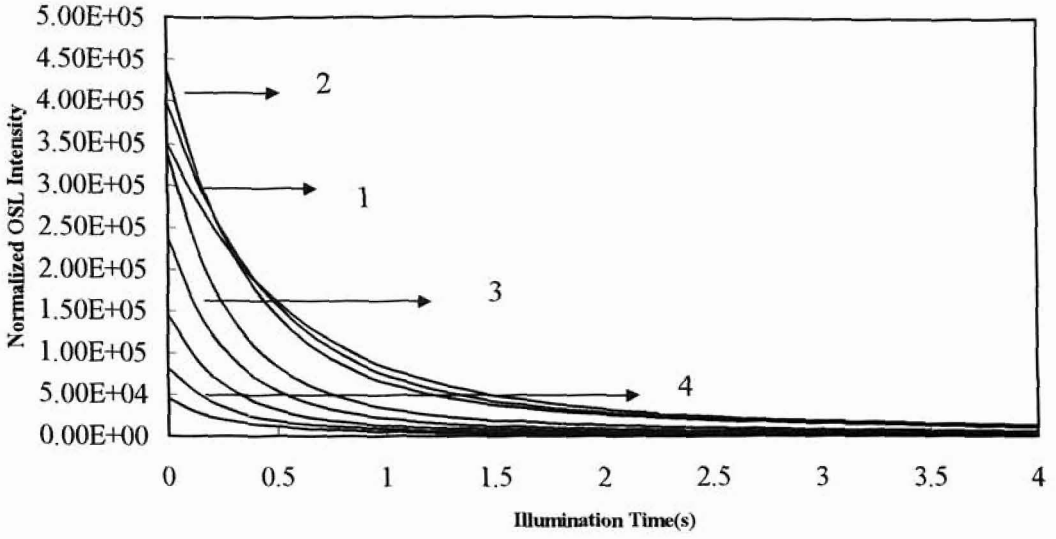

Danish Quartz Sample in the UV emission Region:

A representative set of OSL decay curves is shown for the Danish quartz sample in Fig 4.17 (a) for the heating cycle and 4.17 (b) for the cooling cycle. For this sample too, a preheat of 260°C was used. The curves numbered 1, 2, 3, and 4 are OSL decay curves of sample temperatures of 303 K, 483 K, 463 K and 523 K. The increase in initial intensity for the low temperatures can be seen here too, after which there is a decrease in the intensity of OSL signal as sample temperature is increased further. The area under each curve decreases with increase in the sample temperature. A plot of the integrated signal (area under the curve) against the sample temperature yields the thermal quenching curve.

4.4 (b) Analysis of OSL Decay Curves for the UV Emission Region:

The illumination time of light in each OSL sequence was 40 s. A total of 250 channels (250 data points) were used for measuring the signal for the period of illumination i.e. 40 s i.e. 0.16s per data point (or channel). The signal measured by the last 25 channels was taken as the background signal. Thus, 10 times the signal recorded during the last 25 data points is the total background for each curve. The background signal was subtracted from the total integrated signal in order to calculate the total OSL intensity at each temperature. Plots of quenching curves thus obtained are shown for the two samples in Fig 4.18(a) and Fig 4.18 (b). The maximum intensities have been normalized to unity in both the figures. Data for the heating and cooling cycles for each sample are shown; the closed circle curves in each figure are the quenching curves for the heating cycle (1), and the dashed line with square markers represents the cooling cycle data (2).

Quenching Curves:

In both Fig 4.18(a) and Fig 4.18(b) it can be observed that the quenching curves for the heating cycle and the cooling cycle differ from each other. There is a small peak at low temperatures in the heating cycle of the Arkansas quartz sample, although this is not obvious for the Danish quartz sample.

Heating Cycle: The increase in the signal in this region is because of the presence of the trap that gives raise to the '110 °C' TL peak, which can be seen in the TL glow curves shown in Fig 4.1(a) and Fig 4.2(a). This trap is known to be unstable such that when other measurements are performed at near room temperatures, charges from the deep traps (which are full because of the irradiation in the previous sequence) transfer into this shallow trap and are released during illumination as increased luminescence.

Fig 4.18(a) Arkansas quartz sample: Quenching in the UV emission: Heating (1) and Cooling Cycles (2).

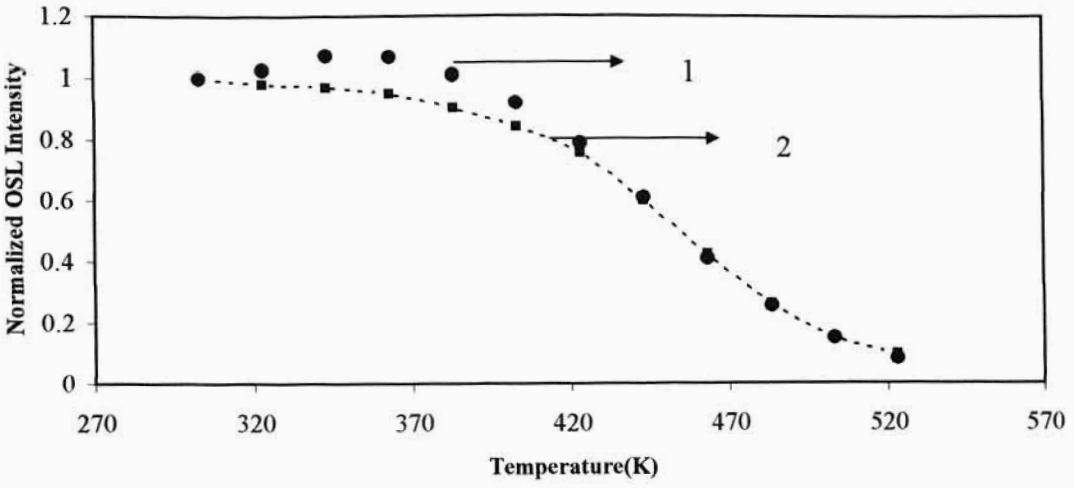

Fig 4.18(b) Danish quartz sample: Quenching in the UV emission: Heating (1) and Cooling Cycles (2).

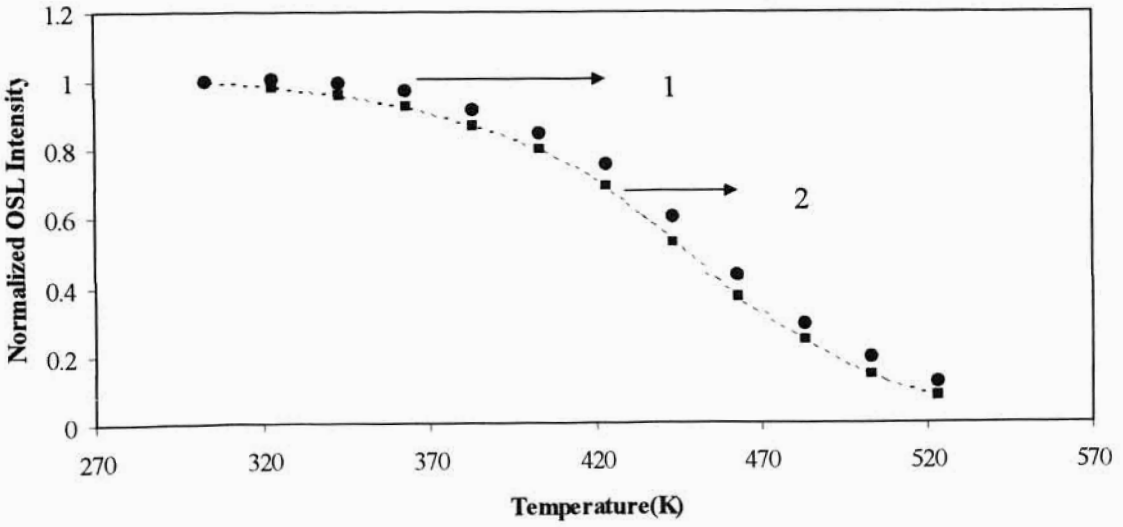

Cooling Cycle:

In the cooling cycle of the Arkansas quartz sample the absence of the peak (which is present in the heating cycle) can be seen. In case of the Danish quartz sample, however, an increase in the extent of the 'flattening' in the quenching curve can be seen in the cooling cycle. In the cooling cycle, as the measurements are first performed at high temperatures, the deep traps do not accumulate the charges and remain empty. Thus when the measurements are performed in the temperature region where the '110°C' peak is unstable, there is no charge transfer into the '110°C' trap from the deeper traps. Thus, no increase in the luminescence intensity can be seen.

This increase in intensity at low temperatures was remarked upon when the OSL decay curves were being discussed in the previous section. This phenomenon can be observed in radio-luminescence data too, which will be presented later in this chapter.

Emission Shift Correction:

Since these measurements were performed in the UV emission region, the effect of emission shift correction had to be explored. Fig 4.19(a) and Fig 4.19(b) show the effect of the emission shift correction on the cooling cycles for the two samples. As can be seen in these figures the effect is significant. In both figures it can be seen that as a result of the emission shift correction, a small peak appears in the quenching curve. Moreover, the curve shifts to higher temperatures and changes shape. This curve, because of the distinctive change in its shape can no longer be fit to the quenching curve from Eq 4.1.

Fig 4.19(a) Arkansas Quartz Sample: Effect of Emission shifts Correction, 'Corrected Data' (1), and 'Uncorrected Data' (2):

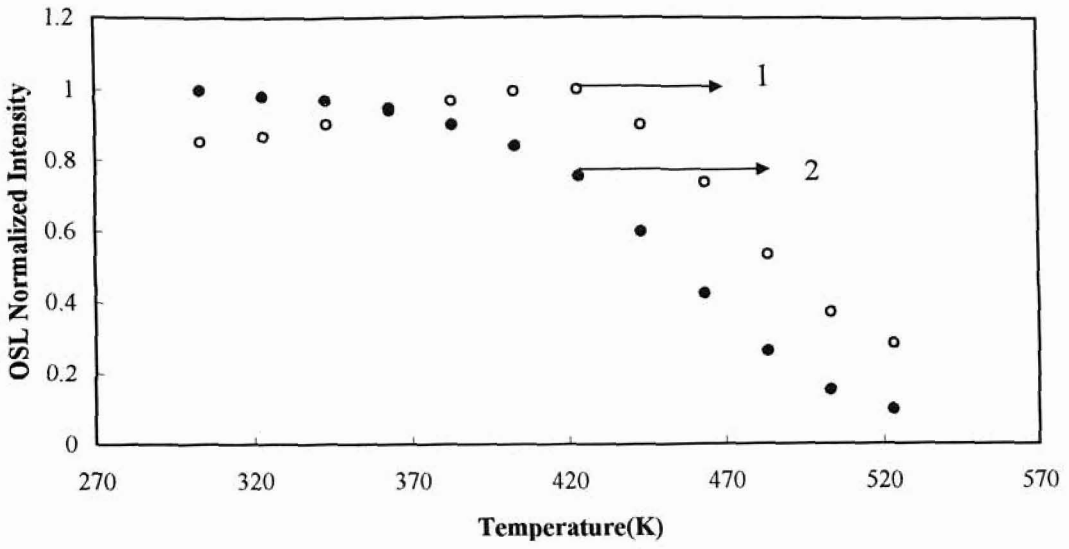

Fig 4.19(b) Danish quartz sample: Emission shifts correction, 'Corrected Data' (1), and 'Uncorrected Data' (2):

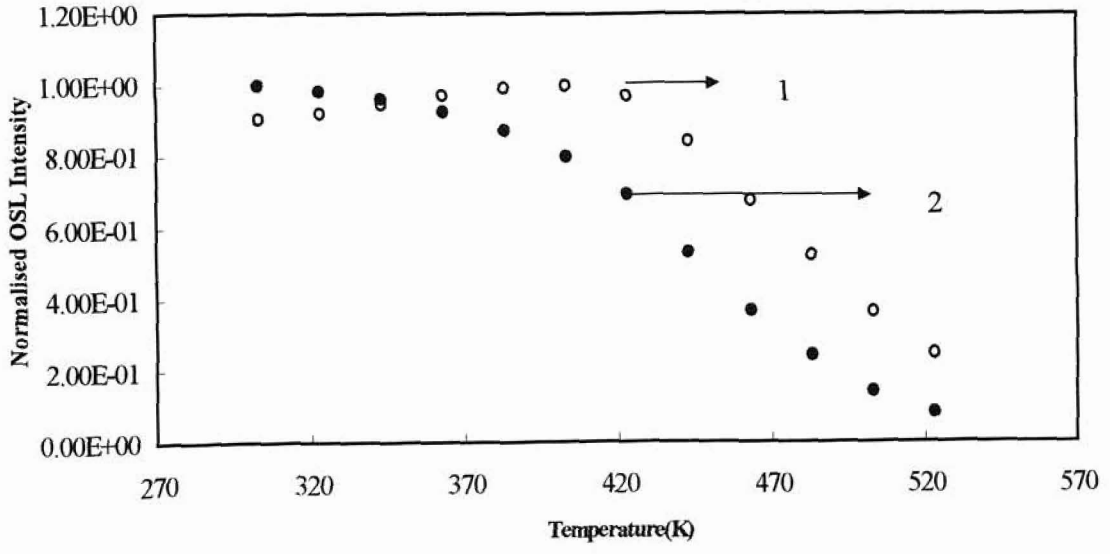

In the heating cycles of the OSL data, the presence of a peak shape was explained as due to transfer of charges from deep traps into the shallow traps. It was also seen that this peak vanishes in the cooling cycle. When the emission shift correction is applied to these cooling curves, a peak also appears but at higher temperatures. This peak can't be explained on the basis of transfer of charges into shallow traps because it is centered at higher temperatures than the '110°C' trap. Thus, the appearance of the latter peak, in the data corrected for emission shift may actually be a result of overcorrecting the data. This fact is also reflected in the TL data that has already been discussed. It will also be shown to be the case in the RL data. Thus, as already mentioned, the emission shift correction will not be applied to the data obtained in the UV emission region in this thesis.

4.4(c) Thermal Quenching Curves and their Parameters:

'Origin 5.0' was used for fitting the quenching curves to Eq 4.1 and yielded the quenching energy E and the constant C. A brief description of the software has already been given along with the results of TL experiments. The fits to the quenching curves for each of the quartz samples in the UV emission region (heating and cooling cycles) are shown in Fig 4.20(a) , 4.20(b) and 4.21(a), 4.21(b).

Fig 4.20 (a) Quenching curve fit: Arkansas quartz sample, UV emission region, Heating Cycle:

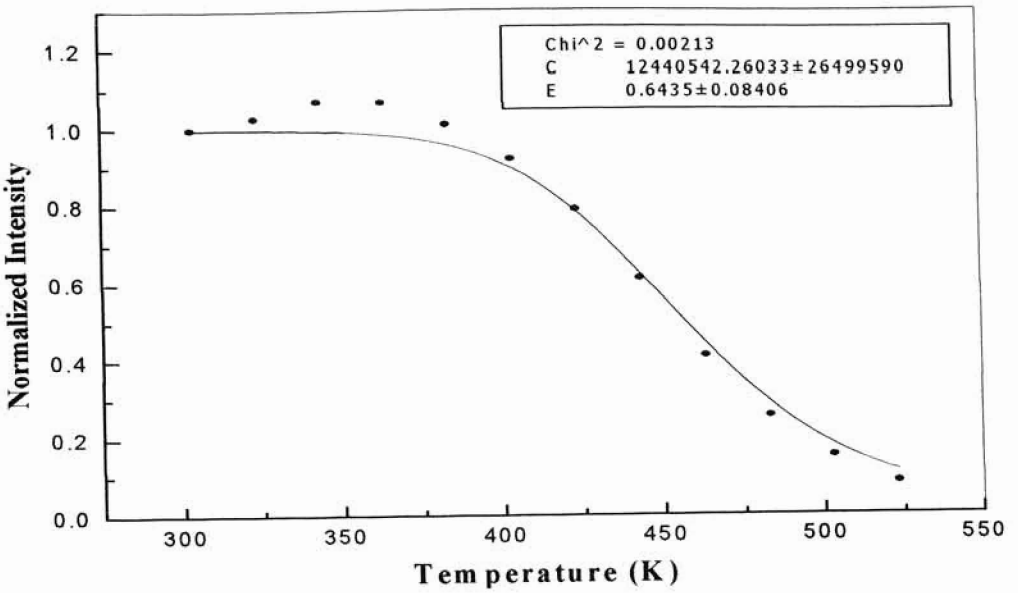

Fig 4.20 (b) Quenching curve fit: Arkansas quartz sample, UV emission region, Cooling Cycle:

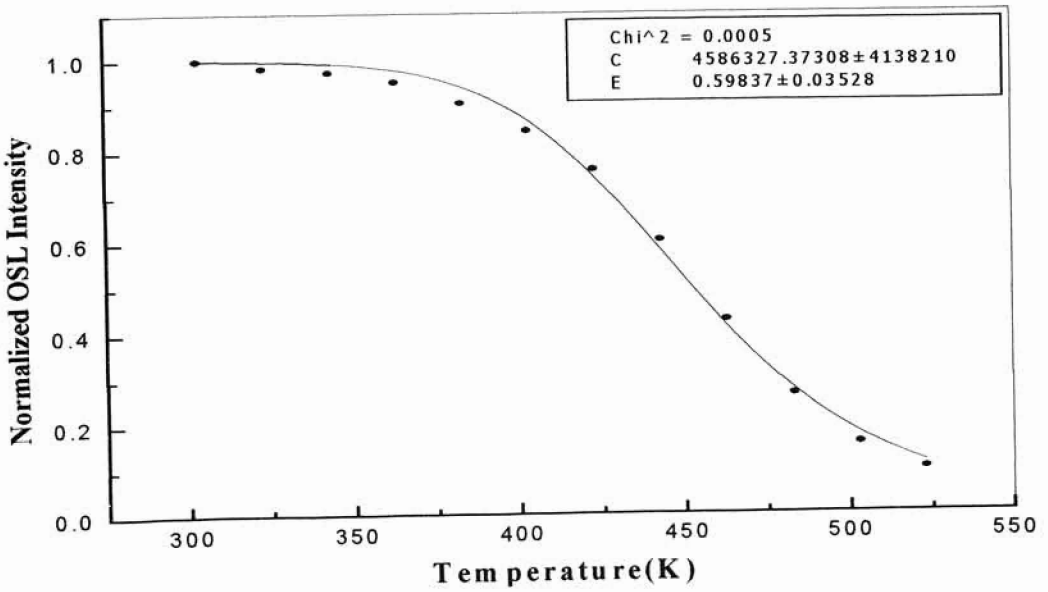

Fig 4.21 (a) Quenching curve fit: Danish quartz sample, UV emission region, Heating Cycle:

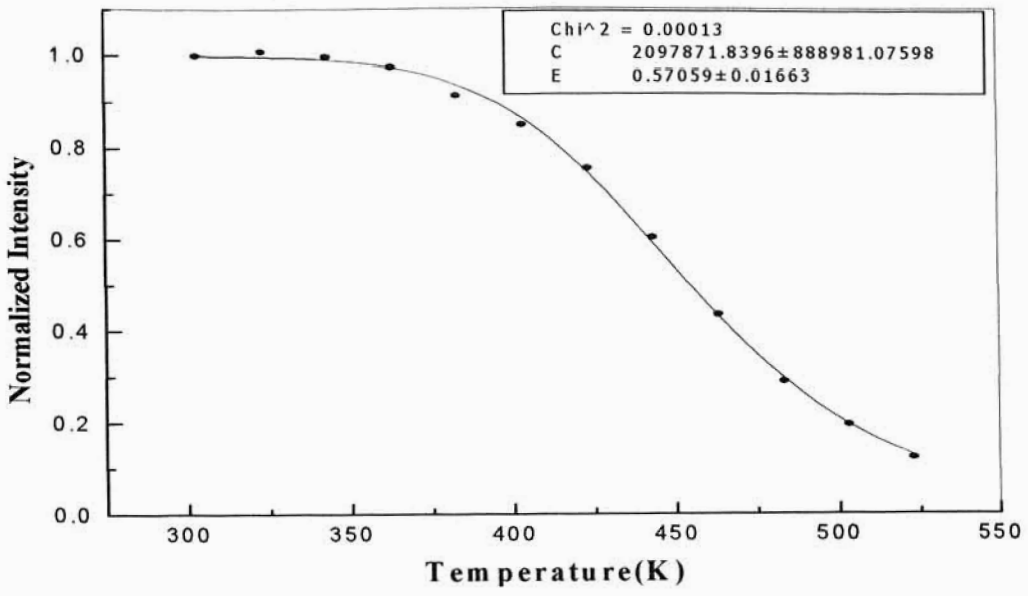

Fig 4.21 (b) Quenching curve fit: Danish quartz sample, UV emission region, Cooling Cycle:

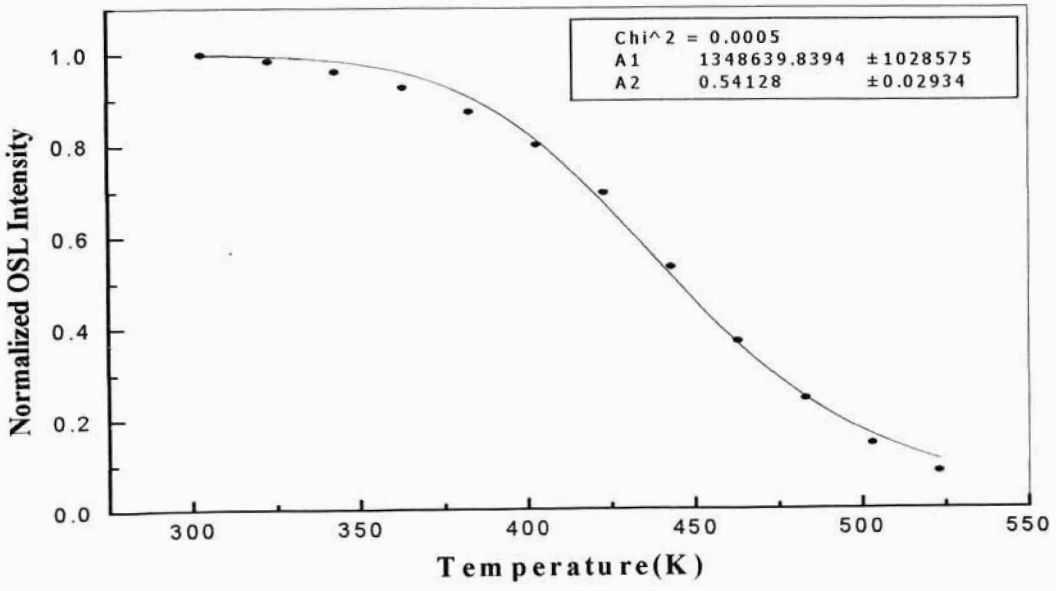

Quenching Parameters:

The values of E and C for the Arkansas quartz sample in the heating cycle are 0.64eV and 1.2*10^7. For the cooling cycle of the Arkansas quartz sample the parameters obtained are 0.6eV and 4.6*10^6.

For the Danish quartz sample in the heating cycle, E and C are 0.57eV and 2.1*10^6. The cooling cycle for this sample gave 0.54eV and 1.3*10^6. A comparison of these values with the values obtained for the TL quenching curves is given in Table 1 at the end of this chapter.

4.5 OSL Experiments in the Blue Emission Region:

The OSL experiments could not performed in the blue emission region because of several problems. These problems are discussed in detail as follows.

Filters and Stimulation light:

As mentioned in the previous chapter, the dosimetry lab here at OSU is equipped with two Risø readers. One of which is has a blue LED with emission centered at 470nm and the other has a green LED and a halogen lamp. The green LED can provide a stimulation light centered at 520nm and the halogen lamp with appropriate filters can provide stimulation light between 420 to 550nm. In order to perform the OSL experiments the wavelength of the stimulation light should not be in the same wavelength region as the emission light. Thus only the green LED or the halogen lamp could be used. The FWHM of the stimulation band that the green LED can provide is 30nm. This bandwidth is too large and overlaps with the wavelength region in which the response of the Corion-Blue 450nm filter lies (cf. Ch.3. Fig 3.1(b), Fig 3.2). The possibility of using other filters,

which had responses at lower wavelength regions, was explored, but no suitable filter could be found. In all the cases the background signal was large enough to saturate the PMT in the reader. Since the halogen lamp can provide stimulation light between 420nm to 550nm, a combination of different filters was used to obtain light in the appropriate wavelength regions. In general most filters have some response outside their specified wavelength regions that they are supposed to respond in. Though this response is very small, the leakage of the excitation light that takes place is large enough to saturate the PMT. Thus the OSL experiments could not be performed in the blue emission region.

4.6 Radioluminescence Experiments:

4.6(a) Results:

As mentioned in Ch 3, both the heating cycle and the cooling cycles were performed on each sample in each of the two emission regions. Each experiment consisted of several sequences with each sequence performed at a specific sample temperature for duration of 200s. In each sequence, background counts were recorded for the first 50s after which the source was switched on and the signal recorded for the next 100s. In the last 50s, background counts were once again recorded. This sequence was repeated for different sample temperatures from room temperature (around 30°C) to 573K (300°C) for the heating cycle, and 573K to room temperature for the cooling cycle. The result obtained for a sequence in the heating cycle of the Arkansas quartz sample at room temperature in the UV emission region is shown in Fig 4.22. In the Fig, data points indicated by 1 were recorded with the source shutter closed and the data points indicated by 2 were recorded with the source shutter open.

Fig 4.22: Signal obtained for the Arkansas quartz sample in the UV emission region at room temperature;

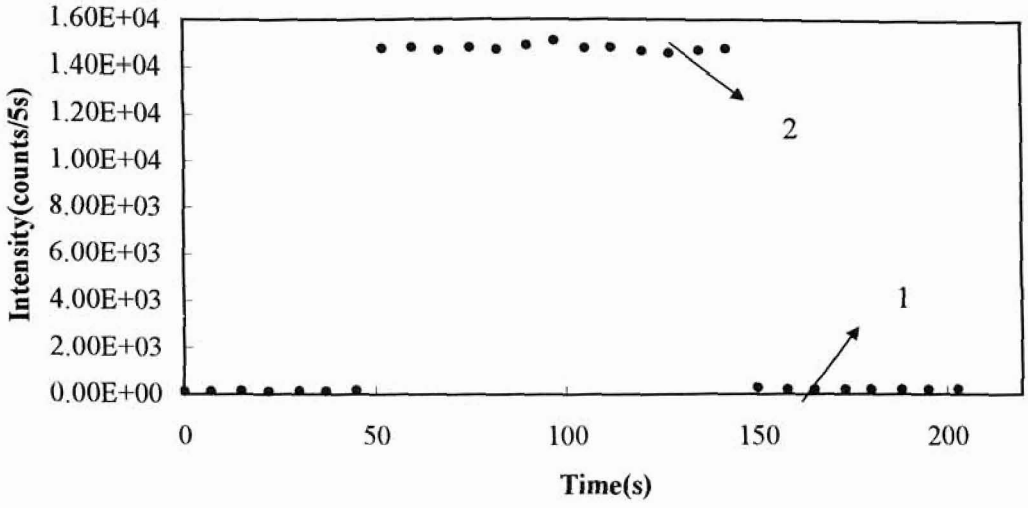

In order to calculate the total signal at each sample temperature, the sum of all the background signal measured was subtracted from the sum total of the signal measured with the source switched on. This was the total signal at that specific sample temperature. This calculation was performed for the data resulting from each sequence within an experiment. Thus, a set of data points was obtained each corresponding to a specific sample temperature. A plot of these data points against their corresponding temperatures will yield the thermal quenching curve. Curves thus obtained for heating and the cooling cycles of the two samples in both the emission regions are shown in Fig 4.23(a) to Fig4.26 (b).

Fig 4.23(a) Quenching curve for Arkansas quartz sample: UV emission region, Heating cycle:

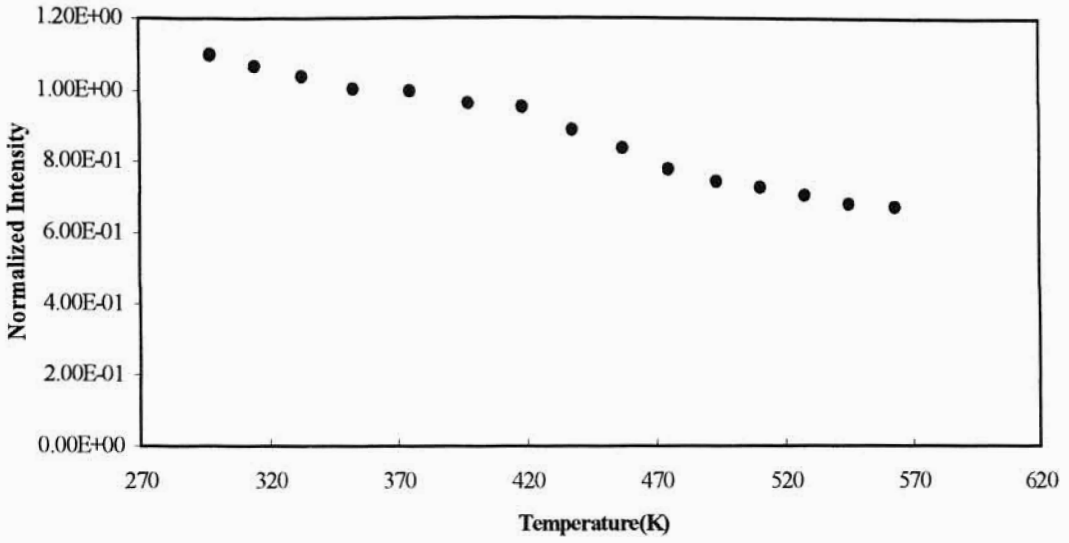

Fig 4.23(b) Quenching curve for Arkansas quartz sample: UV emission region, Cooling cycle:

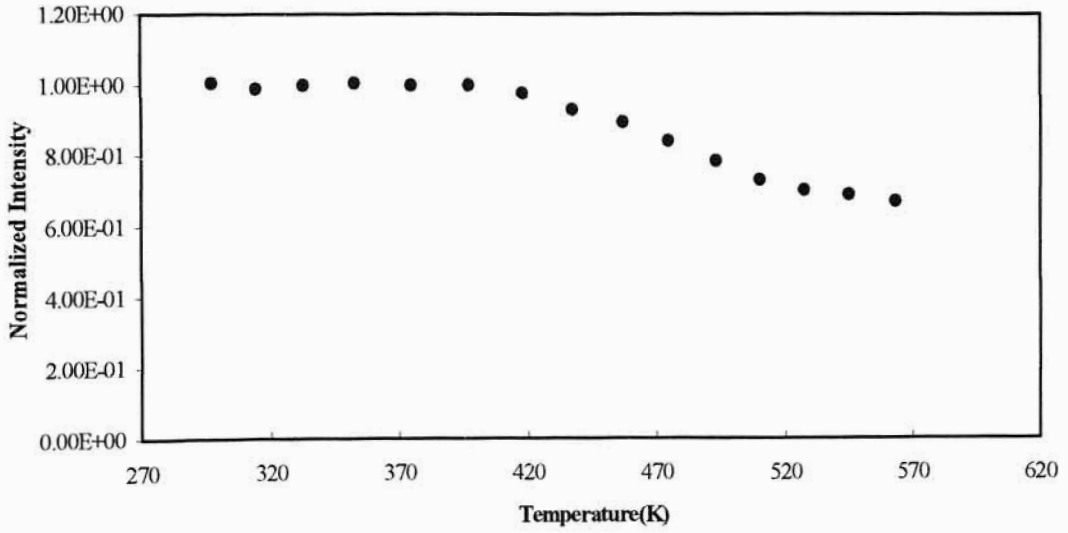

Fig 4.24(a) Quenching curve for Arkansas quartz sample: Blue emission region, Heating cycle:

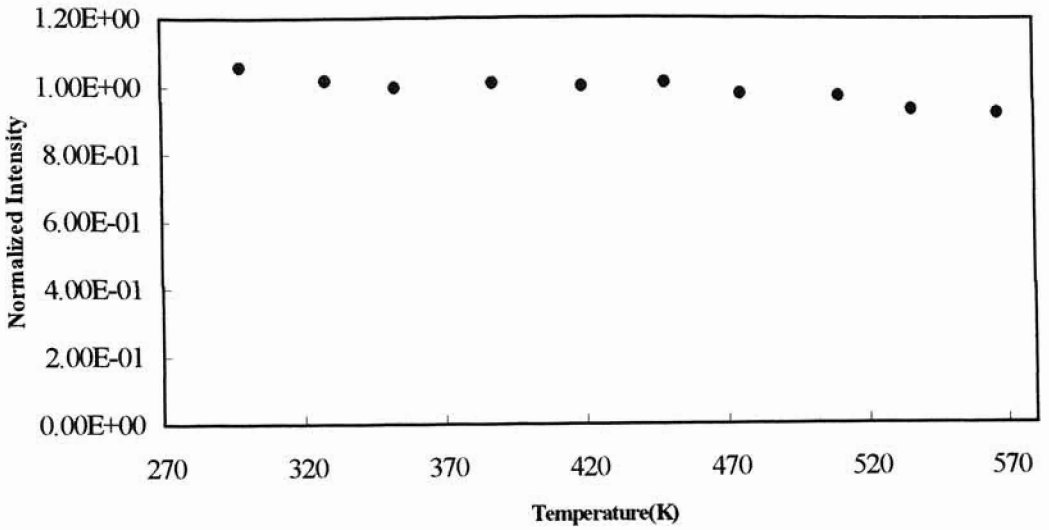

Fig 4.24(b) Quenching curve for Arkansas quartz sample: Blue emission region, Heating cycle:

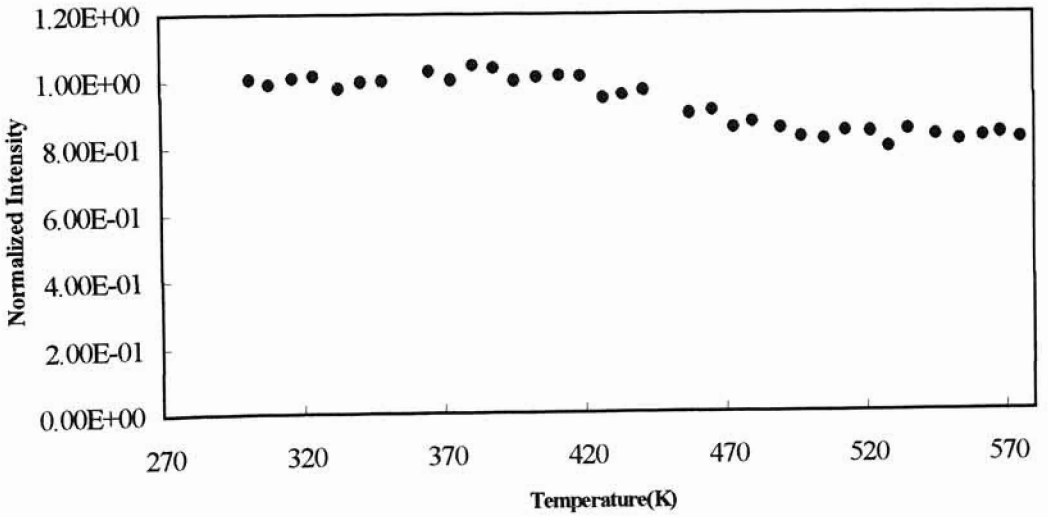

Fig 4.25(a) Quenching curve for Danish quartz sample: UV emission region, Heating Cycle:

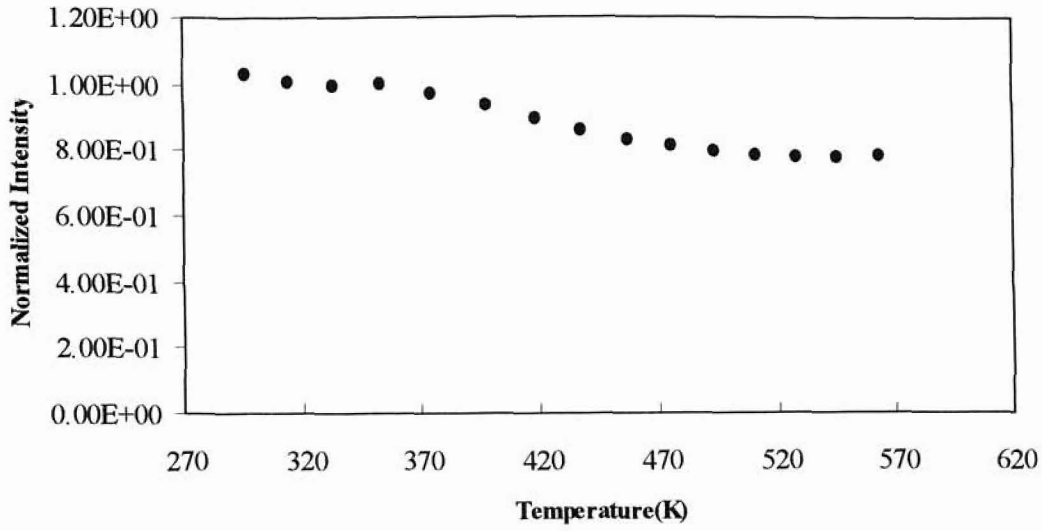

Fig 4.25(b) Quenching curve for Danish quartz sample: UV emission region, Cooling Cycle:

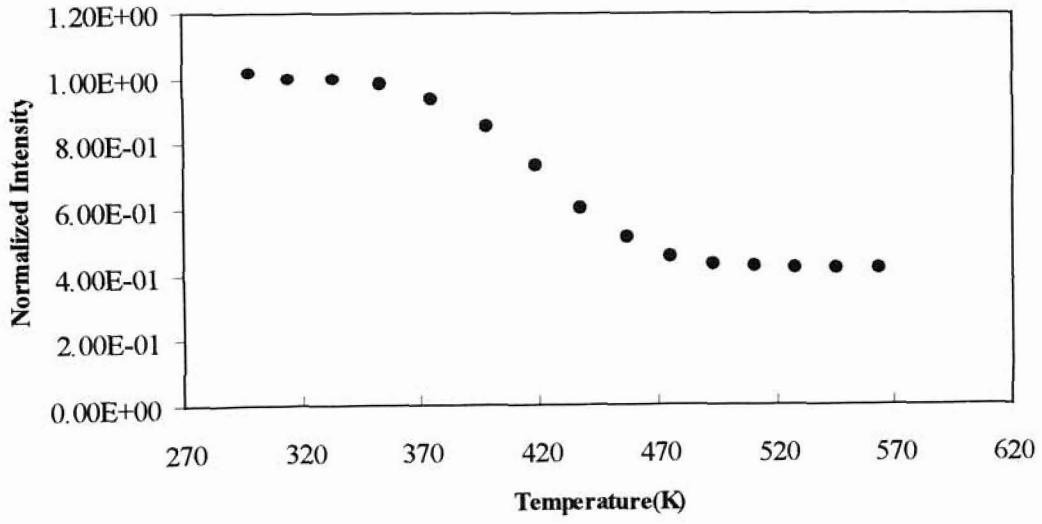

Fig 4.26(a) Quenching curve for Danish quartz sample: Blue emission region, Heating Cycle:

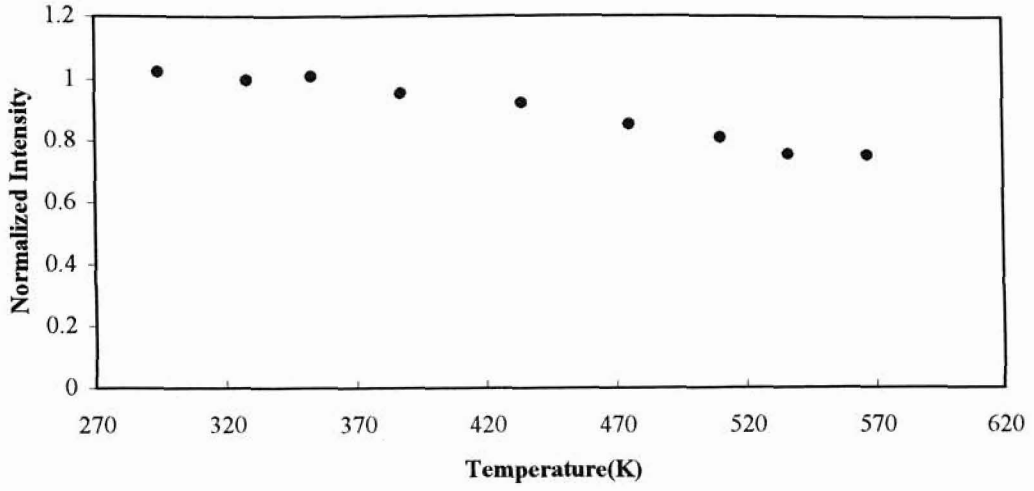

Fig 4.26(b) Quenching curve for Danish quartz sample: Blue emission region, Cooling Cycle:

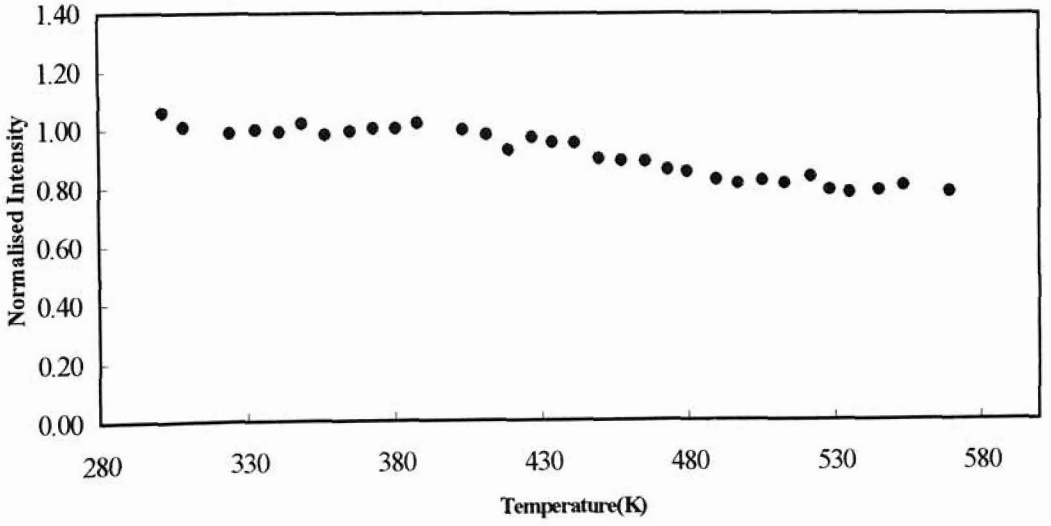

In the graphs shown above it can be seen that the extent of quenching in the UV emission region appears to be very much greater as compared to quenching in the Blue emission region. However it can also be seen that, in all of the graphs, the data points in the tail of the quenching curve have nearly leveled to the same value. Measurements at sample temperatures higher than 573 K was not made because no quenching was observed above this temperature. It can be seen in both the samples and in both the emission regions that beyond 540 K the signal is almost constant. As mentioned in Ch 3, the aluminum disk (to which the sample was affixed) was fixed onto the nickel holder using a thermal compound in order to ensure good thermal contact. However, when exposed to ionizing radiation this compound gives out luminescence. This luminescence, however, does not quench at high temperatures. Thus, depending on the amount of thermal compound present, the intensity of the unquenched signal in the background varied. Moreover, since the RL experimental setup was not isolated from the surrounding, the dust particles in the air were also emitting luminescence when exposed to the ionizing radiation. Another reason, due to which this high background signal is observed when the source shutter is open, can be the 'Cerenkov' radiation. This is luminescence produced due to the radiation passing through the silica fiber. This emission is found to increase at lower wavelength regions and through a fixed detection window it can be recorded as a constant signal, which is generally around twice the background signal with the source shutter closed. It is also possible that the fiber itself may be emitting RL signal since it is made of silica. Thus, the constant unquenched signal observed in all the graphs shown above can be attributed to luminescence being emitted from sources other than the sample. By

subtracting this constant background signal, the correct thermal quenching curves can be obtained. This is shown in Fig 4.27(a), 4.27(b), 4.28(a) and 4.28(b).

Fig 4.27(a) Thermal quenching curves: Arkansas quartz, UV emission region; Heating (1) and Cooling Cycles (2):

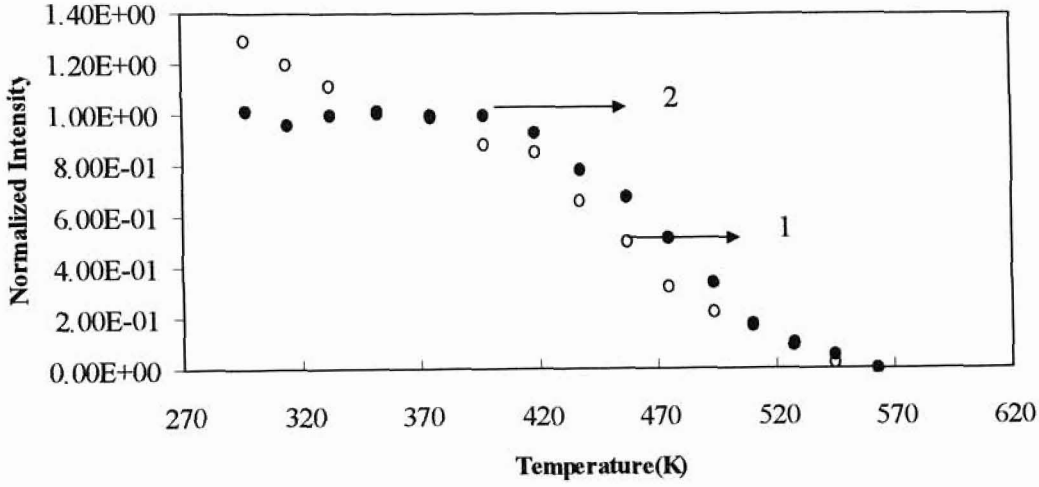

Fig 4.27(b) Thermal quenching curves: Arkansas quartz, Blue emission region; Heating (1) and Cooling Cycles (2):

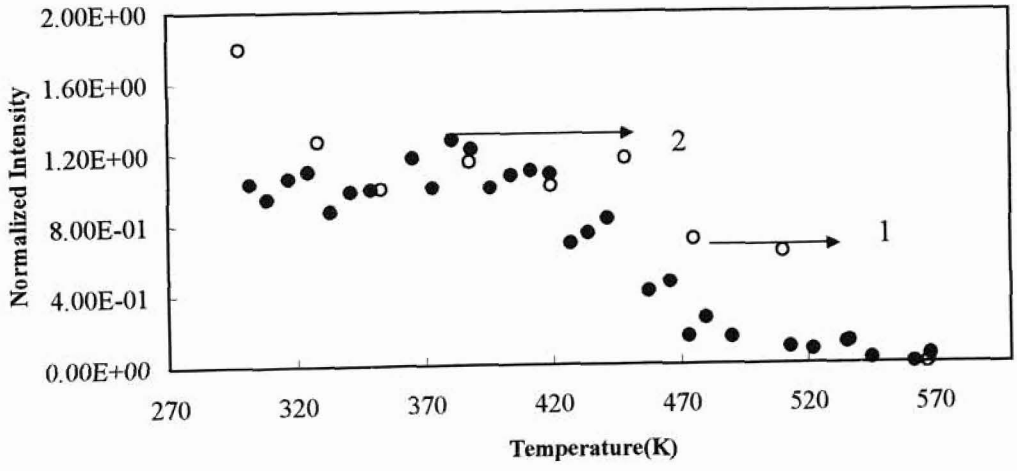

Fig 4.28(a) Thermal quenching curves: Danish quartz, UV emission region; Heating (1) and Cooling Cycles (2):

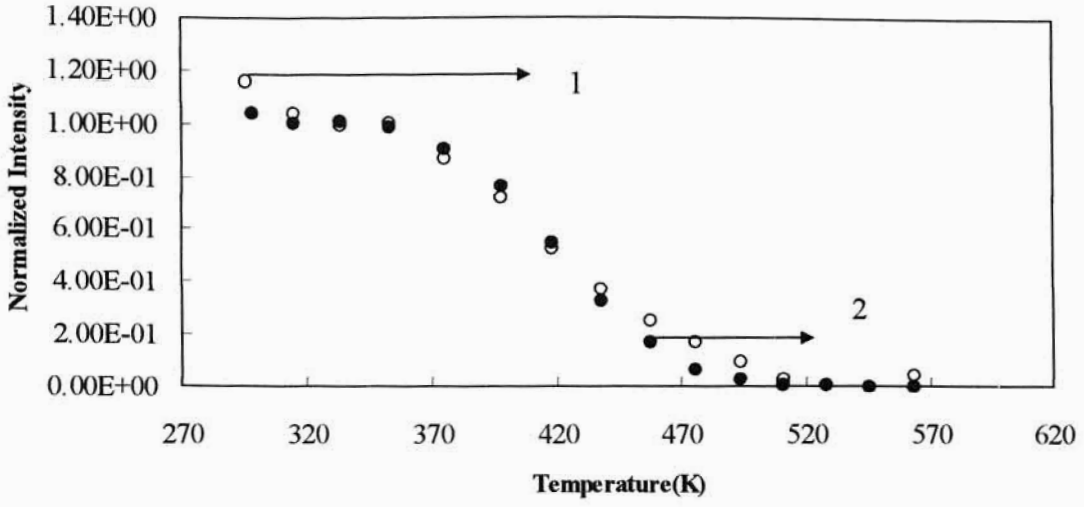

Fig 4.28(b) Thermal quenching curves: Danish quartz, Blue emission region; Heating (1) and Cooling Cycles (2):

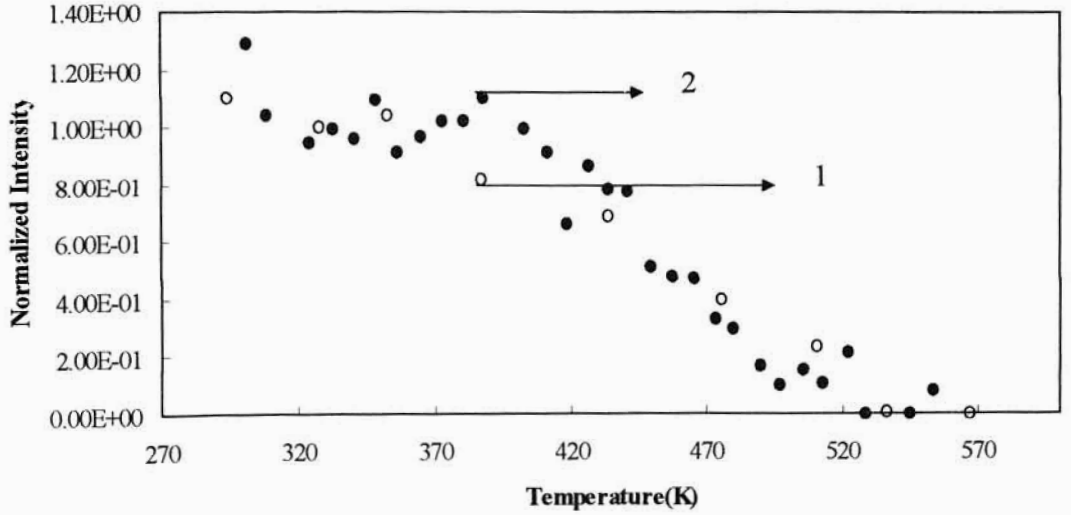

In the graphs shown above, the open circle (1) is data from the heating cycle and the closed circle (2) is data from the cooling cycle. In all the graphs it can be seen that the heating cycle shows an initial increase around 350 K. This fact was also observed in the OSL results wherein the heating cycle data showed a small peak in this same temperature region. As in the other case, here too, the increase in the signal in this region can be attributed to transfer of charges into the low temperature shallow traps from the deeper traps.

It can also be seen that the heating cycle data for the blue emission region does not display as smooth a quenching curve as does the cooling cycle data. Referring back to Fig 4.24(a), (b) and Fig 4.26(a) and (b), wherein the data for the blue emission region of the two samples are shown, it can be seen that the intensity of the quenching signal is not very much greater than the unquenched background signal. Only when the high background is subtracted can the shape of the quenching curve be seen. In case of the cooling cycle for the blue emission region, the data was measured every 10K, and as the effect of the shallow traps is very less here, better data was obtained. For the purpose of obtaining the quenching parameters of E and C, however, only the cooling cycle data will be utilized for the blue emission region.

4.6(b) Emission Shift Correction on Data in the UV emission region:

As in the TL and OSL results, the effect of emission shift correction in the UV emission region will be discussed. This is shown for the cooling cycle data in Fig 4.29(a) and Fig 4.29(b) for the two quartz samples.

Fig 4.29 (a) Effect of emission shift correction: UV emission region; Arkansas quartz sample: (1) 'Uncorrected', (2) 'Corrected':

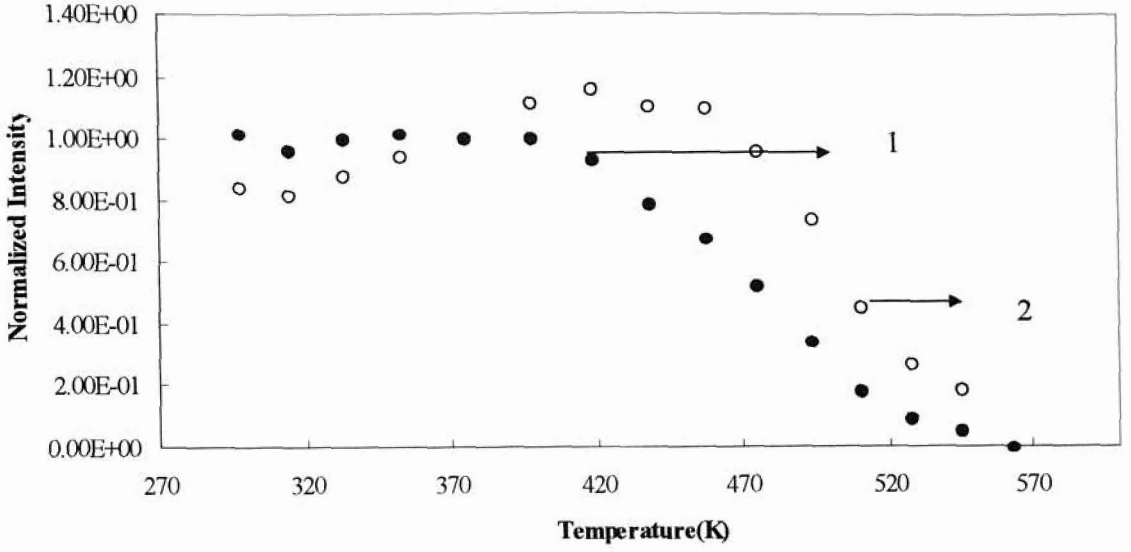

Fig 4.29 (a) Effect of Emission Shift Correction: UV emission region; Danish Quartz sample: (1) 'Uncorrected', (2) 'Corrected':

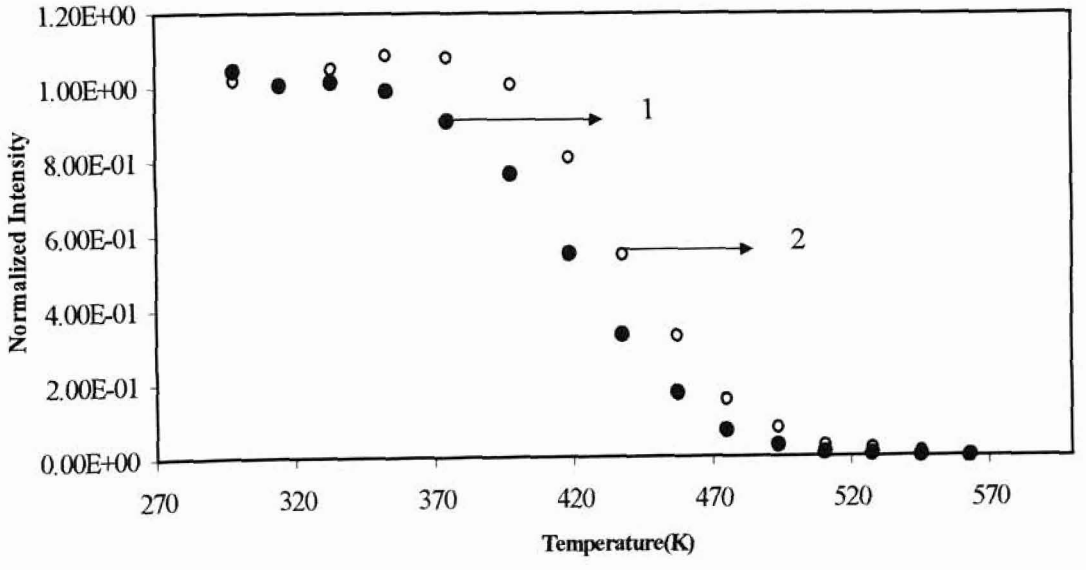

In the above shown graphs, the closed circle (1) is the data uncorrected for emission shift and the open circle (2) is the data that has been corrected for emission shift. It can be seen that emission shift correction not only changes the shape of the curve but it is also shifts the curve to higher temperatures. The small peak around 400 K appears due to the emission shift correction procedure. Referring back to TL and OSL results, the same effect was observed when emission shift correction was applied on the data in the UV region. Again it appears that the experimental data is being overcorrected. This in turn indicates that the emission shift in the UV emission region is not as large as is suggested in the published literature [17]. Thus, as in the TL and OSL case, here too emission shift correction will not be applied to data in the UV emission region for the purpose of this thesis.

4.7 Analysis of Quenching Curves:

Fitting of the quenching curves to Eq 4.1 using 'Origin 5.0' was straightforward for the data obtained in the UV emission region. But the cooling data obtained for the blue emission region was scattered and was more difficult to fit. Fits of the quenching curves obtained in both cooling cycle and the heating cycle of the two quartz samples in the UV emission region are shown in Fig 4.30(a), (b) and Fig 4.31(a) and (b). For the Arkansas quartz sample in the heating cycle the value of E and C are 0.65eV and 1.3*10^7, and for the cooling cycle the values obtained are 0.63eV and 5.4*10^6. For the Danish quartz sample the values of E and C in the heating and cooling cycle are 0.59eV, 9.8*10^6 and 0.63eV and 3.5*10^7 respectively. For the data in the blue emission region, however, the data is very scattered as the measurements were taken at sample temperatures every 10 K.

Fig 4.30(a) Quenching curve fit: Arkansas quartz sample; UV emission region; Heating Cycle data:

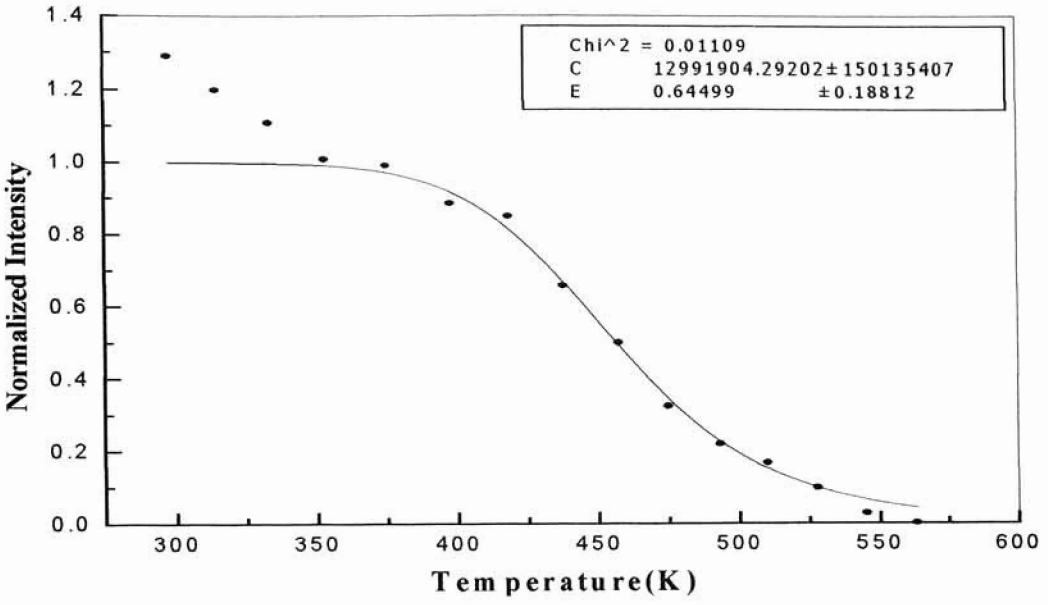

Fig 4.30(b) Quenching curve fit: Arkansas quartz sample; UV emission region; Cooling Cycle data: Error bars indicate the weighting factor

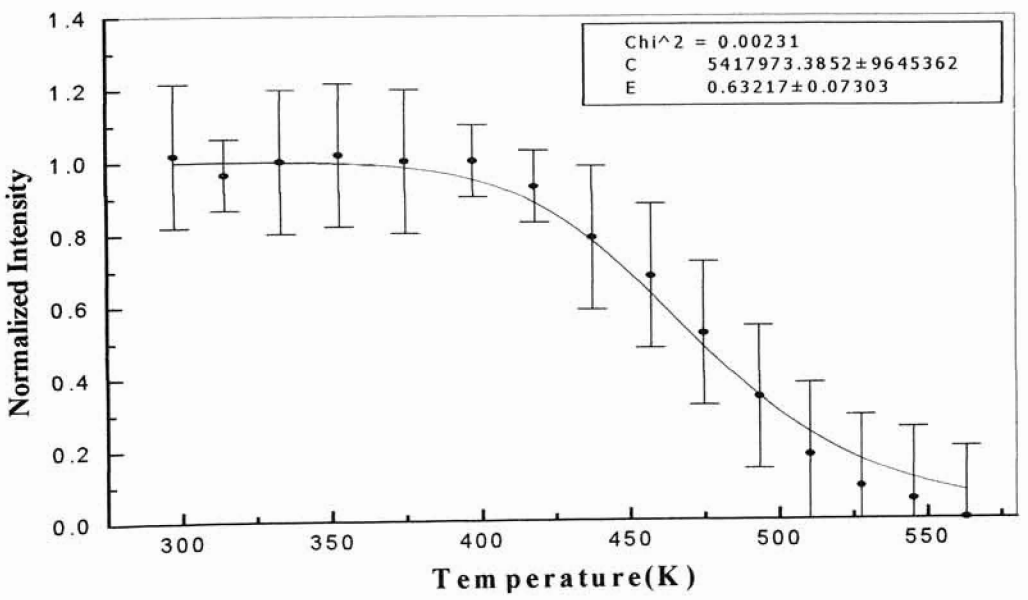

Fig 4.31(a) Quenching curve fit: Danish quartz sample; UV emission region; Heating Cycle data:

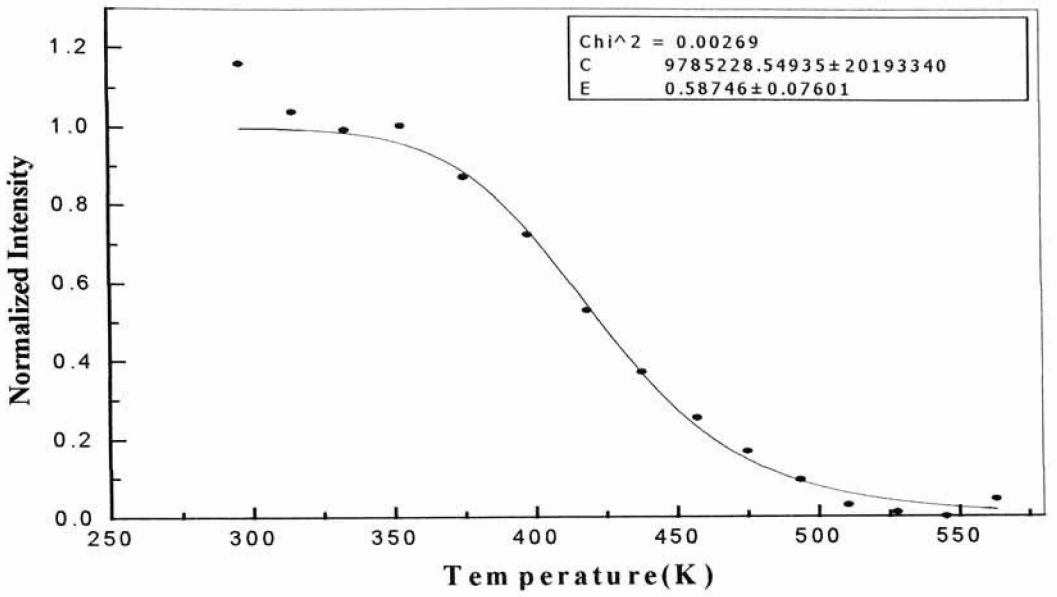

Fig 4.31(b) Quenching curve fit: Danish quartz sample; UV emission region; Cooling Cycle data: Error bars indicate the weighting factor

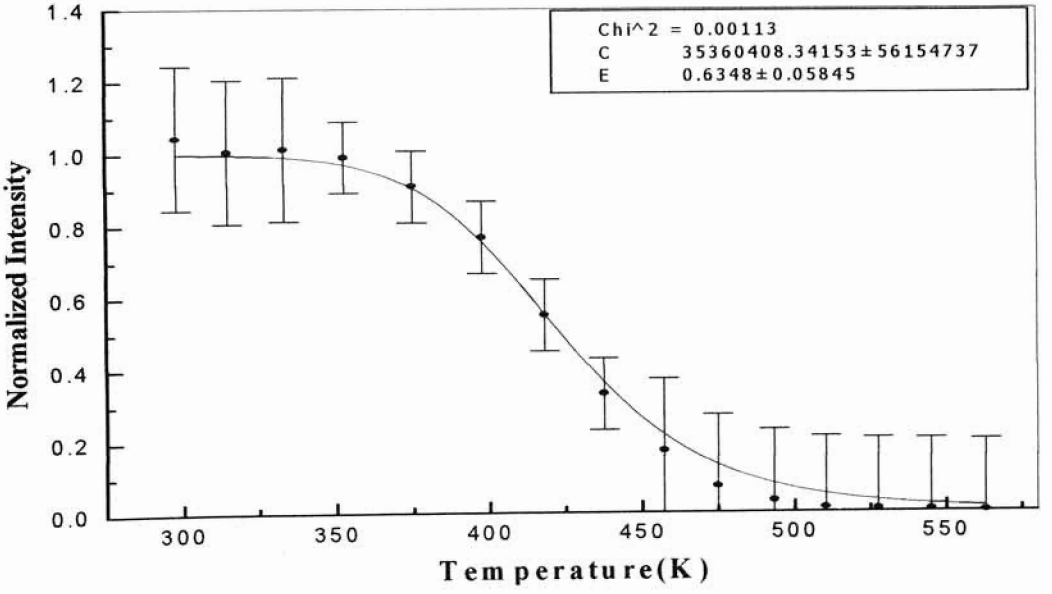

Fig 4.32(a) Quenching curve fit: Arkansas quartz sample; Blue emission region; Cooling Cycle data:

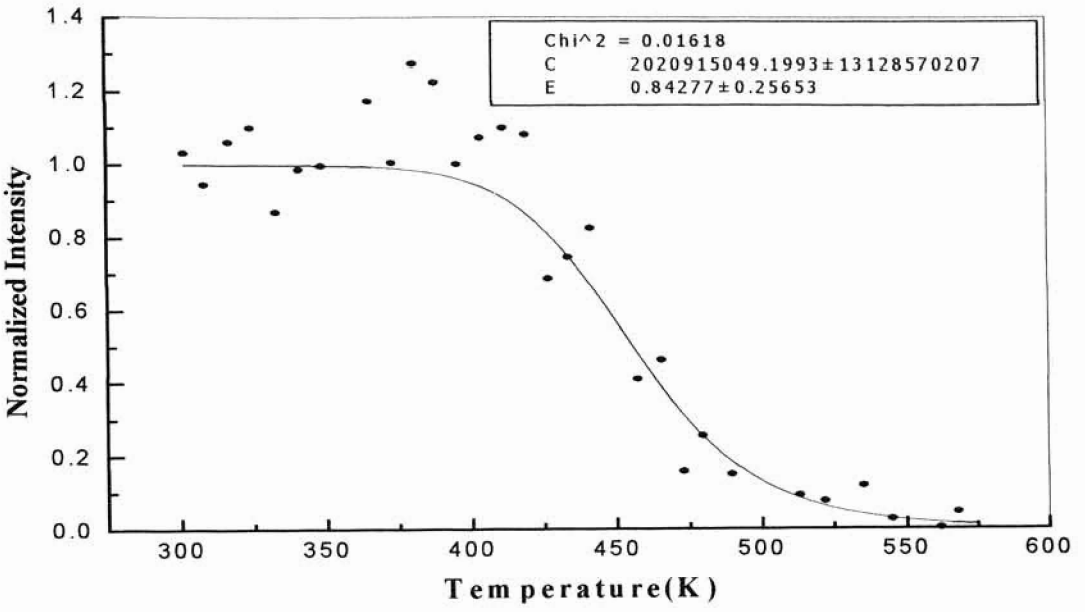

Fig 4.32(a) Quenching curve fit: Danish quartz sample; Blue emission region; Cooling Cycle data:

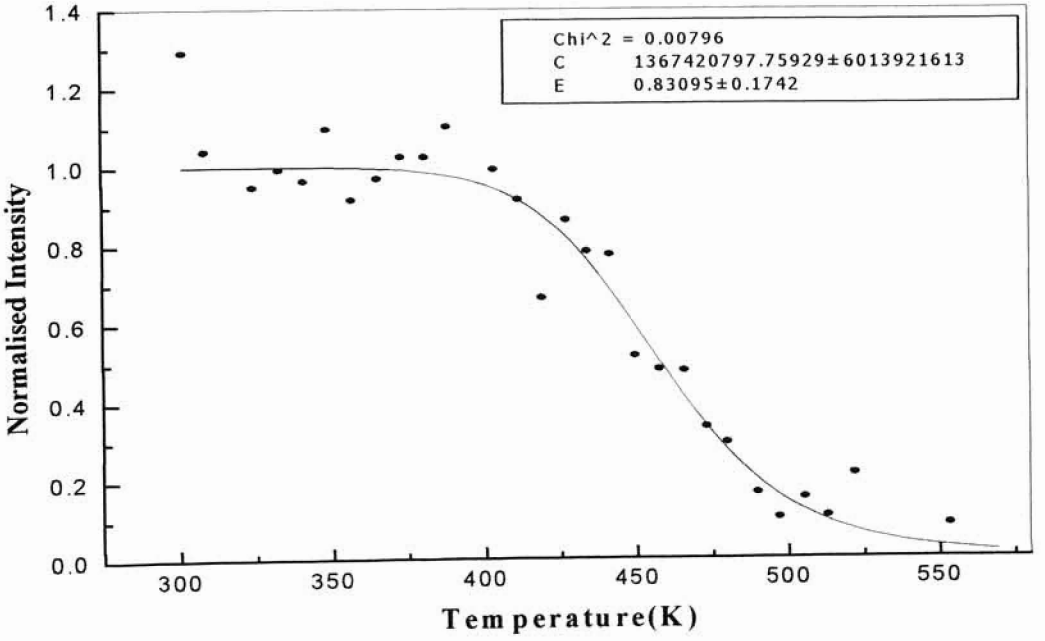

Approximate fits to the data in the blue emission region have been shown in Fig 4.32(a) and (b) for the cooling cycle data. But better estimates can be obtained by comparing these curves with the quenching curves obtained for the samples from the TL experiments. Even though there is uncertainty in the fits to these data because of the wide scatter, it can be seen that the activation is energy is for the blue region is much higher than for the UV emission. For the Arkansas quartz sample the values of E and C are 0.84eV, 2.0*10^9 and for the Danish quartz sample the values are 0.83eV and 1.4*10^10. In Fig 4.33(a) and 4.33(b) comparison between the RL and TL data for the two samples in the blue emission region is shown. The open circle is RL (1) and the closed circle is the TL (2) data. It can be seen that the agreement between TL and RL data for the Arkansas quartz sample is good, but for the Danish quartz sample an apparent shift exists between the two sets of data.

Fig 4.33(a) Comparison of RL (1) and TL (2) data for the Arkansas quartz sample in the Blue emission region:

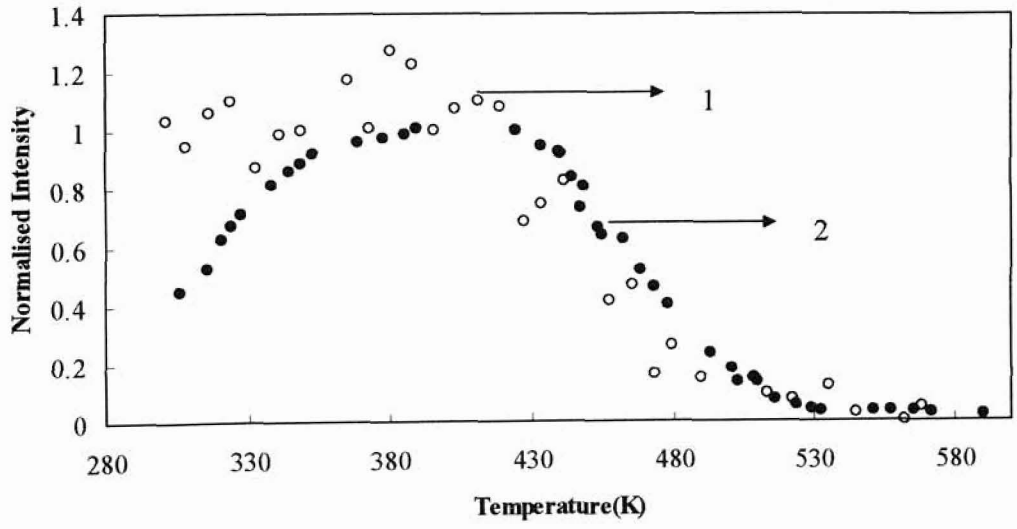

Fig 4.33(a) Comparison of RL (1) and TL (2) data for the Danish quartz sample in the Blue emission region:

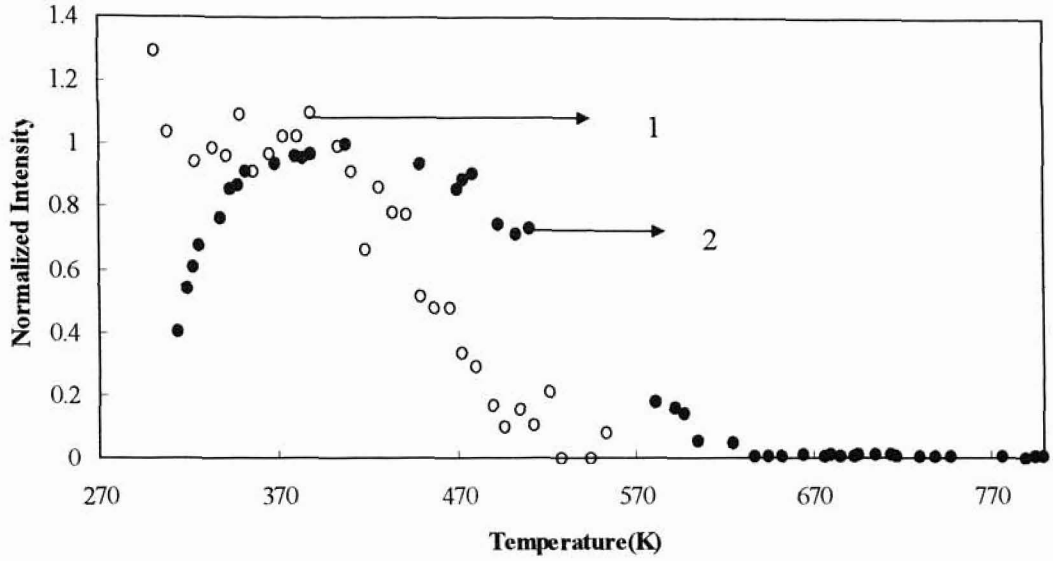

Danish Quartz sample:

Two possible reasons for this to occur emerge with help of the TL spectral emission data. As mentioned in Ch 3, these measurements were performed on the 'Flourolog System' at a heating rate of 1K/s. The TL intensity is given as a function of both temperature and wavelength. The contour plots of the spectral emission for the two samples are shown in Fig 4.34(a) and Fig 4.34(b).

As can be seen in the contour plot of the Arkansas quartz sample, the blue emission region has peaks only at low temperatures. Referring back to the TL glow curves obtained for this sample in Fig 4.1(b), it can be seen that even at the highest heating rate of 9K/s, all the peaks in this emission region are below 300°C. The high intensity around 550nm is the incandescence (**1**).

Fig 4.34(a) Contour plot of the Arkansas quartz sample:

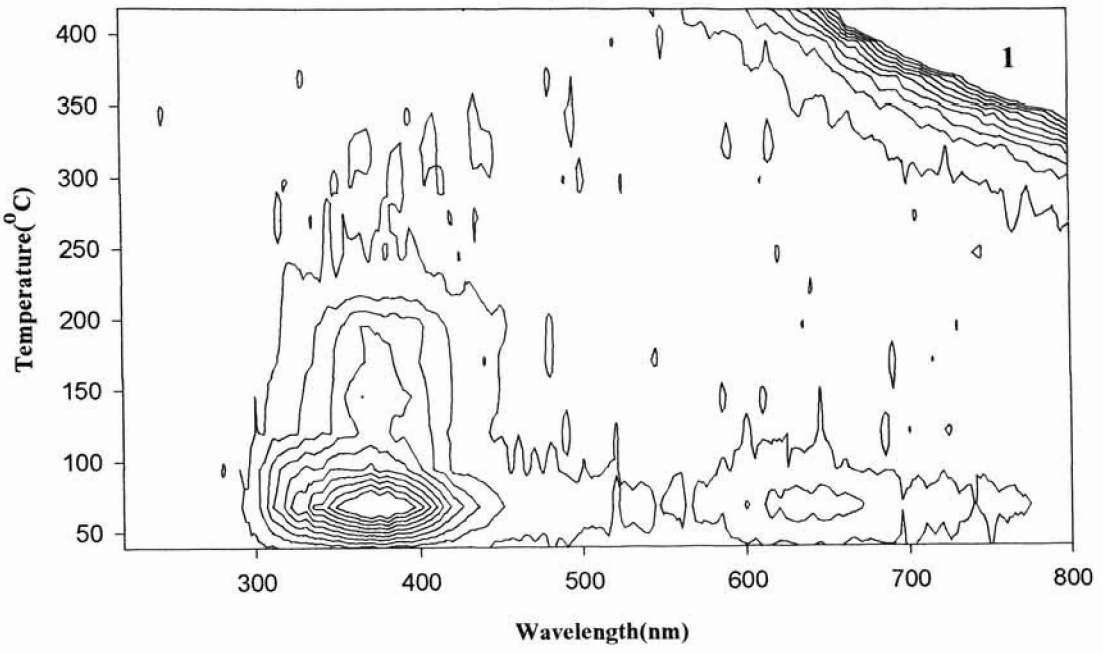

Fig 4.34(b) Contour plot of the Danish quartz sample:

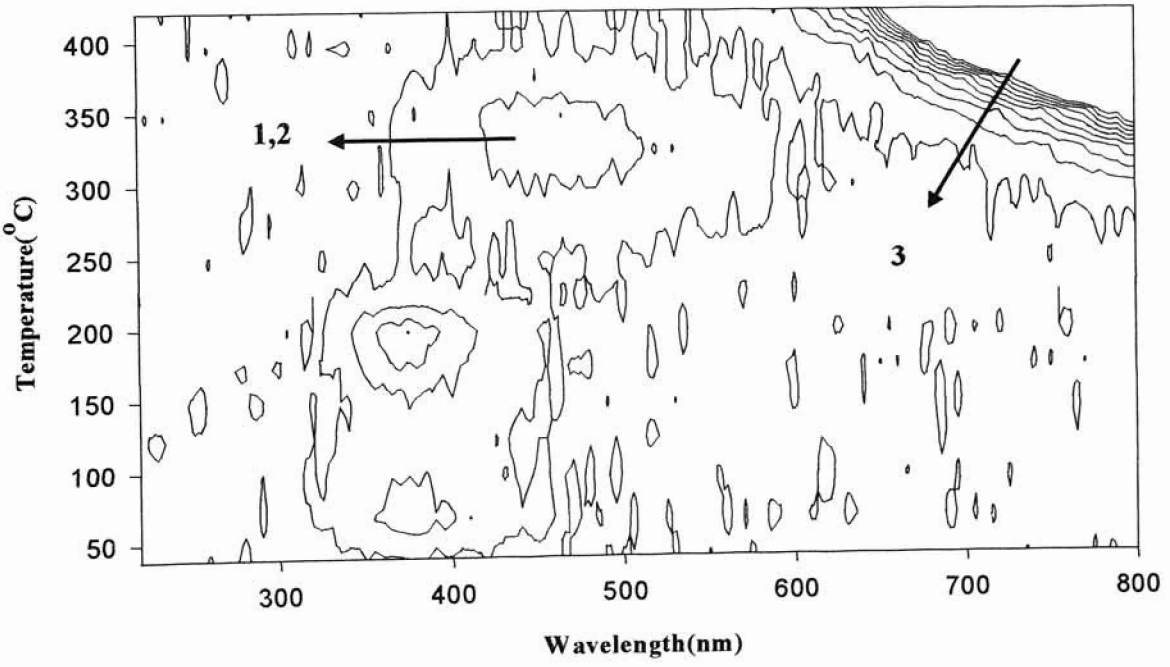

The glow curves obtained for the Danish quartz sample in the blue emission region are shown in Fig 4.2(b). Comparing this to the contour plot shown above, it can be seen that the strong emission peak around 350°C and 460nm (**1,2**) is actually two TL peaks in the temperature region of 320°C to 520°C overlapping each other. At high heating rates the second TL peak moves into the temperature region where the incandescence is emitted and becomes indistinguishable from it. This overlap with the incandescence (**3**) can be seen in the contour plot too.

To explain the temperature shift between the quenching curves obtained in the TL and RL of the Danish quartz sample, the following cases can be considered.

Case 1:

It is possible that the two TL peaks (Fig 4.2(b)) in the Danish quartz sample in the blue emission region in the temperature range of 320°C to 520°C, are being emitted from two different recombination centers. However, they may emit coincidentally in the same emission region, and thus overlap each other. In this case, the rate at which one of the TL peaks is quenching may be different from the other TL peaks in this emission region, or, it is also possible that second peak may not at all be quenching. When the scaling procedure was applied, however, it was under the assumption that all the TL peaks in this emission region quench at the same rate. The possibility that the second peak is quenching at a different rate would introduce an error in the scaling procedure, and would result in the shifting of the scaled TL quenching curve to higher temperatures. The question that now arises concerns whether or not this (possible second) recombination center is also contributing to the RL signal. If the recombination center is contributing to the RL signal, then the high-unquenched background signal (which was earlier attributed

to sources other than the sample) may also include a contribution from this recombination center. In order to verify this theory, RL spectra need to be measured. However in the present study it was not possible to measure RL spectra because of time constraints.

Case 2:

The other possible explanation is that the TL peaks in the 320°C to 520°C temperature region use the same recombination center (different traps) but the overlap of the higher temperature TL peak with incandescence causes the error in the scaling procedure. The overlap of the TL peak with the incandescence is clear from heating rates beyond 0.3K/s. Thus, during the deconvolution of the TL glow curves, this overlap would introduce error. And as a result, the quenching curve from the scaling procedure would be shifted to higher temperatures, thus resulting in the difference between the RL quenching curve and the TL quenching curve (Fig 4.33(a)).

4.8 Comparison of Quenching Parameters Obtained from TL, OSL and RL with Published Values:

This section gives a comparison of the quenching parameters, primarily the activation energy, obtained for quartz in different emission regions by other researchers. The published values of quenching energies have not necessarily been obtained by similar experiments as in this thesis.

UV Emission Region:

The quenching parameters obtained in the UV emission region for TL, OSL and RL experiments agreed very well with published values of the parameters. These values are

given in Table1.The values obtained for E and C by Wintle [5], Wintle and Murray [6], McKeever et al [7], Huntley et al [19], and Galloway [20] in the UV emission region are given in Table 2.

Table1: Values obtained for the quenching parameters in the UV emission region:

Experiment		Arkansas Quartz Sample		Danish Quartz Sample	
		E	***C***	***E***	***C***
TL		0.59eV±0.07	7.9E6	0.63eV±0.1	8.8E6
OSL	**Heating Cycle**	0.64eV±0.08	1.2E7	0.57eV±0.01	2.1E6
	Cooling Cycle	0.60eV±0.03	4.6E6	0.54eV±0.02	1.4E6
RL	**Heating Cycle**	0.65eV±0.2	1.3E7	0.59eV±0.07	9.8E6
	Cooling Cycle	0.63eV±0.07	5.4E6	0.63eV±0.06	3.5E7

Table 2: Published values of quenching parameters in the UV emission region:

Paper		***E***	***C***
Wintle [5]	**RL**	0.64eV	2.8E7
Wintle and Murray [6]	**OSL**	0.636eV, 0.61eV	3.4E7, 2E7
McKeever *et al.* [7]	**OSL**	0.6eV	7.9E6
Huntley *et al.*[19]	**OSL**	0.64eV	2.8E7
Galloway [20]	**(a) Lifetime**	0.74eV±0.06	-
	(b) Intensity	0.73eV±0.14	-

Blue Emission Region:

There are no quenching parameters published for the blue emission region. Wintle [5 concluded in her paper that the quenching parameters for other wavelength regior remain the same as those for the UV. A note by her also indicated that very litt quenching was observed in the 495nm region. The values obtained in the TL and R experiments in this thesis for the blue emission region are given in Table 3.

Table 3: Quenching parameters obtained in the Blue emission region:

Experiment	Arkansas Quartz Sample		Danish quartz sample	
	E	***C***	***E***	***C***
TL	0.89eV± 0.3	3.2E9	0.83eV ±0.24	8.2E7
RL	0.84eV±0.25	2.0E9	0.83eV±0.17	1.4E10

Chapter 5

Summary, Conclusions and Future Work

5.1 Summary:

Luminescence from irradiated quartz is observed over a broad range of wavelengths with major emissions in the UV and blue regions of the spectrum. Additional emissions are observed in the red [16,21]. Early observations by Wintle [5] indicated significant thermal quenching of the luminescence efficiency over all wavelength ranges. She also indicated that the extent of quenching remains almost the same for the different emission regions except for the 495nm. The data presented in this thesis shows good agreement with the quenching parameters for the UV emission region but differs with Wintle [5] in the blue emission region.

The data obtained for UV emission region by TL, RL, and OSL experiments are consistent with the quenching parameters obtained by others from OSL and RL experiments [3,6,14] with an activation energy of the order of 0.60 eV±0.05. However, values from Galloway's [20] luminescence lifetime measurements given in table 1 for UV emission region have higher activation energy of quenching. In contrast to Wintle's [5] conclusions, however, the parameters describing the quenching of the blue emission suggests larger activation energy of the order of 0.85eV±0.15. It should also be noted here that Wintle [5] suggests that emission measured with the 465nm filters yields a quenching energy of 0.64eV but no quenching is observed with the 495nm filter. She also mentions that the quenching energies obtained in with 310nm, 370nm and 410nm are the

same as those obtained with the 465nm. However, filters 465nm and 495nm lie in the same blue- green region. It appears unlikely that quenching is observed at 465nm and not at 495nm. Referring back to the RL data obtained in the blue emission region in this thesis, it was seen that the signal in this region was very low and only after the unquenched high background signal was subtracted, could the actual shape of the quenching curve be seen. It is possible that this same phenomenon was observed by Wintle [5] and she concluded that there was no quenching in the 495nm region. The observation that the quenching parameters differ in UV and blue is consistent with published data by Krbetschek *et al.* [16] on the response of the different emission wavelengths to various sample treatments (pre-heating, pre-irradiation, *etc.*) which suggests that the emissions originate from physically different defect centers. Possible origins for the various emissions are discussed by Krbetschek *et al.*[16]. This conclusion is also consistent with the observations of Spooner and Franklin [21] who determined thermal quenching energies for red TL emission to be of the order of 0. 2eV.

It has been seen that both heating and cooling cycles were performed for the OSL and RL experiments. It was also noted that the cooling cycle yields better quenching curves and that the presence of a small peak in the heating cycle distorts the quenching curve. The presence of this peak has been attributed to the 110°C trap, which also gives raise to the 110°C TL peak.

It has also been seen that the scaling procedure used for obtaining smooth quenching curves in TL relies to a large extent on judgement and thus cannot be completely relied upon. In case of the OSL measurements, a different kind of problem exists: it was not possible to measure the signal in the blue emission region due to the constraints on the

existing system. In case of the RL measurements, the presence of the large unquenched background signal was noted. Possible explanations as to its presence have been presented, but no confirmation could be obtained.

Recent measurements of the photoluminescence lifetime τ from natural quartz in the wavelength range 280 – 380 nm by Bailiff [22] have shown that the lifetime of the luminescence excited state does indeed decrease according to:

$$\tau = \frac{\tau o}{1 + C * Exp\left(-W/kT\right)} \tag{5.1}$$

where τ_o is the lifetime measured at room temperature (varying over the range ~30 - 40 μs), and C and W have the usual definition as in Eq. (4.1). Thus, perhaps the quenching parameters measured from luminescence lifetime will yield better confirmation. However, it was seen that the parameters resulting from luminescence lifetime experiments by Galloway [20] yield comparatively higher quenching energies.

The emission in the UV region has been found to shift to higher wavelength regions [16,17] with an increase in temperature. When the emission shift correction was applied to the data presented in this thesis, it was noted that its effect resulted in the quenching curve changing its shape. It was also seen that the curve no longer follows the known equation given in Eq 4.1. The possible explanation was that the data was being overcorrected, and that though the emission in the UV region does shift to higher wavelengths with increase in temperature, it is not as large as suggested in the published literature [16,17]. Thus emission shift correction was not applied to the data obtained in this thesis.

Finally, the data obtained in this thesis can be understood by considering a fixed thermal quenching curve, independent of heating rate, i.e. the thermal quenching curve is fixed on the temperature space and the glow curves move across the quenching curve with increasing heating rate. This can be seen in Fig 5.1. It shows a simulated quenching curve with the glow curves shifting to higher temperatures with increasing heating rate. The quenching curve was simulated using Eq 4.1 and experimental values for E and C. The glow curves are Gaussian curves with FWHM taken from experimental data.

Fig 5.1 Simulated quenching curve fixed in temperature, with the glow peaks shifting to higher temperatures and quenching with increasing heating rate:

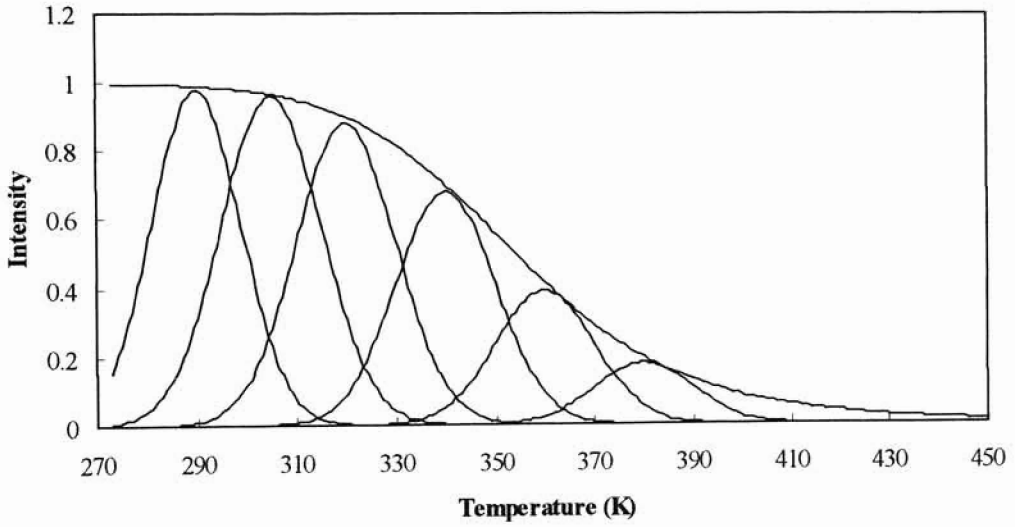

This in turn suggests a Mott-Seitz mechanism for the quenching phenomenon rather than a Schön-Klasens mechanism since in the latter, one would expect that the temperature over which the quenching occurred would shift to higher values as the heating rate

increased, due to the kinetics of the hole release process. Thus, as the heating rate is increased not only would the glow curves shift to higher temperatures but the quenching curve would too.

5.2 Conclusions:

The intent behind the investigation given in this thesis was to examine the thermal quenching characteristics of natural quartz at two different wavelength regions in the UV and blue, and also to discuss the potential of the Mott-Seitz model as the appropriate model to describe the thermal quenching process.

It has been found that the quenching parameters are different for UV and blue. It has also been seen that the observed data fits the Mott-Seitz model rather than the Schön-Klasens mechanism.

5.2 Future Work:

OSL experiments in the blue emission region can be performed to confirm the quenching parameters obtained from the TL and RL experiments. These were not performed at the current time due to constraints on the existing system. RL spectra can be performed in order to confirm or otherwise, the presence of unquenched emission peaks in the blue emission region of the Danish quartz sample.

OSL spectra can be performed on the samples to determine the actual extent of emission shift across wavelength at high temperatures in the UV emission region.

Luminescence lifetime measurements can be performed in both emission regions to obtain the exact values of the quenching parameters.

References:

[1] Aitken, M. J., *An introduction to Optical Dating,* Oxford Univ. Press, (1998).

[2] Huntley, D.J., Godfrey-Smith, D.I., Thewalt, M.L.W., *Optical Dating of Sediments,* Nature. **313**, 105-107 (1985).

[3] McKeever, S.W.S., Bøtter-Jensen, L., Agersnap Larsen N. and Duller, G.A.T., *Temperature dependence of OSL decay curves: Experimental and Theoretical Aspects,* Radiat. Meas. **27**, 161-170 (1997).

[4] Wintle, A.G., *Luminescence Dating: Laboratory Procedures and Protocols,* Radiat. Meas. **27**, 769-817 (1997).

[5] Wintle, A.G., *Thermal quenching of thermoluminescence in quartz,* Geophys. J. Roy. Astron. Soc. **41**, 107-113 (1975).

[6] Wintle A.G. and Murray A.S., *Quartz OSL: Effects of thermal treatment and their relevance to laboratory dating procedures.* Radiat. Meas. **32**, 387-400 (2000)

[7] McKeever, S.W.S., *Thermoluminescence of Solids,* Cambridge Univ. Press, Cambridge (1985)

[8] Chen R. and McKeever, S.W.S., *Theory of Thermoluminescence and Related Phenomena,* World Scientific, Singapore (1997).

[9] Curie, D., *Luminescence in Crystals.* Methuen, London (1960)

[10] Trautman, T., Krebetschek, M. R., Dietrich, A., Stoltz, W., *The basic priciple of radioluminescence dating and a localized transition model* Radiat. Meas. **32** 487-492 (2000).

[11] Trautman, T., Krebetschek, M. R., Dietrich, A., Stoltz, W., *Feldspar radioluminescence: A new dating method and its physical background* J. of Lum **85** 45-58 (1999)

[12] Markey, B.G., Botter-Jensen, L., Duller, G.A.T., *A new flexible system for measuring TL and OSL,* Radiat. Meas. **27** 83-89 (1997).

[13] Botter-Jensen, L., *Development of Optically stimulated luminescence techniques using natural minerals and ceramics, and their application to retrospective dosimetry*, Ph.D thesis University of Copenhagen (2000).

[14] Spooner N.A., *On the optical dating signal from quartz,* Radiat. Meas. **23**, 593-600 (1994).

[15] Petrov, S.A., Bailiff, I.K., *Thermal Quenching and Initial rise technique of trap depth evaluation*, J. Luminescence **65**, 289-291 (1996)

[16] Krbetschek, M.R., Götze, J., Dietrich, A. and Trautman, T., *Spectral information from minerals relevant for luminescence dating,* Radiat. Meas. **27**, 695-748 (1997).

[17] Franklin, A.D., Prescott, J.R. and Scholefield, R.B., *The mechanism of thermoluminescence in an Australian sedimentary quartz*. J. Luminescence **63**, 317-326 (1995)

[18] Huntley, D.J., Godfrey-Smith, D.I. and Haskell, E.H., *Light-induced emission spectra from some quartz and feldspars*. Radiat. Meas. **18**, 127-131 (1991).

[19] Huntley, D.J., Short, M.A., Dunphy, K., *Deep traps in quartz and their use for optical dating* Can. J. Phys. **74**, 81-91.(1996).

[20] Galloway, R.B., *Luminescence lifetimes in quartz: dependence on annealing temperature prior to beta irradiation,* Radiat. Meas. **35** 67-77 (2002).

[21] Spooner, N.A. and Franklin, A.D., *Effect of the heating rate on the red TL of quartz*, Radiat. Meas. **35** 59-66 (2002).

[22] Bailiff, I.K. *Characteristics of time-resolved luminescence in quartz*, Radiat. Meas. **32**, 401-405 (2000).

[23] Bailey, R.M., Smith, B.W., Rhodes, E.J., *Partial bleaching and the decay form characteristics of quartz OSL*, Radiat. Meas, **27** 123-136 (1997)

[24] Banerjee, D., *Supralinearity and sensitivity changes in optically stimulated luminescence of annealed quartz*, Radiat. Meas. **33** 47-57 (2001).

[25] Townsend, P. D., Kelly, J. C., *Colour centers and imperfections in insulators and semiconductors*, Sussex Univ. Press, (1973)

VITA 2

Rashmi Nanjundaswamy

Candidate for the Degree of

Master of Science

Thesis: THERMAL QUENCHING OF LUMINESCENCE IN QUARTZ

Major Field: Physics

Biographical:

Personal Data: Born in Karnataka, India, on January 20, 1977.

Education: Received Bachelor's degree in Physics from St.Xavier's College of Gujarat University, Gujarat, India (June, 1997); Received Master's degree in Physics from Saurashtra University, Gujarat, India (June, 1999); Completed the requirements for the Master of Science degree with a major in Physics at Oklahoma State University (August, 2002).

Experience: Department of Physics, Oklahoma State University, as a graduate research assistant and teaching assistant from August 1999 to June 2002.